Université de Liège

Vibration Testing & Modal Identification

Jean-Claude Golinval

References

- D. J. EWINS

  Modal Testing : theory, practice and application

  Second Edition, Research Studies Press LTD, 2000

  ISBN 0 86380 218 4

- N. MAIA, J. SILVA

  Theoretical and Experimental Modal Analysis

  Research Studies Press LTD, 1997

  ISBN 0 86380 208 7

Two Routes to Vibration Analysis

Theoretical Approach – Direct Problem

Structural Model → Modal Model → Response Model

Structural Model	Modal Model	Response Model
Description of the structure in terms of its mass, stiffness and damping properties	Natural frequencies, Modal damping factors, Mode shapes	Frequency Response Functions, Impulse Response Functions

Experimental Approach – Inverse Problem

Response Measurements → Modal Model (Identification) → Structural Model

Analyse et identification modale

Définition

Développement d 'un modèle mathématique du comportement dynamique d 'une structure à partir de tests expérimentaux.

Relation fondamentale

Réponse	=	Excitation	×	Propriétés du système

Bref historique

Avant 1947 : mesures de la réponse seule

1947 : mesures de la réponse et de l 'excitation
Kennedy, Pancu : mesures des fréquences de résonance et de l 'amortissement de structures d 'avions.

1960-70 : progrès techniques des moyens de mesures (capteurs, électronique, ...) et d 'acquisition (analyseurs de spectre digitaux)

1965 : algorithme FFT (Cooley et Tukey)

Single-Degree-Of-Freedom (SDOF) System

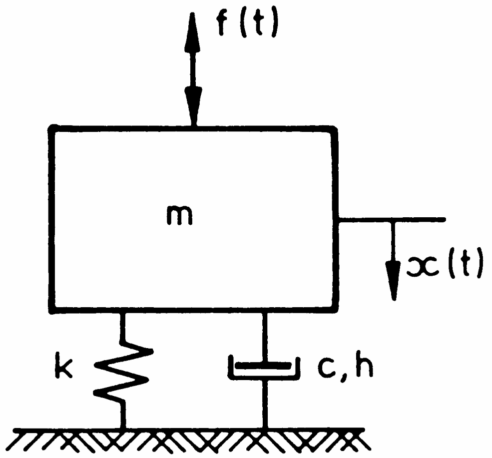

Governing equation of motion

$$m\,\ddot{x} + c\,\dot{x} + k\,x = f(t)$$

In case of no external forcing ($f(t) = 0$,

the trial solution : $x(t) = X\,e^{\lambda t}$

leads to the requirement that : $m\,\lambda^2 + c\,\lambda + k = 0$

Roots : $$\lambda_{1,2} = -\frac{c}{2\,m} \pm \frac{\sqrt{c^2 - 4\,k\,m}}{2\,m} = -\zeta\,\omega_0 \pm i\,\omega_0\,\sqrt{1-\zeta^2}$$

where $\omega_0 = \sqrt{\dfrac{k}{m}}$ and $\zeta = \dfrac{c}{2\,\omega_0\,m}$

Natural frequency **Viscous damping ratio**

Free vibration characteristic of damped SDOF system $(\zeta < 1)$

$$x(t) = X\ e^{-\zeta\omega_0 t}\ e^{i\,\omega_0 \sqrt{1-\zeta^2}\ t}$$

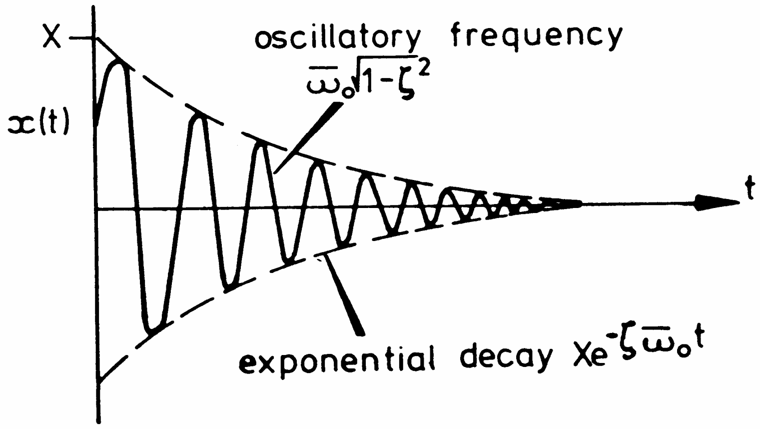

Forced response to harmonic excitation: $f(t) = F\ e^{i\,\omega\, t}$

$$\boxed{X(\omega) = H(\omega)\, F(\omega)}$$

$$H(\omega) = \frac{1}{(k-\omega^2\ m) + i\,(\omega\, c)} = \frac{1}{k}\,\frac{1}{\left(1-\dfrac{\omega^2}{\omega_0^2}\right) + i\left(2\,\zeta\,\dfrac{\omega}{\omega_0}\right)}$$

Frequency Response Function (FRF)

Alternative Forms of FRF

Force → Structure → Response → Displacement / Velocity / Acceleration

FRF = Response / Force

	Standard FRF	Inverse FRF
Displacement	Receptance Admittance	Dynamic stiffness
Velocity	Mobility	Mechanical impedance
Acceleration	Accelerance Inertance	Apparent mass

Graphical Displays of FRF Data

The FRF is a complex quantity.

$$H = \overbrace{\Re(H(\omega))}^{\text{Real Part}} + i\,\overbrace{\Im(H(\omega))}^{\text{Imaginary Part}}$$

Frequency

The most common forms of presentation are:

- Bode plot: Modulus and Phase of FRF vs. Frequency (2 graphs);
- Nyquist plot: Imaginary Part (of FRF) vs. en Real Part (of FRF) (a single graph which does not contain frequency information explicitely);
- Cartesian plots: Real Part (of FRF) vs. Frequency and Imaginary Part (of FRF) vs. Frequency (2 graphs);

- **Bode Plot**

Linear scales

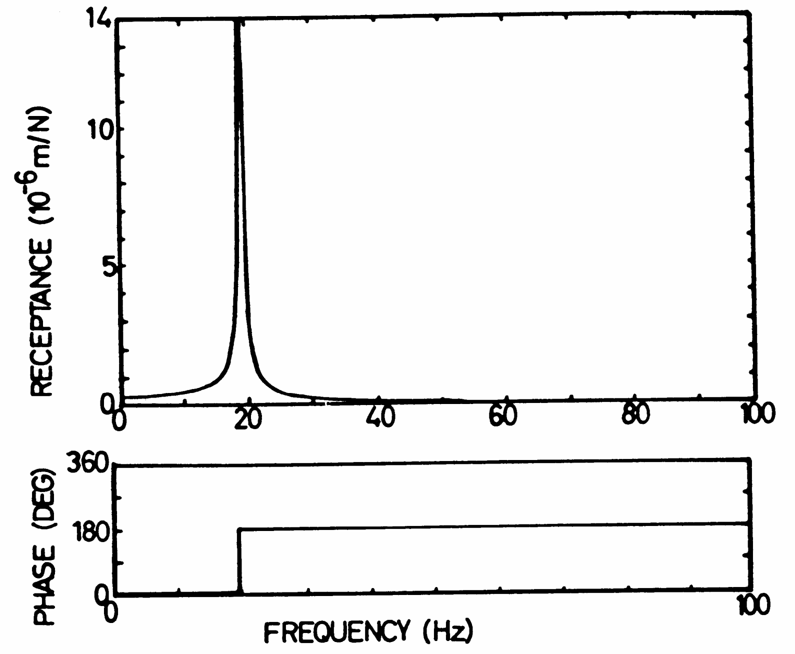

Log-Log scales

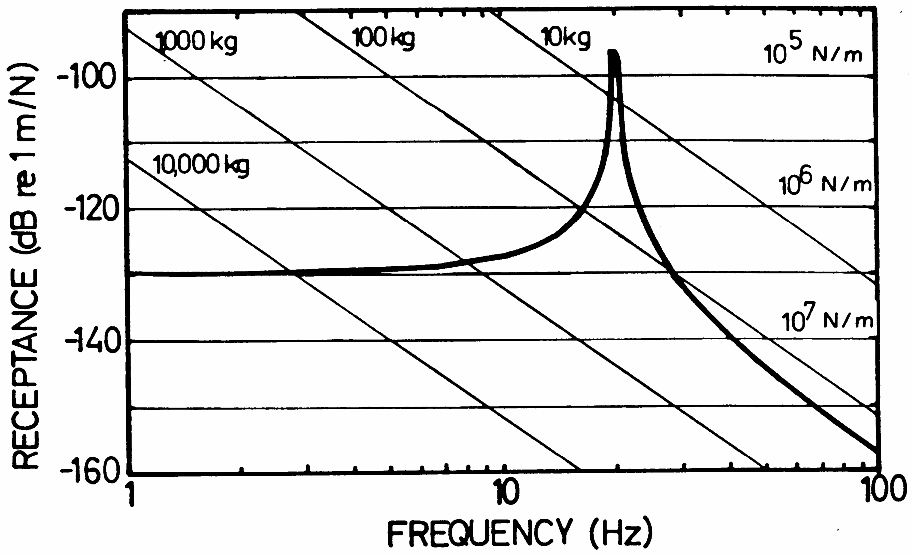

Receptance	Mass	Stiffness
$H(\omega)$	$-1/\omega^2\, m$	$1/k$
$\log(H(\omega))$	$-\log(m) - 2\log(\omega)$	$-\log(k)$

- **Nyquist Plot**

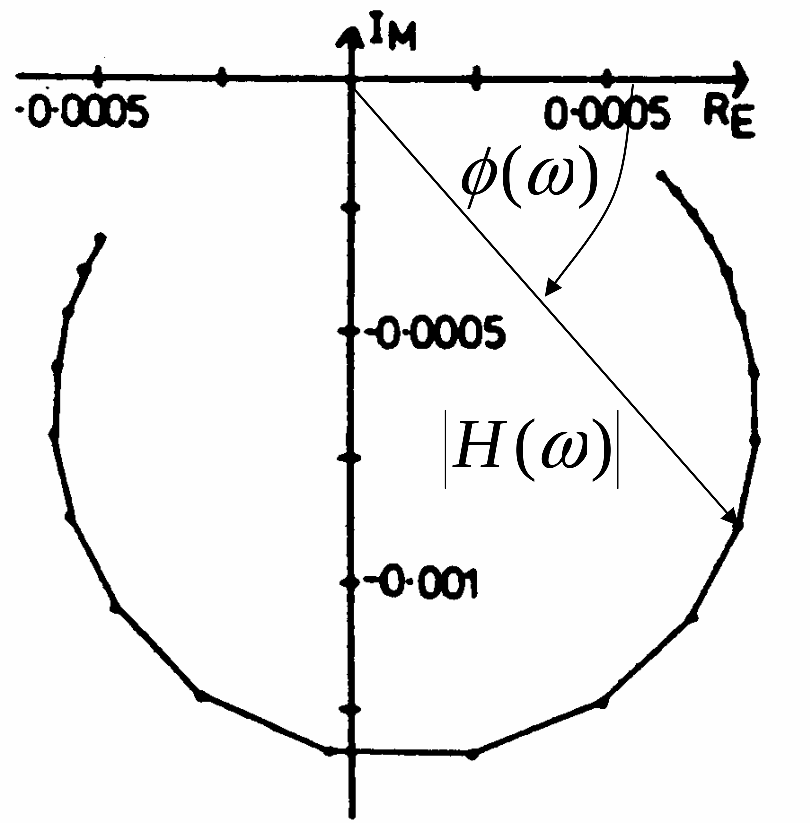

- **Cartesian Plots**

Real Part

Imaginary Part

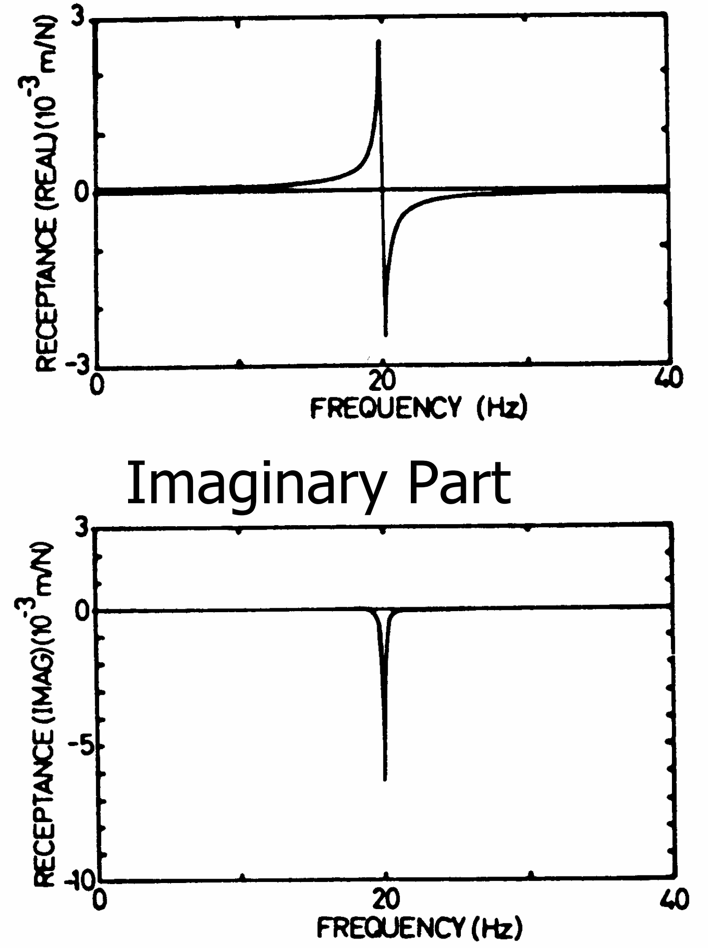

- **Three-dimensional plot of SDOF system FRF**

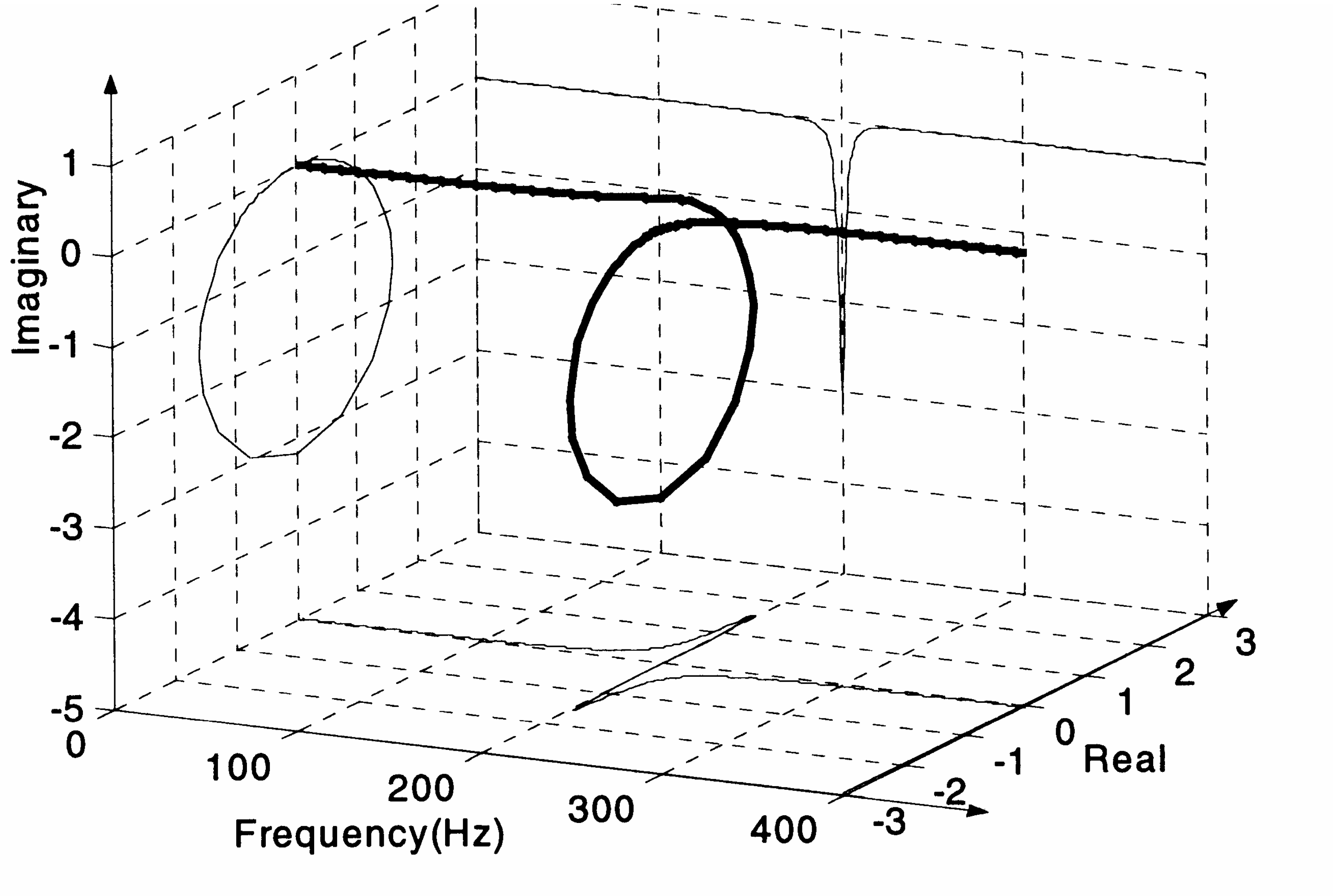

Multi-Degree-Of-Freedom Systems

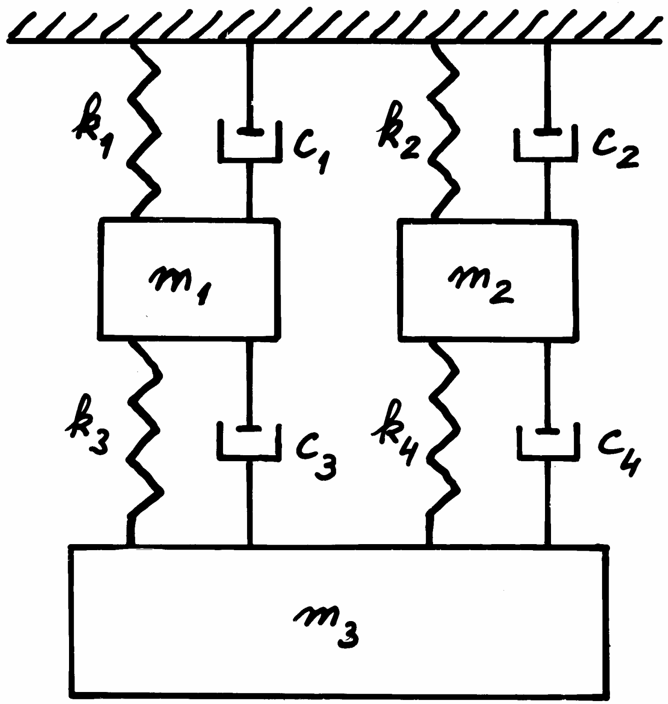

Governing equation of motion

$$\mathbf{M}\,\ddot{\mathbf{q}} + \mathbf{C}\,\dot{\mathbf{q}} + \mathbf{K}\,\mathbf{q} = \mathbf{f}(t)$$

$\mathbf{q}$ = vector of displacements

$\mathbf{f}(\mathrm{t})$ = vector of forces

$\mathbf{M}$ = mass matrix

$\mathbf{K}$ = stiffness matrix

$\mathbf{C}$ = damping matrix

$\mathbf{M}$, $\mathbf{K}$ and $\mathbf{C}$ constitute the **Spatial Model**.

Undamped MDOF Systems

Free Vibration Solution – The Modal Properties

$$\mathbf{M}\,\ddot{\mathbf{x}} + \mathbf{K}\,\mathbf{x} = 0$$

The undamped system's natural frequencies are the solutions of

$$dtm \left| \mathbf{K} - \omega^2\,\mathbf{M} \right| = 0$$

and the corresponding mode shapes are the solutions of

$$\left(\mathbf{K} - \omega_r{}^2\,\mathbf{M}\right)\boldsymbol{\psi}_{(r)} = 0$$

$\Rightarrow$ N eigensolutions

$$\begin{array}{ccccccc} \omega_1 & \le & \omega_2 & \le & \cdots & \le & \omega_N \\ \boldsymbol{\psi}_{(\mathbf{1})} & & \boldsymbol{\psi}_{(\mathbf{2})} & & \cdots & & \boldsymbol{\psi}_{(N)} \end{array}$$

Let us define

$$\boldsymbol{\Psi} = \begin{bmatrix} \boldsymbol{\psi}_{(1)} & \boldsymbol{\psi}_{(2)} & \cdots & \boldsymbol{\psi}_{(N)} \end{bmatrix}$$ Modal matrix

$$\left[\omega_r^2\right] = diag\begin{bmatrix} \omega_1^2 & \omega_2^2 & \cdots & \omega_N^2 \end{bmatrix}$$ Spectral matrix

$\boldsymbol{\Psi}$ and $\left[\omega_r^2\right]$ constitute the **Modal Model**.

Orthogonality properties:

$$\boldsymbol{\Psi}^T \ \mathbf{M} \ \boldsymbol{\Psi} = \left[m_r\right]$$ Modal mass matrix

$$\boldsymbol{\Psi}^T \ \mathbf{K} \ \boldsymbol{\Psi} = \left[k_r\right]$$ Modal stiffness matrix

And thus $\left[\omega_r^2\right] = \left[m_r\right]^{-1} \left[k_r\right]$

Remark :
Mass-normalisation is the most relevant scaling in modal testing, i.e.

$$[m_r] = [\mathbf{1}]$$

in which case, the mass-normalised eigenvectors are written as

$$\mathbf{X} = \begin{bmatrix} \mathbf{x}_{(1)} & \mathbf{x}_{(2)} & \cdots & \mathbf{x}_{(N)} \end{bmatrix}$$ Mass-normalised modal matrix

Orthogonality properties:

$$\mathbf{X}^T \ \mathbf{M} \ \mathbf{X} = [\mathbf{1}]$$
$$\mathbf{X}^T \ \mathbf{K} \ \mathbf{X} = \left[\omega_r^2\right]$$

Forced Response Solution – The FRF Characteristics

$$\mathbf{M}\,\ddot{\mathbf{q}} + \mathbf{K}\,\mathbf{q} = \mathbf{f}(t) = \mathbf{F}\,e^{i\,\omega\,t}$$

Solution of the form: $\mathbf{q} = \mathbf{Q}\,e^{i\,\omega\,t}$

Modal transformation: $\mathbf{Q} = \sum_{k=1}^{N} a_k\;\mathbf{x}_{(k)} = \mathbf{X}\,\mathbf{a}$

The equations of motion then becomes: $\left(\mathbf{K} - \omega^2\;\mathbf{M}\right)\mathbf{X}\,\mathbf{a} = \mathbf{F}$

Premultiply both sides by $\mathbf{X}^T$ to obtain

$$\left(\left[\omega_r^2\right] - \omega^2\,[\mathbf{1}]\right)\,\mathbf{a} = \mathbf{X}^T\;\mathbf{F}$$

which leads to $\mathbf{Q} = \mathbf{X}\left(\left[\omega_r^2\right] - \omega^2\,[\mathbf{1}]\right)^{-1}\,\mathbf{X}^T\;\mathbf{F}$

From the definition of the FRF matrix, it follows that:

$$\mathbf{H}(\omega) = \mathbf{X}\left(\left[\omega_r^2\right] - \omega^2\left[\mathbf{1}\right]\right)^{-1}\mathbf{X}^T$$

$$\mathbf{H} = \begin{bmatrix}\mathbf{x}_{(1)} & \cdots & \mathbf{x}_{(N)}\end{bmatrix}\begin{bmatrix}\ddots & & \\ & \dfrac{1}{\omega_r^2 - \omega^2} & \\ & & \ddots\end{bmatrix}\begin{bmatrix}\mathbf{x}_{(1)}^T \\ \vdots \\ \mathbf{x}_{(N)}^T\end{bmatrix}$$

Hence the spectral representation of the FRF matrix:

$$\boxed{\mathbf{H}(\omega) = \sum_{k=1}^{N}\frac{\mathbf{x}_{(k)}\,\mathbf{x}_{(k)}^T}{\omega_k^2 - \omega^2}}$$

Any individual FRF coefficient linking coordinates r and s (called dynamic influence coefficient) is written:

Modal Constant (or Residue)

$$H_{rs}(\omega) = \sum_{k=1}^{N} \frac{A_{rs(k)}}{\omega_k^2 - \omega^2} \quad \text{with} \quad A_{rs(k)} = \phi_{rk}\,\phi_{sk}$$

Natural Frequency (Pole)

Damped Systems

$$\mathbf{M}\,\ddot{\mathbf{q}} + \mathbf{C}\,\dot{\mathbf{q}} + \mathbf{K}\,\mathbf{q} = \mathbf{f}(t)$$

Modal transformation: $$\mathbf{q}(t) = \sum_{k=1}^{N} \eta_k\, \mathbf{x}_{(k)} = \underbrace{\mathbf{X}}_{\text{Modal matrix}}\, \boldsymbol{\eta}$$

Pre-multiplying the equation of motion by $\mathbf{X}^T$

$$[m_r]\,\ddot{\boldsymbol{\eta}}(t) + \underbrace{\mathbf{X}^T\;\mathbf{C}\;\mathbf{X}}_{\text{Modal damping matrix}}\,\dot{\boldsymbol{\eta}}(t) + [k_r]\,\eta(t) = \mathbf{X}^T\;\mathbf{f}(t)$$

Proportional Damping

In this case, the matrix $\mathbf{X}^T \, \mathbf{C} \, \mathbf{X} = \left[c_k \right]$ is diagonal

where $[c_k]$ = modal damping matrix.

Using the notation introduced above for the SDOF analysis, the damping coefficient of mode k is written in the form:

$$c_k = 2 \, \zeta_k \, \omega_k \, m_k$$

The forced response to an harmonic excitation

$$\mathbf{M} \, \ddot{\mathbf{q}} + \mathbf{C} \, \dot{\mathbf{q}} + \mathbf{K} \, \mathbf{q} = \mathbf{F} \, e^{i \, \omega \, t}$$

is in the form: $\mathbf{q} = \mathbf{Q} \, e^{i \, \omega \, t}$

Modal transformation: $\mathbf{Q} = \sum_{k=1}^{N} a_k \, \mathbf{x}_{(k)} = \mathbf{X} \, \mathbf{a}$

Thus, the equation of motion takes the form:

$$\left(\mathbf{K} - \omega^2\, \mathbf{M} + i\, \omega\, \mathbf{C}\right) \mathbf{X}\, \mathbf{a} = \mathbf{F}$$

Pre-multiplying par $\mathbf{X}^T$, we have:

$$\left(\left[\omega_k^2\right] - \omega^2\, [\mathbf{1}] + i\, \omega \left[2\, \zeta_k\, \omega_k\right]\right) \mathbf{a} = \mathbf{X}^T\, \mathbf{F}$$

$$\mathbf{Q} = \mathbf{X} \left(\left[\omega_k^2\right] - \omega^2\, [\mathbf{1}] + i\, \omega \left[2\, \zeta_k\, \omega_k\right]\right)^{-1} \mathbf{X}^T\, \mathbf{F}$$

We obtain: $\mathbf{H}(\omega) = \mathbf{X} \left(\left[\omega_k^2\right] - \omega^2\, [\mathbf{1}] + i\, \omega \left[2\, \zeta_k\, \omega_k\right]\right)^{-1} \mathbf{X}^T$

and the expression of the FRF matrix is:

$$\boxed{\mathbf{H}(\omega) = \sum_{k=1}^{N} \frac{\mathbf{x}_{(k)}\, \mathbf{x}_{(k)}^T}{\omega_k^2 - \omega^2 + 2\, i\, \zeta_k\, \omega\, \omega_k}}$$

The receptance frequency response function (FRF) at coordinate r , resulting from a single force applied at coordinate s , is :

$$H_{rs}(\omega) = \sum_{k=1}^{N} \frac{A_{rs(k)}}{\omega_k^2 - \omega^2 + 2\, i\, \zeta_k\, \omega\, \omega_k} \quad \text{with} \quad A_{rs(k)} = \mathbf{x}_{r(k)}\, \mathbf{x}_{s(k)}$$

Example:

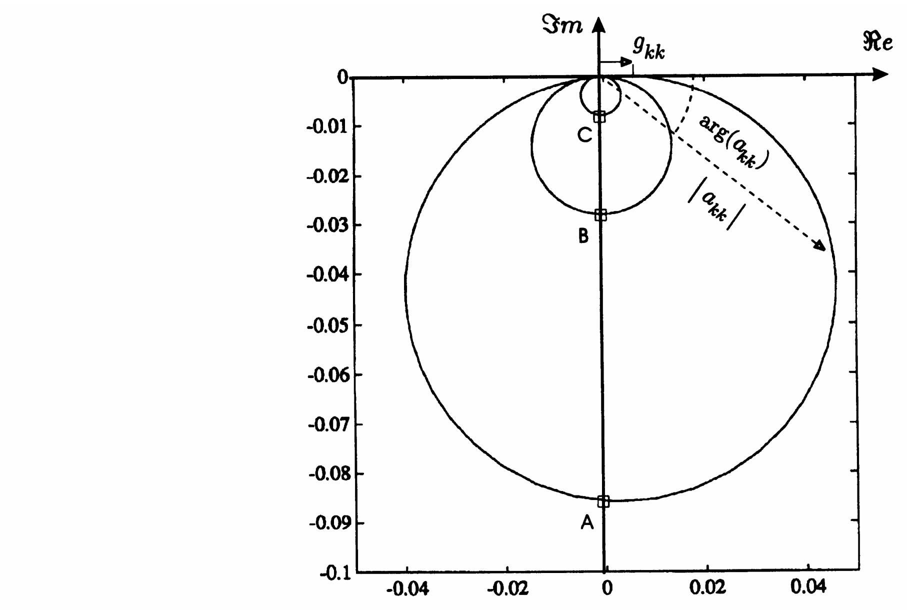

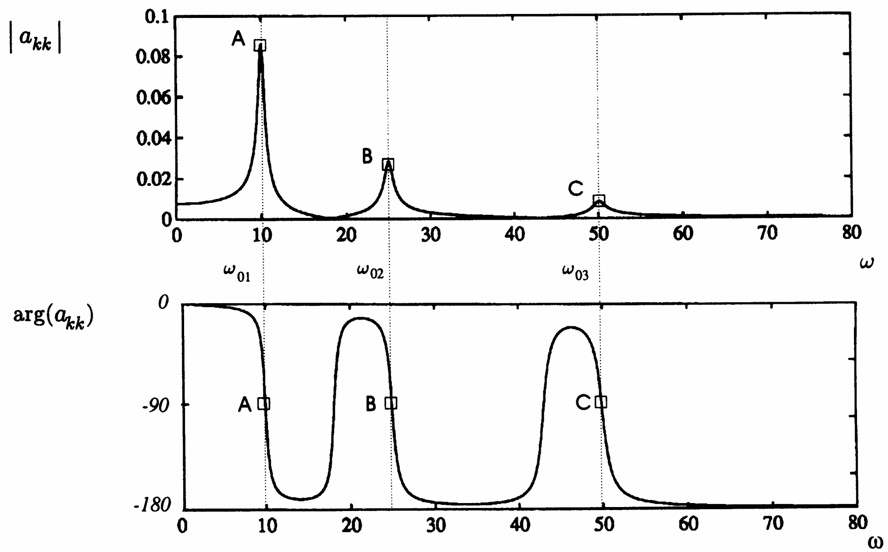

Particular form of proportional damping

$$\mathbf{C} = \beta\,\mathbf{K} + \gamma\,\mathbf{M}$$

In this case, the eigenvalues and eigenmodes take the form:

$$\omega_k^d = \omega_k \sqrt{1-\zeta_k^2}$$

$$\zeta_k = \frac{1}{2}\left(\beta\,\omega_k + \frac{\gamma}{\omega_k}\right)$$

$$\mathbf{X}_{damped} = \mathbf{X}_{undamped}$$

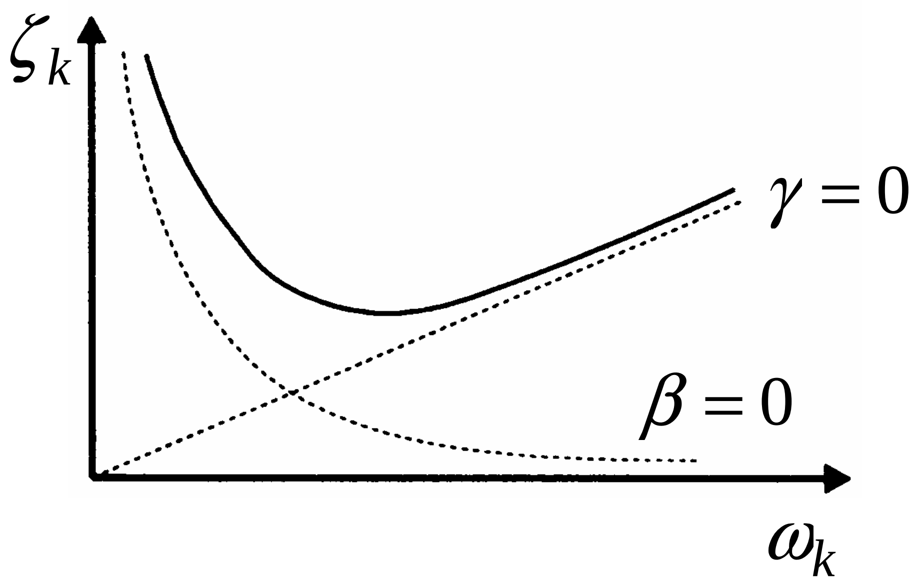

Viscous damping (General case)

In this case, the matrix $\mathbf{X}^T \, \mathbf{C} \, \mathbf{X}$ is not diagonal anymore.

Consider the homogeneous system:

$$\mathbf{M}\,\ddot{\mathbf{q}} + \mathbf{C}\,\dot{\mathbf{q}} + \mathbf{K}\,\mathbf{q} = \mathbf{0}$$

It can be shown that the eigensolutions of the appropriate equation

$$\left(\lambda^2\,\mathbf{M} + \lambda\,\mathbf{C} + \mathbf{K}\right)\mathbf{Q} = 0$$

occur as complex conjugates.

$$\left.\begin{array}{l} \lambda_k,\ \lambda_k^* \\ \\ \boldsymbol{\Psi}_{(k)},\ \boldsymbol{\Psi}_{(k)}^* \end{array}\right\} \quad k = 1, \cdots, N$$

with: $\lambda_k = \omega_k \left(-\zeta_k + i\sqrt{1-\zeta_k^2} \right)$

This approach is not particularly convenient for numerical application.

In the general case of viscous damping, it is better to recast the equations into the state-space form:

$$\begin{cases} \mathbf{M}\,\ddot{\mathbf{q}} + \mathbf{C}\,\dot{\mathbf{q}} + \mathbf{K}\,\mathbf{q} = \mathbf{F}\,e^{i\,\omega\,t} \\ \mathbf{M}\,\dot{\mathbf{q}} - \mathbf{M}\,\dot{\mathbf{q}} = \mathbf{0} \end{cases}$$

or

$$\begin{bmatrix} \mathbf{C} & \mathbf{M} \\ \mathbf{M} & \mathbf{0} \end{bmatrix} \begin{Bmatrix} \dot{\mathbf{q}} \\ \ddot{\mathbf{q}} \end{Bmatrix} + \begin{bmatrix} \mathbf{K} & \mathbf{0} \\ \mathbf{0} & -\mathbf{M} \end{bmatrix} \begin{Bmatrix} \mathbf{q} \\ \dot{\mathbf{q}} \end{Bmatrix} = \begin{Bmatrix} \mathbf{F} \\ \mathbf{0} \end{Bmatrix} e^{i\,\omega\,t}$$

$$\mathbf{A}\,\dot{\mathbf{u}} + \mathbf{B}\,\mathbf{u} = \mathbf{P}\,e^{i\,\omega\,t}$$

$\mathbf{A}$ and $\mathbf{B}$ are real and symmetric matrices of dimension $2N$ x $2N$.

Homogeneous equation: $\mathbf{A}\,\dot{\mathbf{u}} + \mathbf{B}\,\mathbf{u} = \mathbf{0}$

Solution of the form: $\mathbf{u} = \mathbf{U}\, e^{\lambda\, t}$

Eigenvalue problem: $\left(\lambda\, \mathbf{A} + \mathbf{B}\right)\mathbf{z} = \mathbf{0}$

$\Rightarrow$ $2N$ eigenvalues λ_k and eigenvectors $\mathbf{z}_{(k)}$ verifying the orthogonality properties:

$$\mathbf{Z}^T\ \mathbf{A}\,\mathbf{Z} = \left[a_k\right]$$

$$\mathbf{Z}^T\ \mathrm{B}\,\mathbf{Z} = \left[b_k\right]$$

and which have the usual characteristic that

$$\lambda_k = -\frac{b_k}{a_k} \quad ; \quad (k = 1, \cdots, 2N)$$

Forced response to harmonic excitation

$$\mathbf{A}\,\dot{\mathbf{u}} + \mathbf{B}\,\mathbf{u} = \mathbf{P}\,e^{i\,\omega\,t}$$

Development in the series of eigenmodes:

$$\mathbf{u} = \sum_{k=1}^{2N} \eta_k\; e^{i\,\omega\,t}\mathbf{z}_{(k)}$$

Substituting into the state-space equation and pre-multiplying by $\mathbf{z}_{(k)}^T$ we have:

$$i\,\omega\,a_k\;\eta_k + b_k\;\eta_k = \mathbf{z}_{(k)}^T\;\mathbf{P} \qquad (k = 1,\cdots,2N)$$

$$\Longrightarrow \qquad \eta_k = \frac{\mathbf{z}_{(k)}^T\;\mathbf{P}}{a_k\;(i\omega - \lambda_k)} \qquad (k = 1,\cdots,2N)$$

Thus, the solution may be written as:

$$\mathbf{u} = \sum_{k=1}^{2N} \frac{\mathbf{z}_{(k)}\;\mathbf{z}_{(k)}^T\;\mathbf{P}}{a_k\;(i\,\omega - \lambda_k)}\,e^{i\,\omega\,t}$$

However, because the eigensolutions occur in complex conjugate pairs, the solution may be rewritten as:

$$\begin{Bmatrix} \mathbf{Q} \\ \cdots \\ i\,\omega\,\mathbf{Q} \end{Bmatrix} = \sum_{k=1}^{N} \left(\frac{\mathbf{z}_{(k)}\,\mathbf{z}_{(k)}^{T}}{a_k\,(i\,\omega - \lambda_k)} + \frac{\overline{\mathbf{z}}_{(k)}\,\overline{\mathbf{z}}_{(k)}^{T}}{\overline{a}_k\,(i\,\omega - \overline{\lambda}_k)} \right) \mathbf{P}$$

If we extract the response vector $\mathbf{Q}$, we obtain the expression of the FRF matrix in the form:

$$\boxed{\mathbf{H} = \sum_{k=1}^{N} \frac{\mathbf{z}_{(k)}\,\mathbf{z}_{(k)}^{T}}{a_k\,(i\,\omega - \lambda_k)} + \frac{\overline{\mathbf{z}}_{(k)}\,\overline{\mathbf{z}}_{(k)}^{T}}{\overline{a}_k\,(i\,\omega - \overline{\lambda}_k)}}$$

$$\boxed{\mathbf{H} = \sum_{k=1}^{N} \frac{\mathbf{z}_{(k)}\,\mathbf{z}_{(k)}^{T}}{a_k\,(i\,\omega - \lambda_k)} + \frac{\overline{\mathbf{z}}_{(k)}\,\overline{\mathbf{z}}_{(k)}^{T}}{\overline{a}_k\,(i\,\omega - \overline{\lambda}_k)}}$$

A single response parameter takes the form:

Modal constants (Residues)

$$H_{rs}(\omega) = \sum_{k=1}^{N} \frac{\overbrace{\mathbf{z}_{r(k)}\,\mathbf{z}_{s(k)}}}{a_k\,(i\,\omega - \lambda_k)} + \frac{\overbrace{\overline{\mathbf{z}}_{r(k)}\,\overline{\mathbf{z}}_{s(k)}}}{\overline{a}_k\,(i\,\omega - \overline{\lambda}_k)}$$

Poles (complex)

Complex Modes

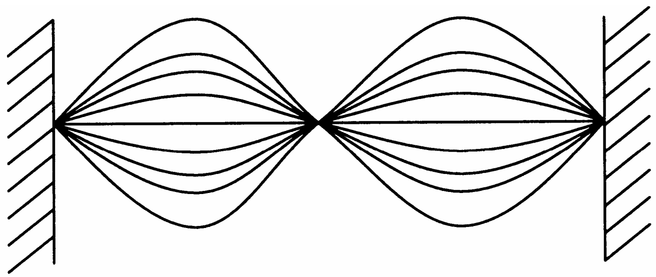

Real mode: in-phase vibration, (standing wave)

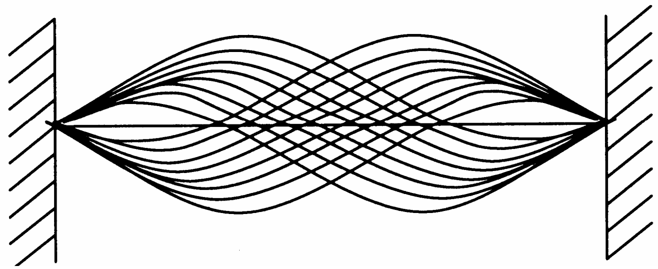

Complex mode: out-of-phase vibration (travelling wave)

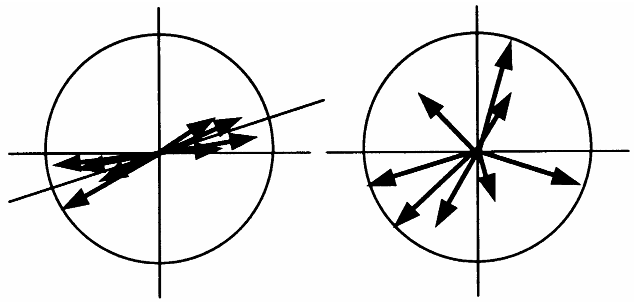

Measurement of modal complexity (complex mode shapes plotted on Argand diagrams)

Example:

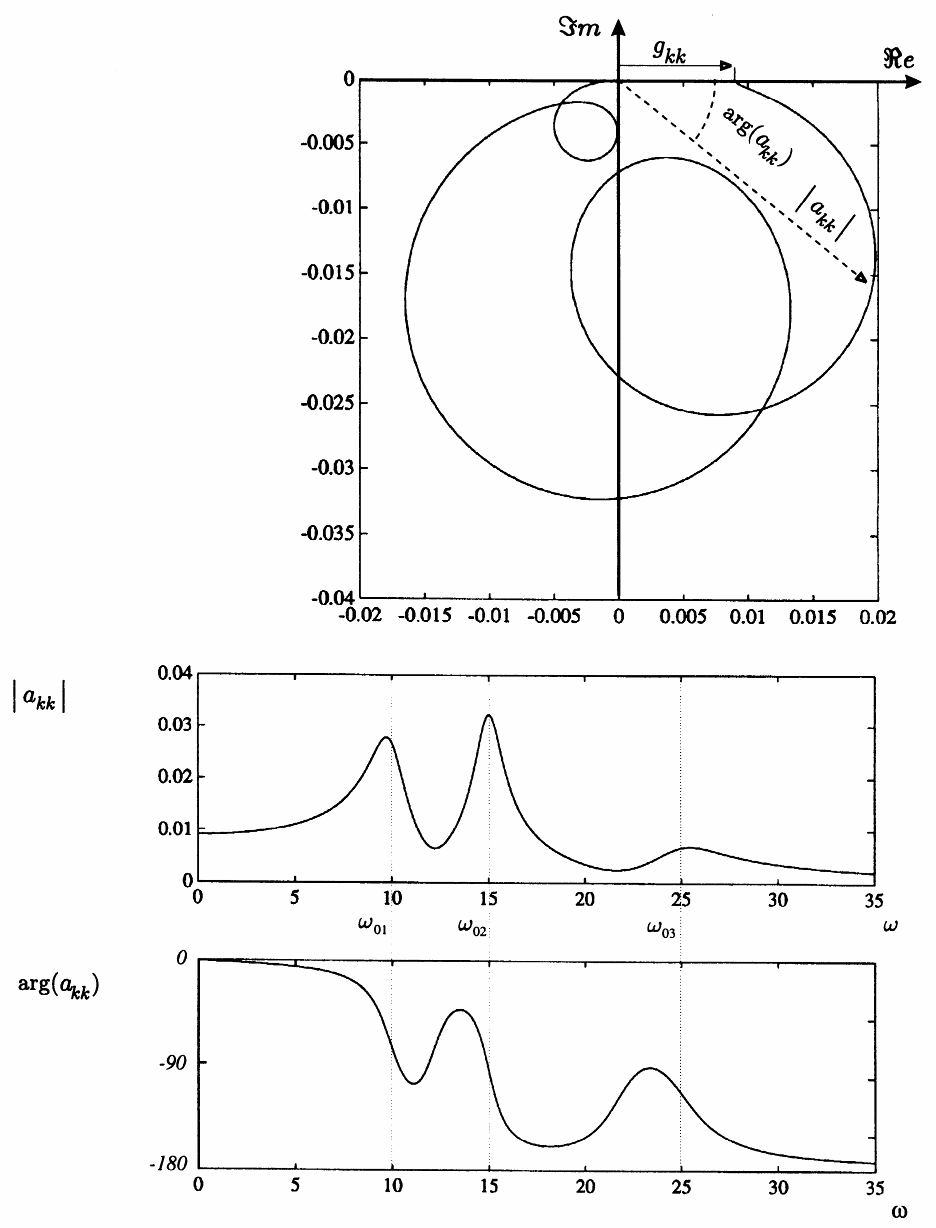
$\Im m$
g_{kk}
$\Re e$
$\arg(a_{kk})$
$|a_{kk}|$
0
-0.005
-0.01
-0.015
-0.02
-0.025
-0.03
-0.035
-0.04
-0.02 -0.015 -0.01 -0.005 0 0.005 0.01 0.015 0.02
$|a_{kk}|$
0.04
0.03
0.02
0.01
0
0 5 10 15 20 25 30 35
ω_{01} ω_{02} ω_{03} ω
$\arg(a_{kk})$
0
-90
-180
0 5 10 15 20 25 30 35
ω

Summary

The fundamental relations used for experimental modal analysis are:

a) Undamped systems

$$H_{rs}(\omega) = \sum_{k=1}^{N} \frac{A_{rs(k)}}{\omega_k^2 - \omega^2} \quad \text{with} \quad A_{rs(k)} = \mathbf{x}_{r(k)}\,\mathbf{x}_{s(k)}$$

b) Damped systems (proportional damping)

$$H_{rs}(\omega) = \sum_{k=1}^{N} \frac{A_{rs(k)}}{\omega_k^2 - \omega^2 + 2\, i\, \zeta_k\, \omega\, \omega_k} \quad \text{with} \quad A_{rs(k)} = \mathbf{x}_{r(k)}\,\mathbf{x}_{s(k)}$$

c) Damped systems (general case of viscous damping)

$$H_{rs}(\omega) = \sum_{k=1}^{N} \frac{\mathbf{z}_{r(k)}\,\mathbf{z}_{s(k)}}{a_k\,(i\,\omega - \lambda_k)} + \frac{\overline{\mathbf{z}}_{r(k)}\,\overline{\mathbf{z}}_{s(k)}}{\overline{a}_k\,(i\,\omega - \overline{\lambda}_k)}$$

Test Planning

- Definition of the objectives
  - estimation of vibration amplitude levels
  - estimation of natural frequencies, mode shapes and damping factors
  - model validation
- Selection of the frequency range
- Selection of measurement and excitation coordinates
- Selection of excitation devices and transducers
- Selection of the support points (to minimise external influence)
- Checking the quality of measured data
- Measured data consistency, including reciprocity
- Measurement repeatability
- Measurement reliability

General Layout of FRF Measurement System

Excitation mechanism

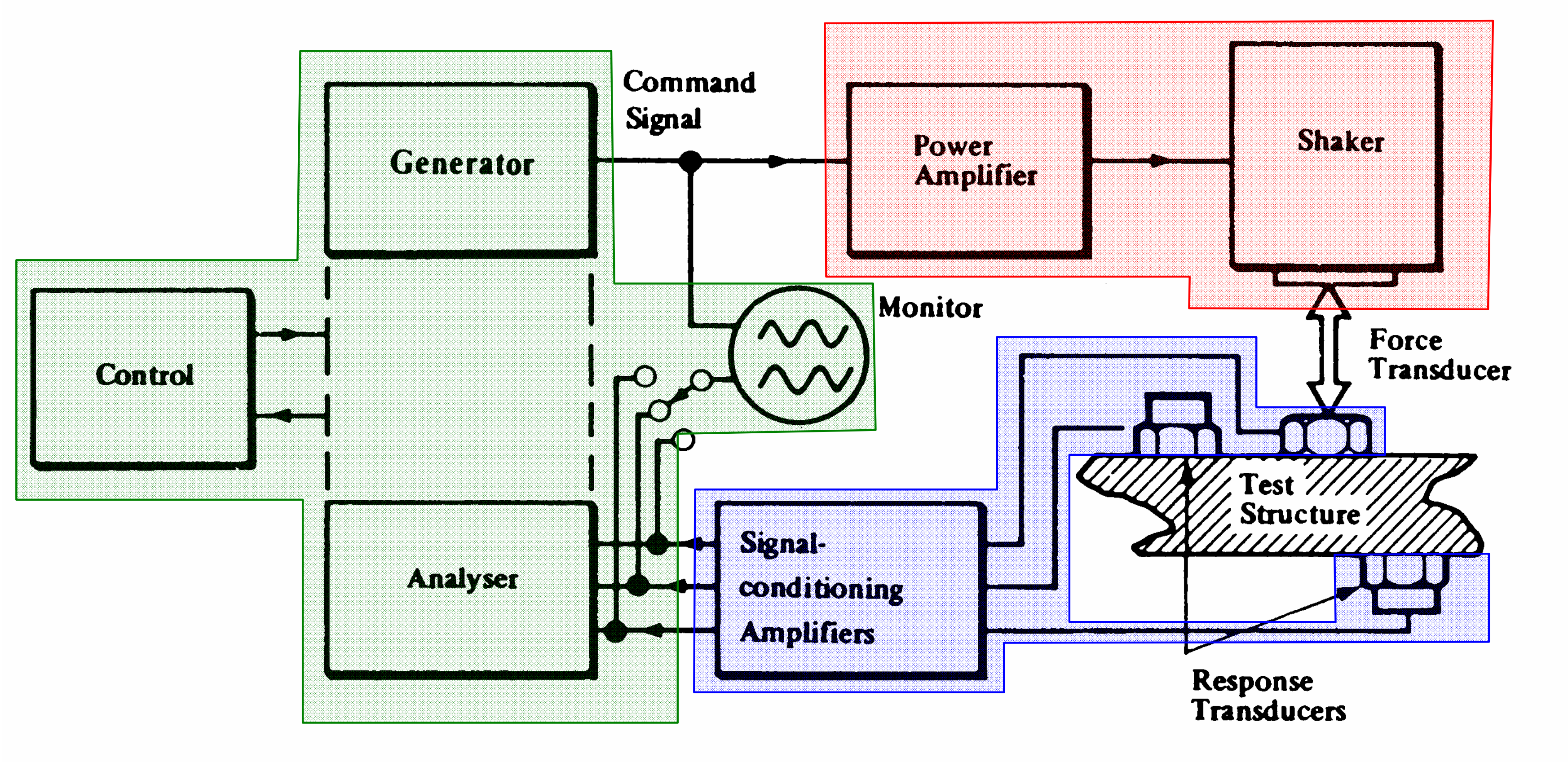

Analyser

Transduction system

Excitation of the Structure

- **Mechanical Exciters**

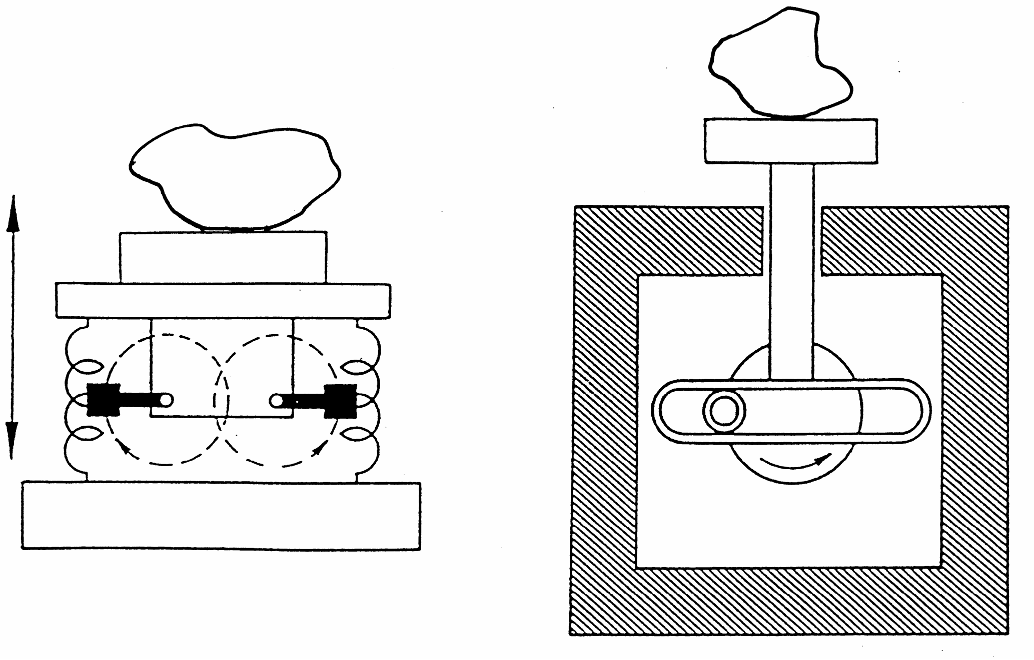

- little flexibility or control

- **Electrohydraulic Exciters**

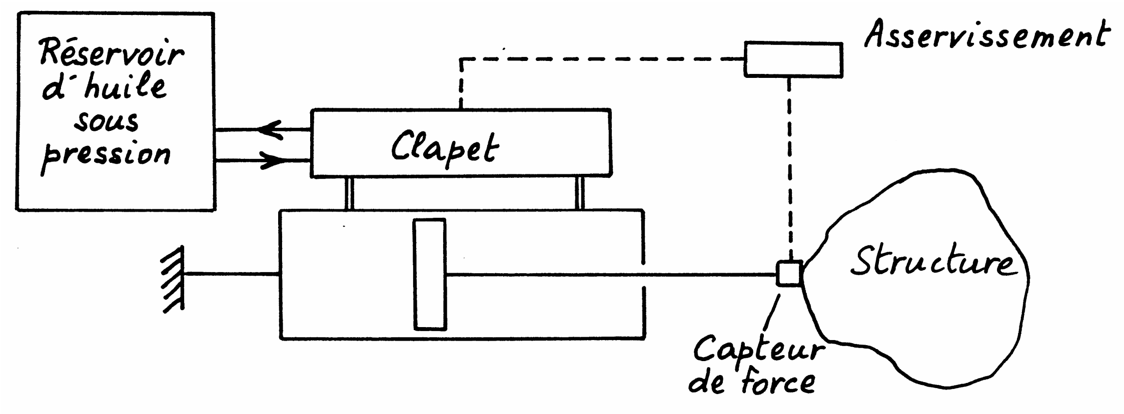

- substantial forces are generated
- possibility to apply simultaneously a static load to the dynamic vibratory load
- large displacement amplitudes
- limited frequency range
- hydraulic shakers are complex and expansive

• Electrodynamic Exciters

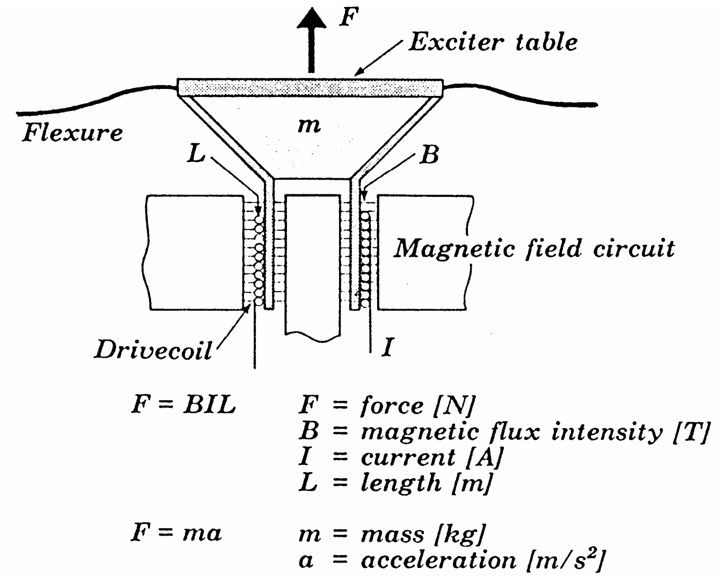

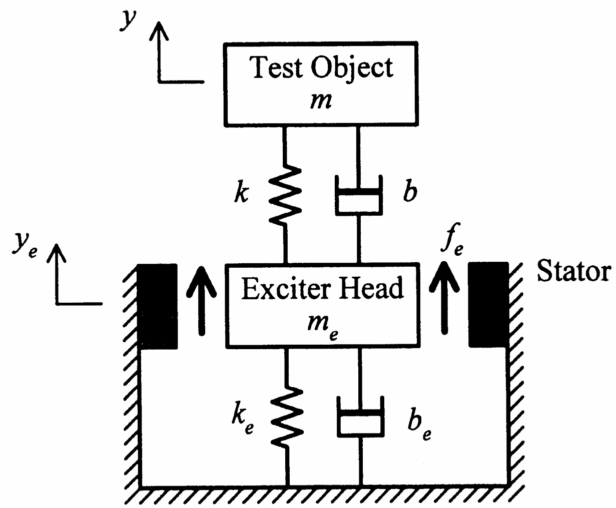

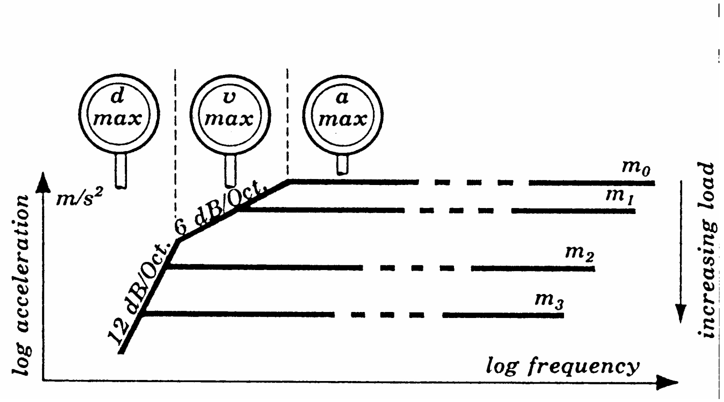

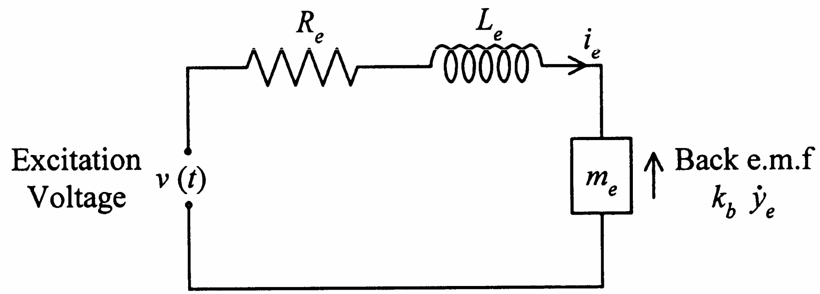

Characteristics of a shaker

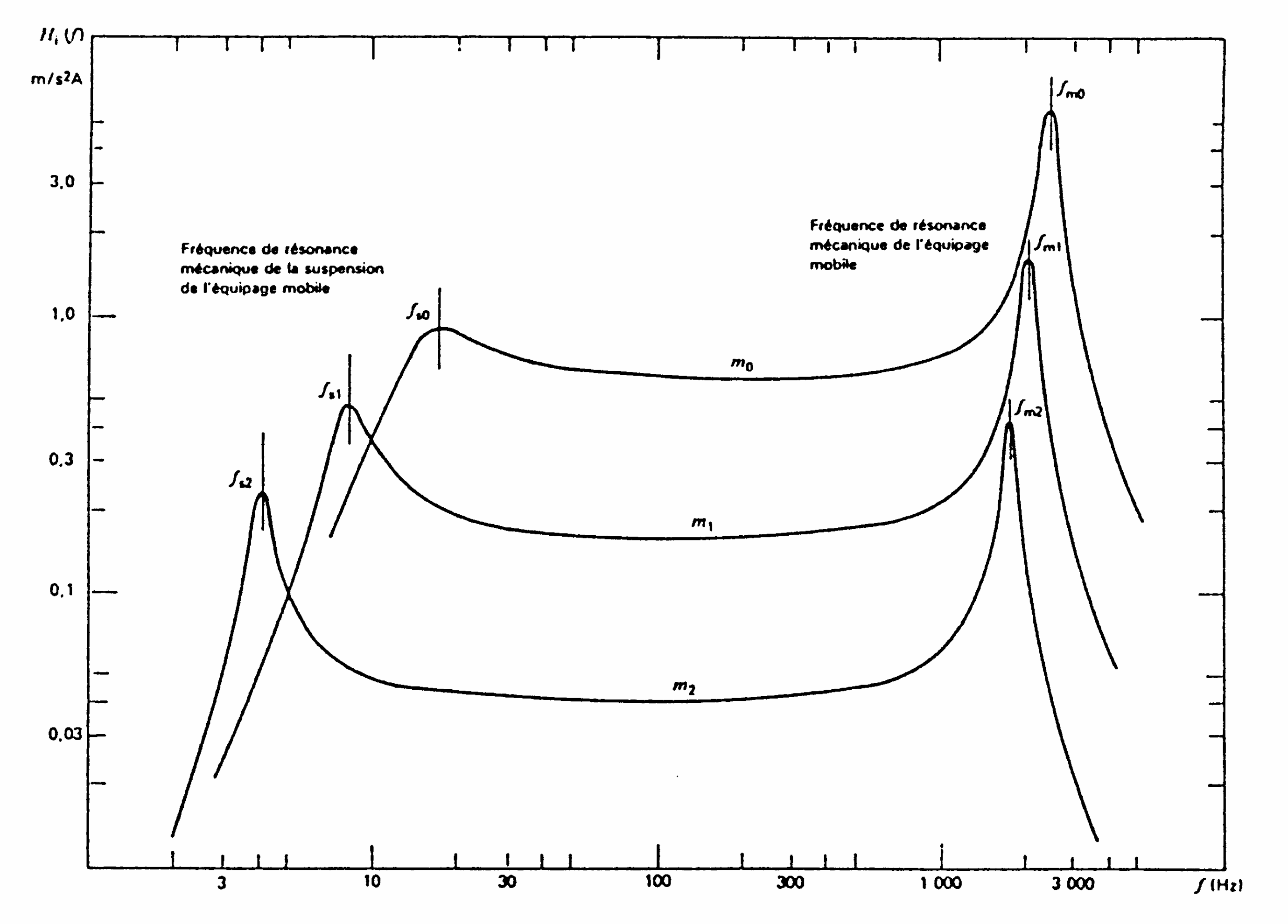

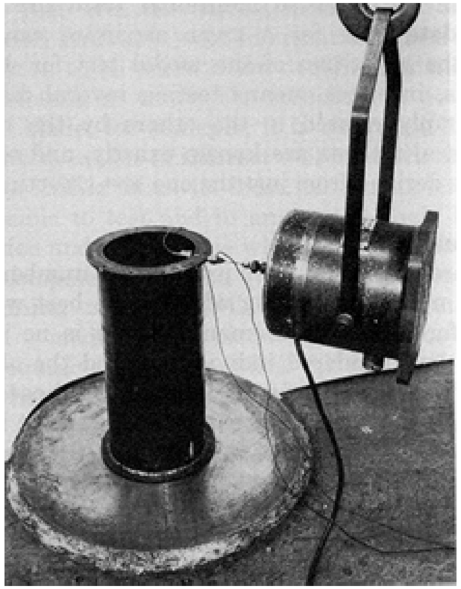

Example of grounded structure

Examples of freely-supported structure

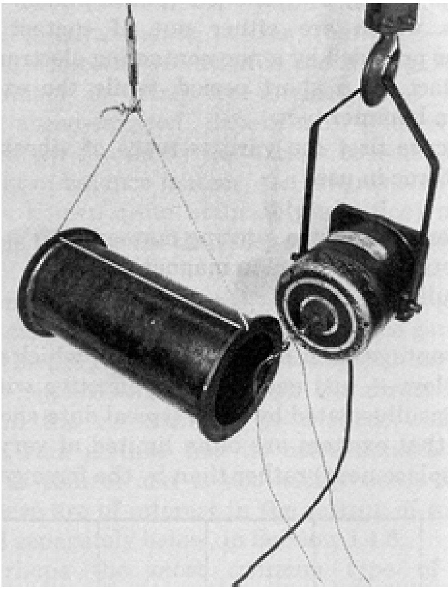

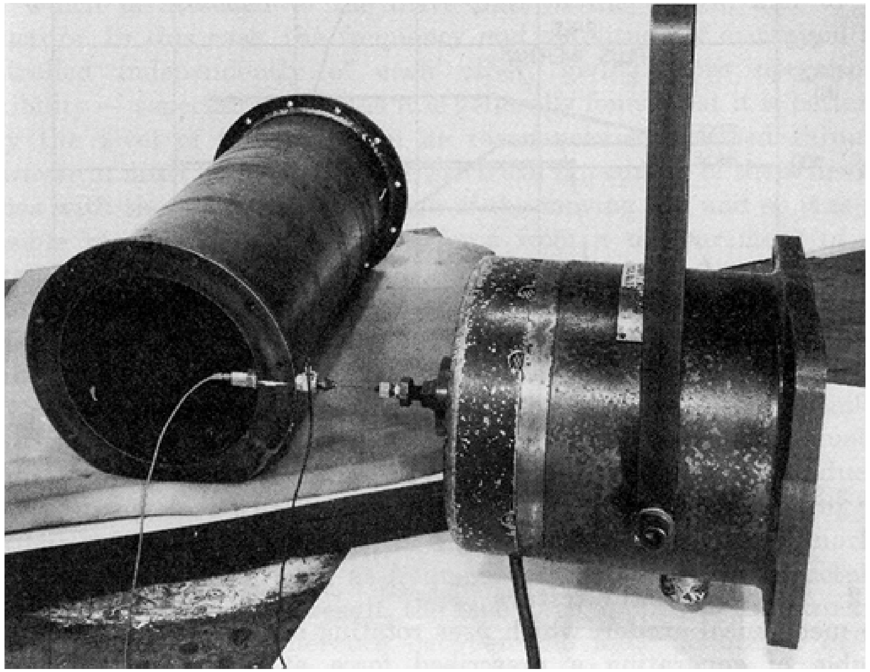

Exciter attachment

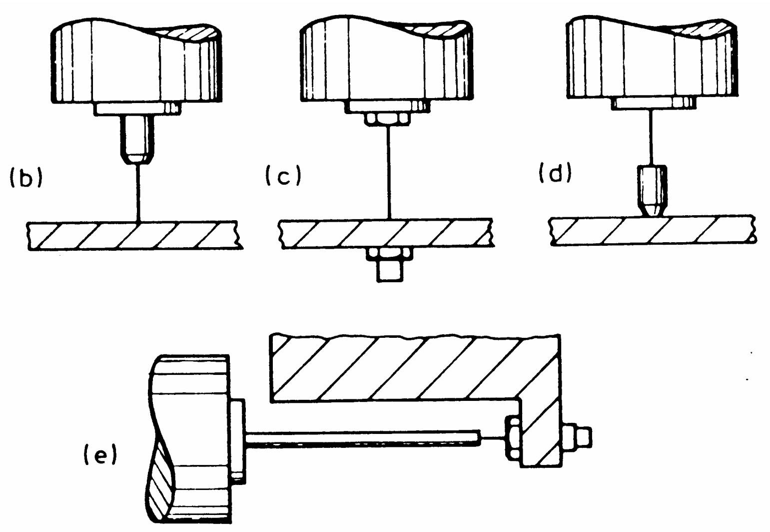

(b) Unsatisfactory assembly

(c) et (d) Acceptable assembly

(e) Use of a push rod or stinger

Various mounting arrangements for exciter

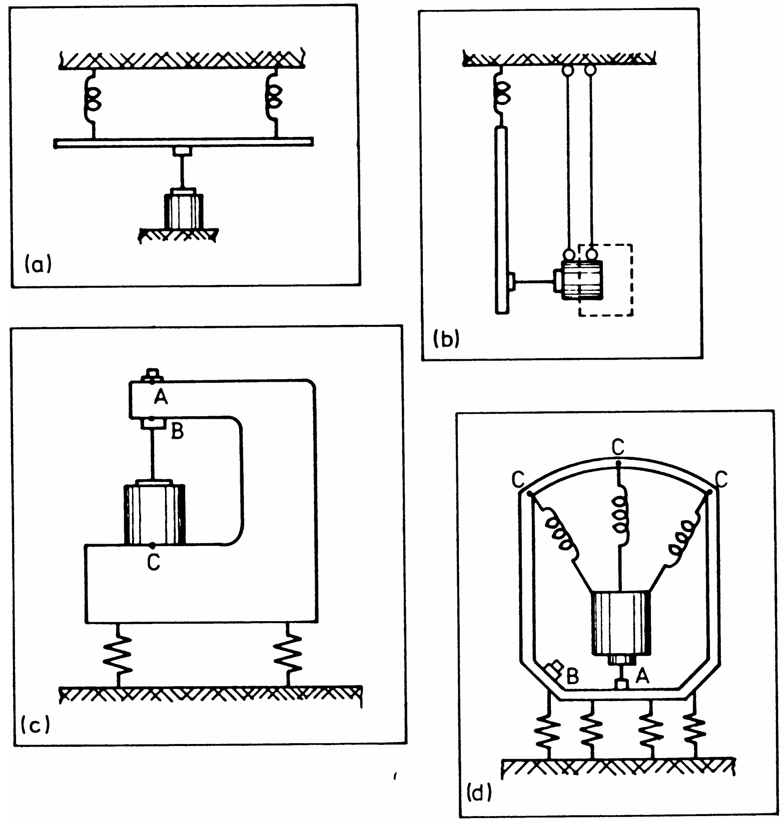

(a) Ideal configuration

(b) Suspended shaker plus inertia mass

(c) et (d) Compromise configurations

Example of electrodynamic shaker used for environmental testing (qualification, fatigue)

Gearing & Watson V2664

Max. force = 26.6 kN (sinus et random) ;

Max. displ. = 50 mm (peak-peak) ;

Max. velocity = 1.52 m/s.

- **Piezoelectric exciters**
  - Operational at high frequency range
  - Low excitation amplitude

- **Non-Contact Magnetic Excitation**
  - Electromagnetic force
  - Measurement of the reaction force on the body of the magnet (not directly the force applied to the structure)
  - Application to rotating machinery

- **Hammer Excitation**

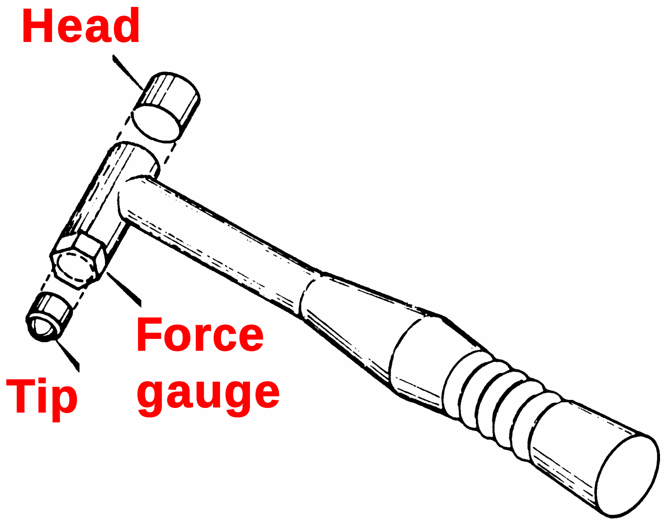

Typical impact force pulse and spectrum

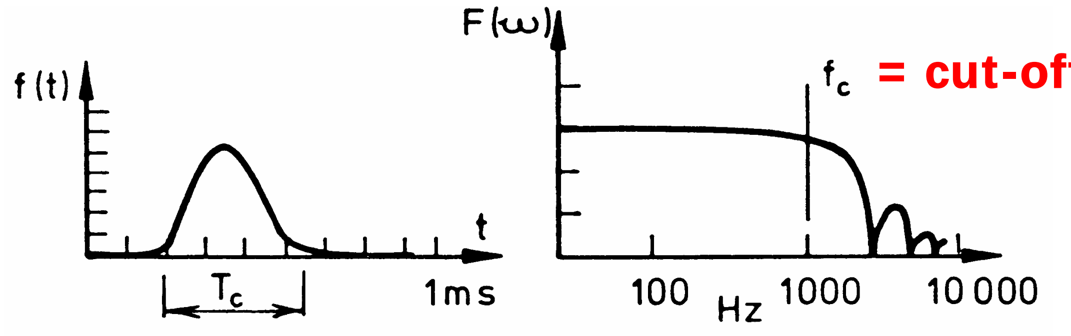

= cut-off frequency

Duration of the pulse

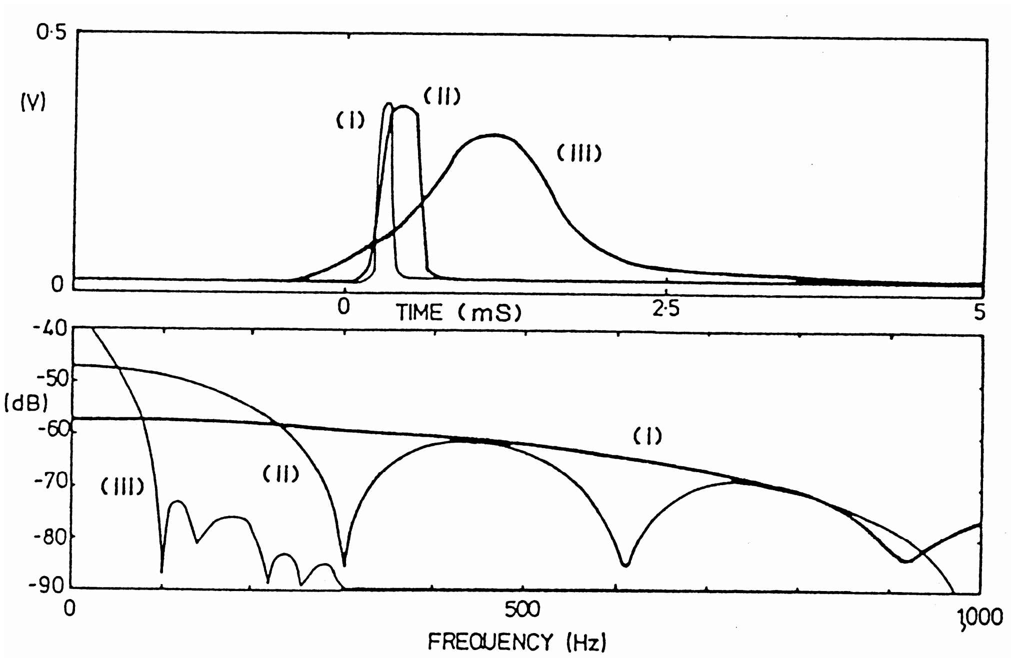

(I) Stiff tip (steel)

(II) Medium tip (vinyl)

(III) Soft tip (rubber)

Use of different excitation devices

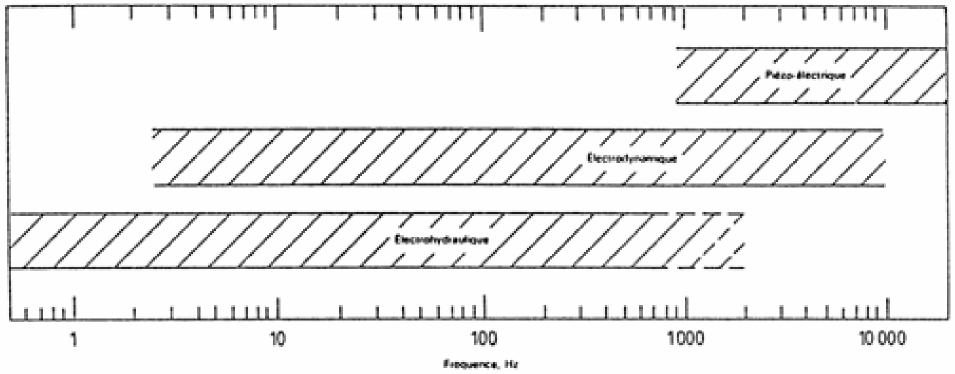

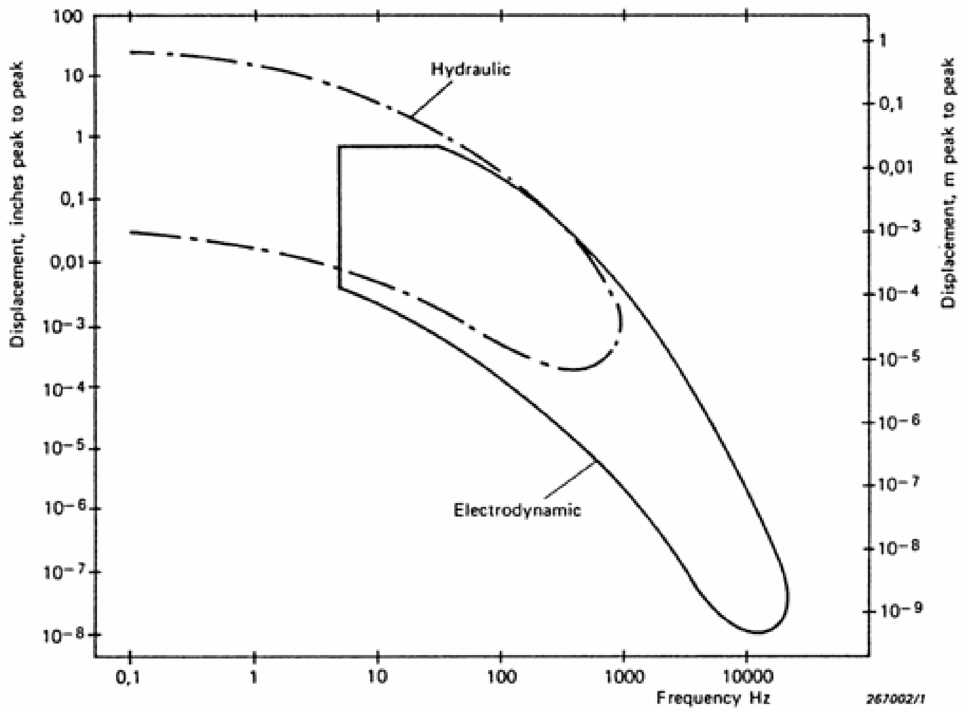

Transducers

Consider a sinusoidal signal

Signal		Response parameter	
$f = F \sin \omega t$	$\Rightarrow$	Force	F
$x = X \sin \omega t$	$\Rightarrow$	Displacement	X
$\dot{x} = \omega X \sin \omega t$	$\Rightarrow$	Velocity	ωX
$\ddot{x} = -\omega^2 X \sin \omega t$	$\Rightarrow$	Acceleration	$\omega^2 X$

Example:

frequency	displacement	acceleration	
0,5 Hz	1 μm	$10^{-5}\ m/s^2$	→ Not detectable
15800 Hz	1 μm	$10^{4}\ m/s^2$	

Choice of the physical quantity to be measured

- Displacement : measurement of gaps, orbits of rotor inside journals, thermal dilatations, …
- Velocity : used in standards to characterise vibration intensity
- Acceleration : measurement of high frequency signals (shocks)

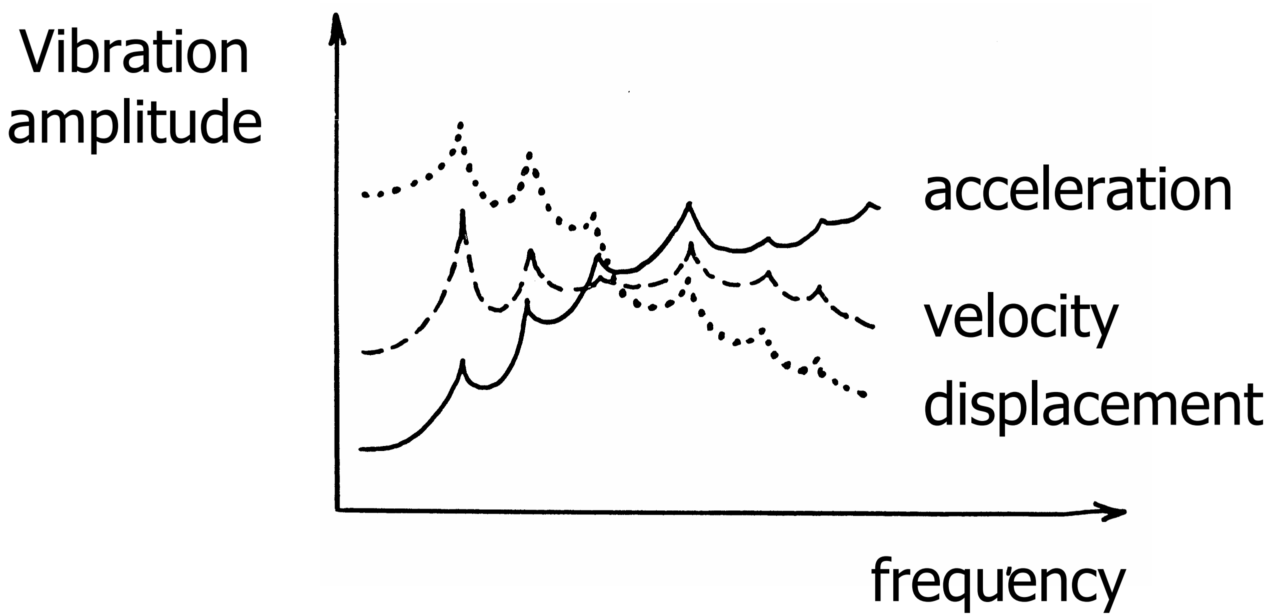

Vibration Transducers

Definition

Physical quantity

(force, displacement, velocity, acceleration)

absolute or relative

↓

TRANSDUCER

(sensitivity)

↓

Electrical quantity

(voltage, current, charge)

Specifications

- Measurement Range (e.g. 0 to 10 g,
  -1 mm to +1mm)
- Frequency Range (e.g. 1hz to 1,5 kHz)
- Sensitivity (e.g. 10 pC/g, 300 mV/(cm/s))
- Transverse Sensitivity
- Environmental:
  - Magnetic Sensitivity (e.g. 0,1 g/tesla)
  - Acoustic Sensitivity (e.g. 0,01 pC/db)
  - Temperature Transient Sensitivity
- Physical
  - Weight, Dimensions
- Mounting Techniques

Vibration Transducer Basics

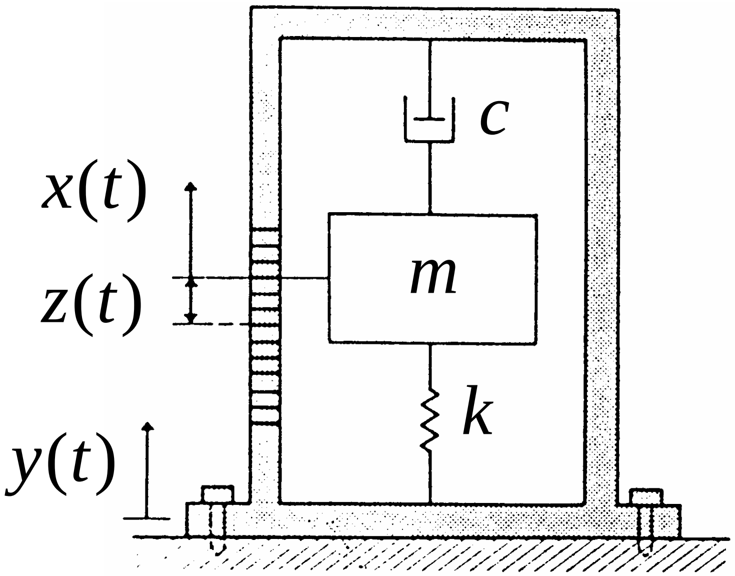

Governing equation of motion

$$m\,\ddot{x} + c\,(\dot{x} - \dot{y}) + k\,(x - y) = f\,(t)$$

In terms of relative displacement

$$m\,\ddot{z} + c\,\dot{z} + k\,z = f\,(t) - m\,\ddot{y} = R(t)$$

The forced response to harmonic excitation $y(t) = Y\,e^{i\,\omega\,t}$ applied to the body (with $f(t)=0$) is written in the form

$$z(t) = \frac{m\,\omega^2\,Y\,e^{i\,\omega\,t}}{k - \omega^2\,m + i\,\omega\,c} = Z\,e^{i\,\omega\,t}$$

amplitude

$$\left|\frac{Z}{Y}\right| = \frac{(\omega/\omega_0)^2}{\sqrt{\left(1 - \omega^2/\omega_0^2\right)^2 + (2\,\zeta\,\omega/\omega_0)^2}}$$

phase

$$\tan\phi = \frac{2\,\zeta\,\omega/\omega_0}{1 - \omega^2/\omega_0^2}$$

Displacement transducer

(sismographs)

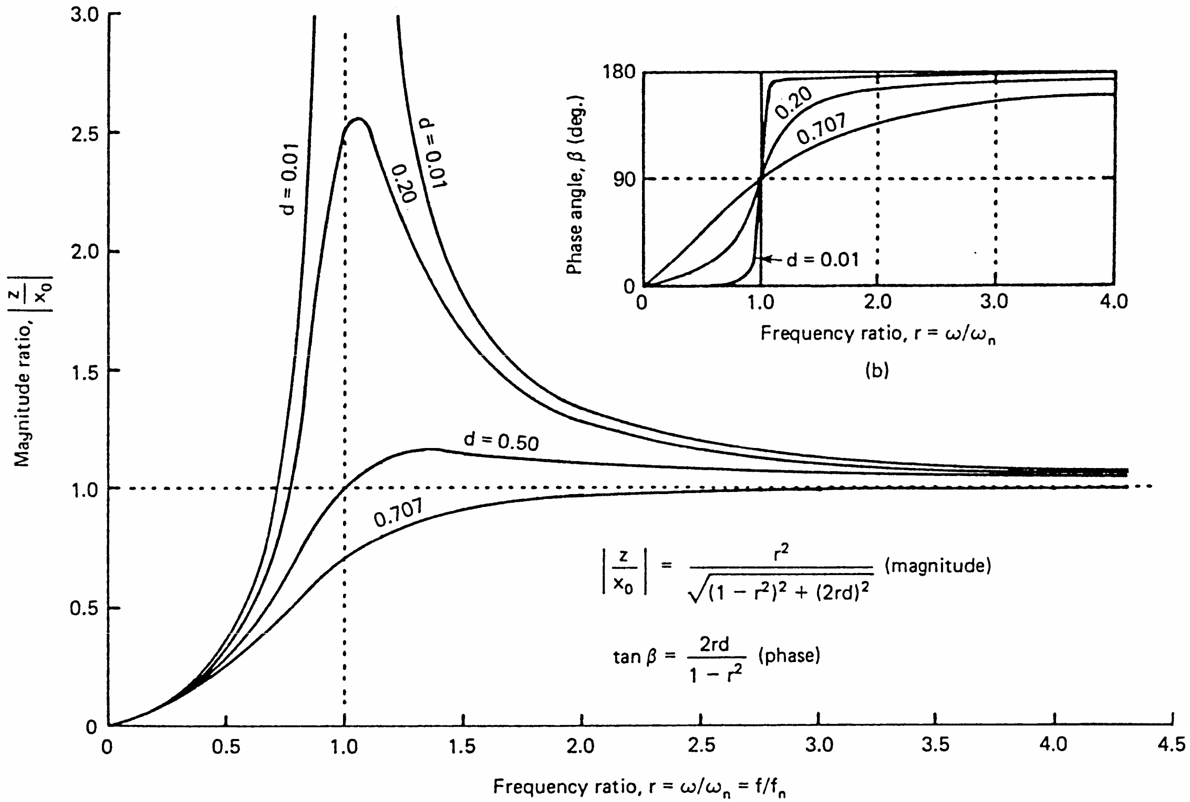

For $\dfrac{\omega}{\omega_0} > 4,$ we have $\left\{ \begin{array}{l} \left|\dfrac{Z}{Y}\right| \to 1 \quad \forall\, \zeta \\ \phi \to 180^\circ \end{array} \right\rangle \quad \Rightarrow \quad z = -y$

When $\zeta = 0{,}707$, the amplitude peak disappears

Design requirement: $\omega_0 <<<$

k low

m high

$\Rightarrow$ Transducer is relatively large and heavy

Example: LVDT (Linear Variable Differential Transformer)

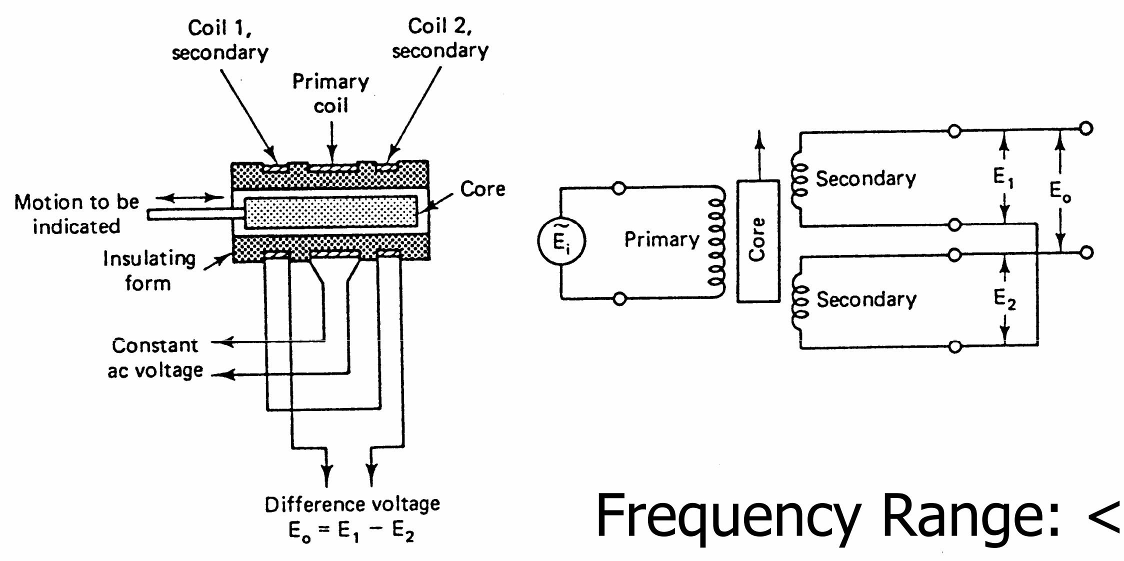

Frequency Range: < 500 Hz

Velocity Transducer (same working principles as for the displacement transducer)

Practical example

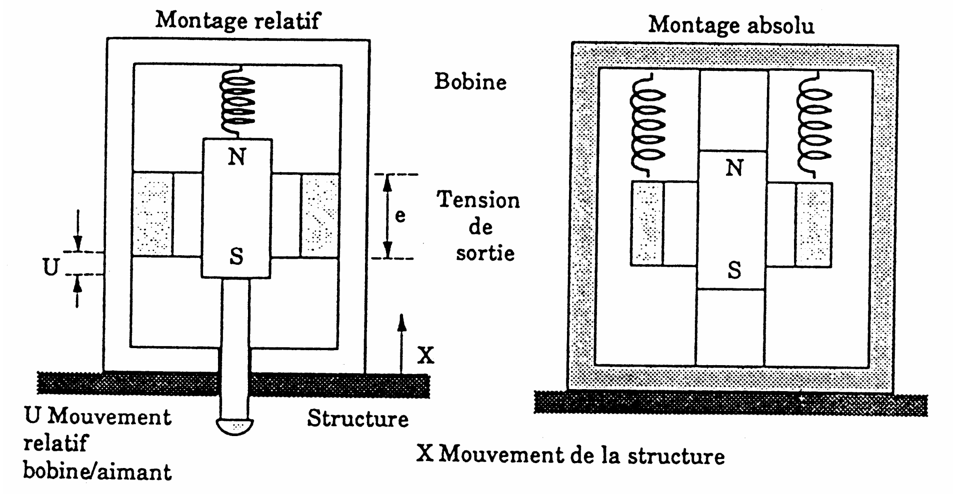

Voltage

Magnetic flux

$$e = -\frac{\partial \phi}{\partial t} = \lambda \frac{\partial U}{\partial t}$$

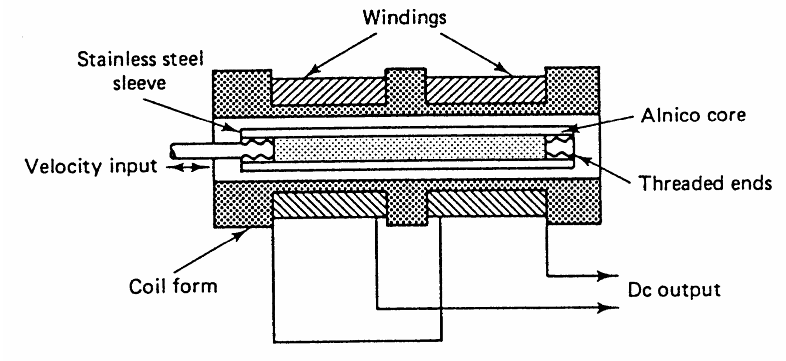

Advantages:

- reliability, robustness (no power supply needed)
- high sensitivity (e.g. 300 mV/(cm/s))
- low impedance (no conditioning amplifier needed)

Drawbacks: - heavy and large, frequency range < 2000 Hz

Accelerometers

System response: $$z(t) = \frac{m\,\omega^2\,Y\,e^{i\,\omega\,t}}{k - \omega^2\,m + i\,\omega\,c} = Z\,e^{i\,\omega\,t}$$

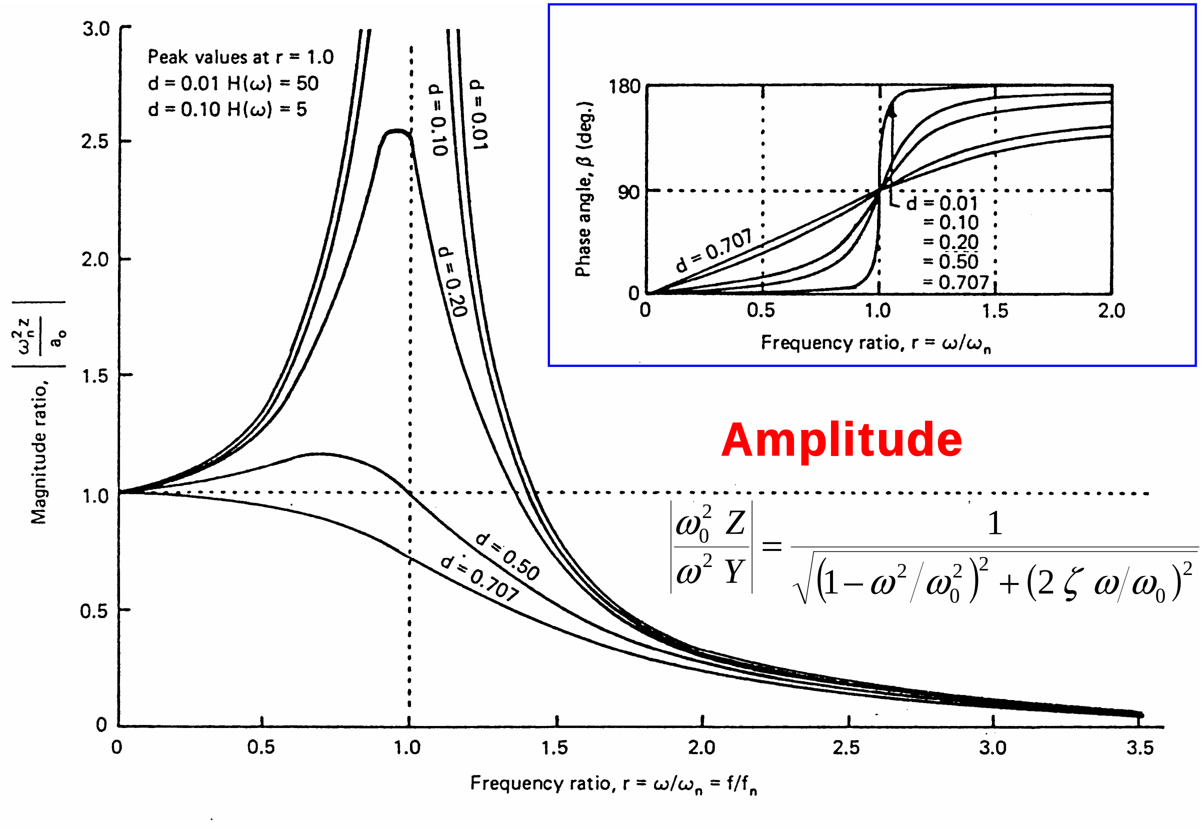

Phase

$$\tan\phi = \frac{2\,\zeta\,\omega/\omega_0}{1-\omega^2/\omega_0^2}$$

Amplitude

$$\left|\frac{\omega_0^2\,Z}{\omega^2\,Y}\right| = \frac{1}{\sqrt{\left(1-\omega^2/\omega_0^2\right)^2 + \left(2\,\zeta\,\omega/\omega_0\right)^2}}$$

Amplitude: $$\left|\frac{\omega_0^2\ Z}{\omega^2\ Y}\right| = \frac{1}{\sqrt{\left(1-\omega^2/\omega_0^2\right)^2 + \left(2\ \zeta\ \omega/\omega_0\right)^2}}$$

Measurement of the acceleration of the support

As $\dfrac{\omega}{\omega_0} \to 0$, we get $Z \to -\dfrac{\omega^2\ Y}{\omega_0^2} = \underbrace{\dfrac{m}{k}}_{\text{Accelerometer sensitivity}} \Big(\underbrace{-\,\omega^2\ Y}_{\text{Acceleration of the support}}\Big)$

Design requirement: $\omega_0 >>>$

k high

m small

$\Rightarrow$ Transducer is small and light

Sensitivity ÷ seismic mass

Optimise the choice for any given application

Typical examples of piezoelectric accelerometers

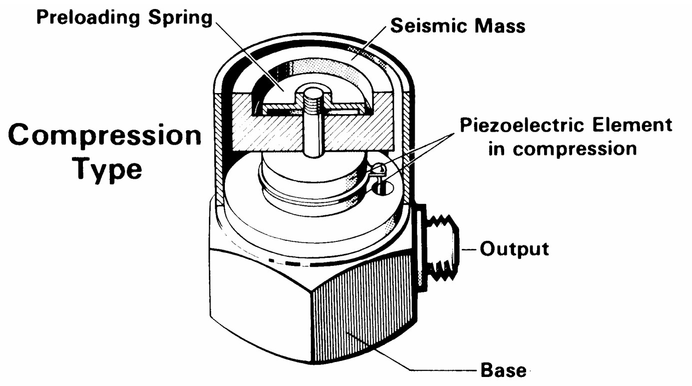

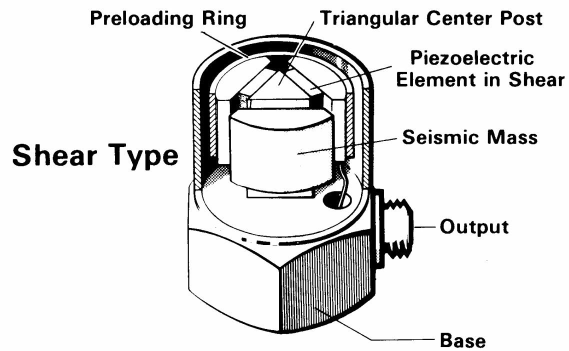

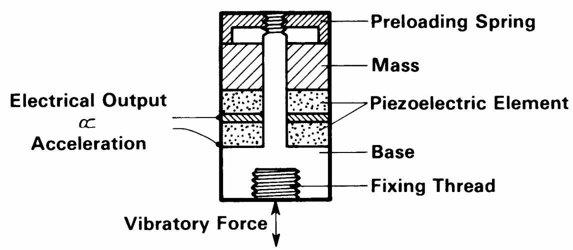

$$Q = \lambda_1 \ \ddot{y}$$

Sensitivity in pC/g

Advantages:

- high frequency range
- excellent linearity
- low sensitivity to environmental noises
- small size, lightness

Drawbacks:

- very high impedance

  → charge amplifier

Selection of accelerometers

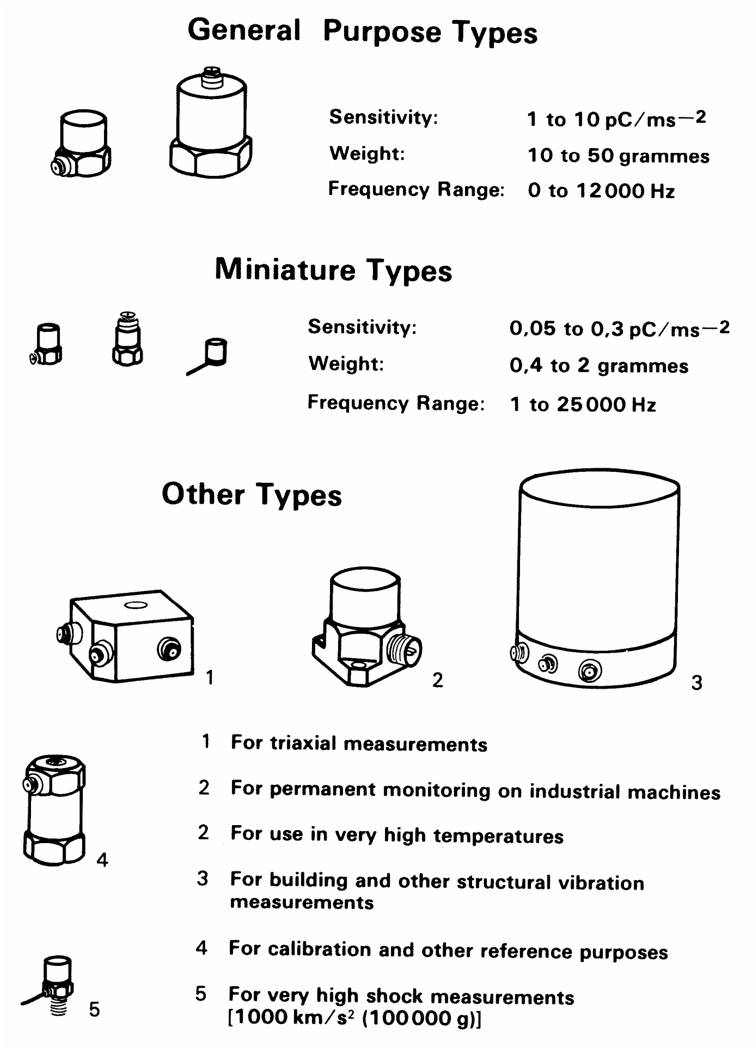

Attachment and location of accelerometers

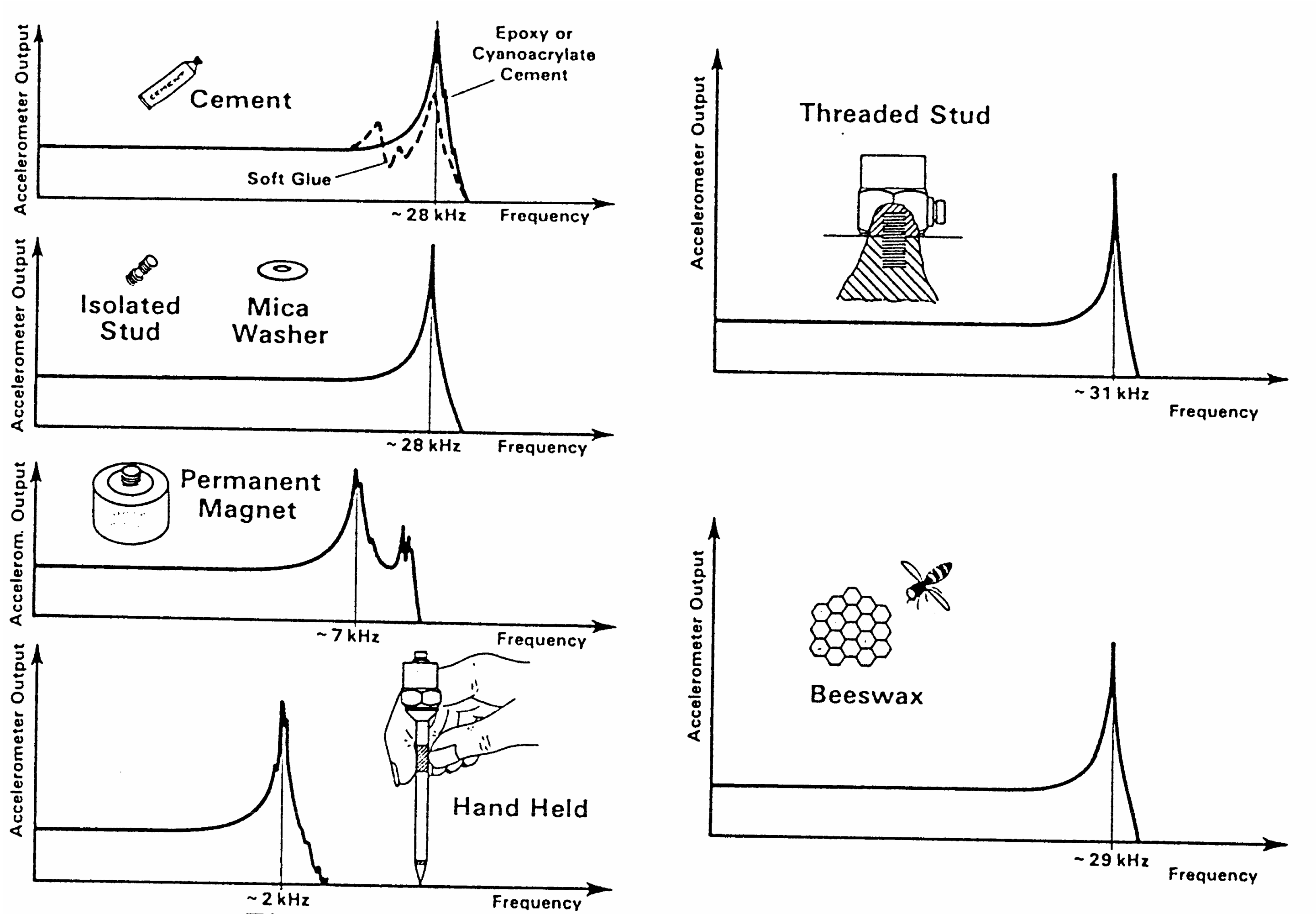

Force Transducers

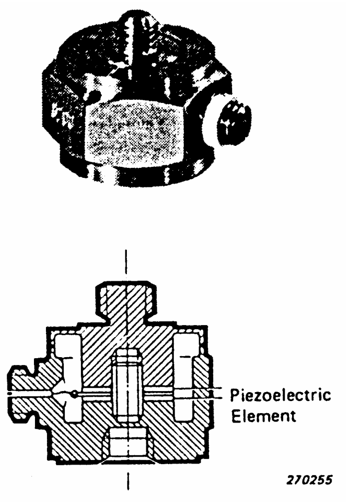

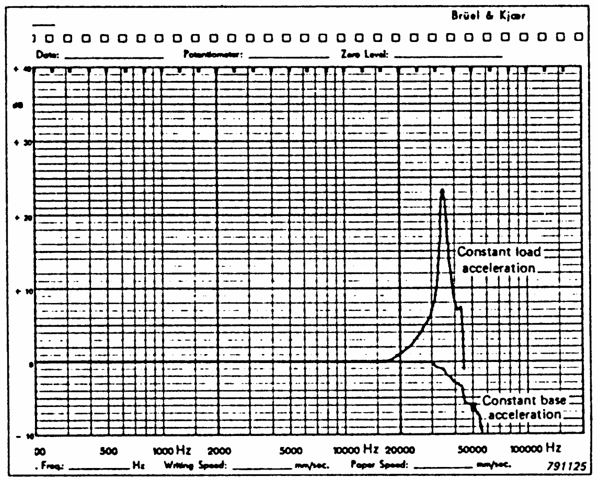

Impedance Heads

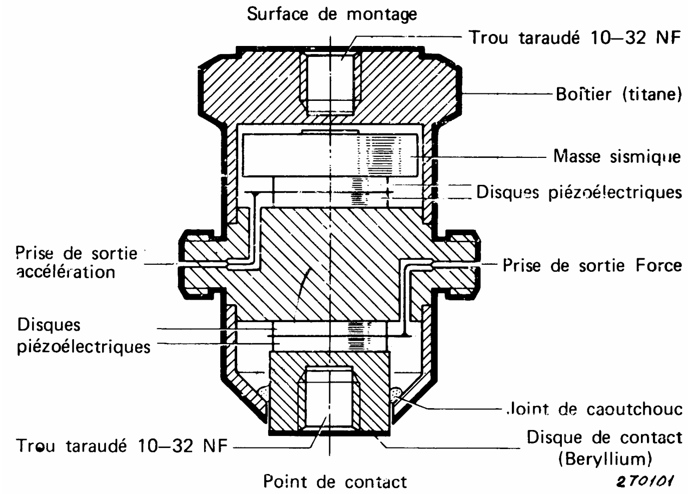

Combination of 2 transducers:
force + acceleration

Laser Transducers

- Laser Doppler velocimeter (LDV)
  - Characteristics for a typical device:
  - Frequency range: 0-250 kHz
  - Vibration velocity range: 0.01 - 20000 mm/s
  - Target distance: 0.2 - 30 m
  - Signal/noise: excellent (depends on target, type of scan and measurement range)
  - Sensitivity: 1 - 1000 mm/s/V
- Holographic interferometry (ESPI, DSPI)

General case

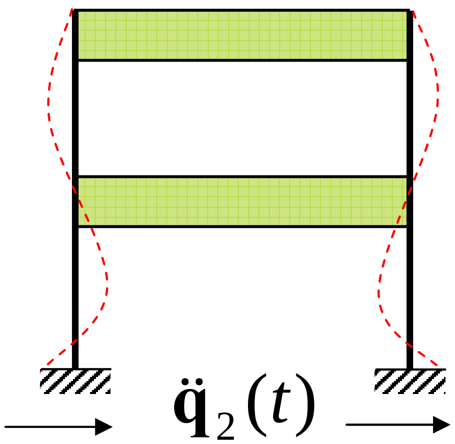

Partition of the DOF :

- n_1 free displacements $\mathbf{q}_1$
- n_2 imposed displacements $\mathbf{q}_2$

Equations of motion

$$\begin{bmatrix} \mathbf{M}_{11} & \mathbf{M}_{12} \\ \mathbf{M}_{21} & \mathbf{M}_{22} \end{bmatrix} \begin{Bmatrix} \ddot{\mathbf{q}}_1 \\ \ddot{\mathbf{q}}_2 \end{Bmatrix} + \begin{bmatrix} \mathbf{K}_{11} & \mathbf{K}_{12} \\ \mathbf{K}_{21} & \mathbf{K}_{22} \end{bmatrix} \begin{Bmatrix} \mathbf{q}_1 \\ \mathbf{q}_2 \end{Bmatrix} = \begin{Bmatrix} \mathbf{0} \\ \mathbf{r}_2(t) \end{Bmatrix}$$

Université de Liège

The response takes the form

$= \mathbf{S}$ (static condensation matrix at foundation level)

$$\mathbf{q}(t) = \begin{bmatrix} \mathbf{I} & \boxed{-\mathbf{K}_{11}^{-1}\,\mathbf{K}_{12}} \\ 0 & \mathbf{I} \end{bmatrix} \begin{Bmatrix} \mathbf{y}_1 \\ \mathbf{q}_2 \end{Bmatrix}$$

Dynamic part of the response solution of

$$\mathbf{M}_{11}\,\ddot{\mathbf{y}}_1 + \mathbf{K}_{11}\,\mathbf{y}_1 = \mathbf{g}_1(t)$$

$$\mathbf{g}_1(t) = -(\mathbf{M}_{11}\,\mathbf{S} + \mathbf{M}_{12})\,\ddot{\mathbf{q}}_2(t)$$

(equivalent load)

System submitted to global support acceleration

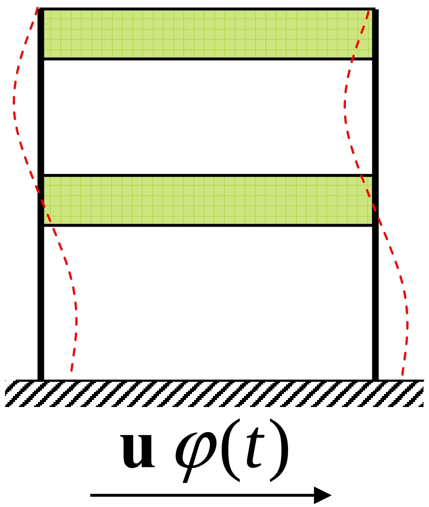

$$\Rightarrow \qquad \ddot{\mathbf{q}} = \begin{Bmatrix} \ddot{\mathbf{q}}_1 \\ \ddot{\mathbf{q}}_2 \end{Bmatrix} = \begin{Bmatrix} \ddot{\mathbf{y}}_1 \\ \mathbf{0} \end{Bmatrix} + \begin{Bmatrix} \mathbf{u}_1 \\ \mathbf{u}_2 \end{Bmatrix} \varphi(t)$$

where
$$\begin{cases} \mathbf{u}_1 = -\mathbf{K}_{11}^{-1}\,\mathbf{K}_{12}\,\mathbf{u}_2 \\ \mathbf{g}_1(t) = -\left(\mathbf{M}_{11}\,\mathbf{u}_1 + \mathbf{M}_{12}\,\mathbf{u}_2\right)\varphi(t) \end{cases}$$

Method of additional masses

Modification of the equations of motion

$$\begin{bmatrix} \mathbf{M}_{11} & \mathbf{M}_{12} \\ \mathbf{M}_{21} & \mathbf{M}_{22} + \boxed{\mathbf{M}_{22}^{0}} \end{bmatrix} \begin{Bmatrix} \ddot{\mathbf{q}}_1 \\ \ddot{\mathbf{q}}_2 \end{Bmatrix} + \begin{bmatrix} \mathbf{K}_{11} & \mathbf{K}_{12} \\ \mathbf{K}_{21} & \mathbf{K}_{22} \end{bmatrix} \begin{Bmatrix} \mathbf{q}_1 \\ \mathbf{q}_2 \end{Bmatrix} = \begin{Bmatrix} \mathbf{0} \\ \boxed{\mathbf{f}(t)} \end{Bmatrix}$$

with $\mathbf{M}_{22}$ of high amplitude level $\qquad \mathbf{f}(t) \cong \mathbf{M}_{22}^{0}\,\ddot{\mathbf{q}}_2$

Effective modal masses

Governing motion equation for the unrestrained DOF

$$\mathbf{M}_{11}\,\ddot{\mathbf{y}}_1 + \mathbf{K}_{11}\,\mathbf{y}_1 = \mathbf{g}_1(t) \quad \text{with} \quad \mathbf{g}_1(t) = -(\mathbf{M}_{11}\,\mathbf{S} + \mathbf{M}_{12})\,\ddot{\mathbf{q}}_2(t)$$

⇨ Normal equations

$$\boldsymbol{\Omega}^2\,\boldsymbol{\eta} + \ddot{\boldsymbol{\eta}} = \boxed{-\mathbf{X}^T\,(\mathbf{M}_{11}\,\mathbf{S} + \mathbf{M}_{12})}\;\ddot{\mathbf{q}}_2$$

$\boldsymbol{\Gamma}$ = modal participation matrix of dimension n_1 x n_2

Concept of effective modal mass : $\boldsymbol{\Gamma}\,\boldsymbol{\Gamma}^{\mathrm{T}}$

⇨ $$\boxed{m_T - m_S = \sum_{j=1}^{n_1} \frac{(\boldsymbol{\Gamma}\,\mathbf{e}_i)_j^2}{\mu_j}}$$

Effective mass of mode j in direction i

Total mass

Mass associated with the support

Different types of signals

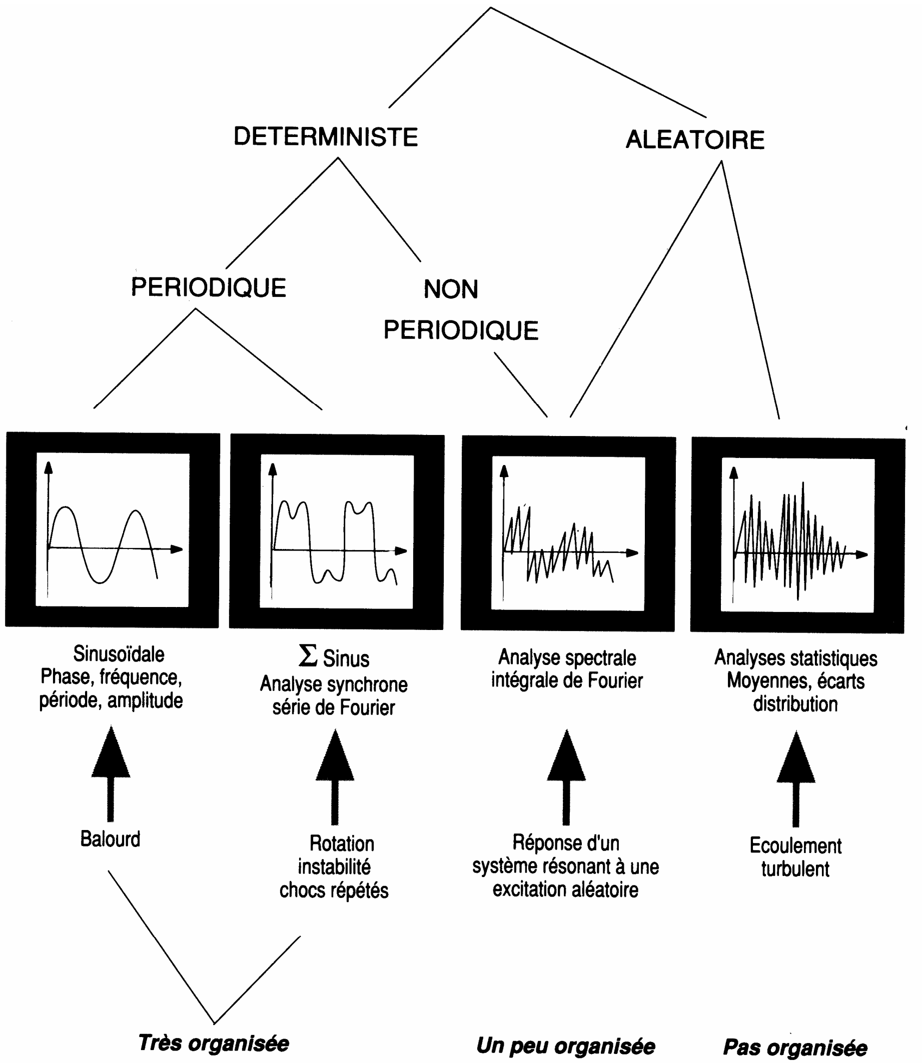

Basic Theory of Fourier Analysis

A function $x(t)$, **periodic** in time T, can be written in an infinite series of sinusoids:

$$x(t)=\frac{a_0}{2}+\sum_{n=1}^{\infty}\left(a_n\cos(n\,\omega\,t)+b_n\sin(n\,\omega\,t)\right)\quad \left(\text{with } \omega=\frac{2\,\pi}{T}\right)$$

where $$a_n=\frac{2}{T}\int_0^T x(t)\cos(n\,\omega\,t)\,dt\qquad (n=0,1,2,\cdots)$$

$$b_n=\frac{2}{T}\int_0^T x(t)\sin(n\,\omega\,t)\,dt\qquad (n=1,2,\cdots)$$

Alternative forms

$$x(t)=\sum_{n=-\infty}^{\infty}X_n\,e^{i\,n\,\omega\,t}\quad \text{where}\quad X_n=\frac{1}{T}\int_0^T x(t)\,e^{-i\,n\,\omega\,t}\,dt$$

The Fourier Transform

A **nonperiodic** function $x(t)$ which satisfies the condition

$$\int_{-\infty}^{\infty} |x(t)|\, dt < \infty$$

can be represented by the integral

$$x(t) = \int_{-\infty}^{\infty} \left(A(\omega)\cos(\omega\, t) + B(\omega)\sin(\omega\, t)\right) d\omega$$

where $A(\omega) = \dfrac{1}{\pi}\displaystyle\int_{-\infty}^{\infty} x(t)\cos(\omega\, t)\, dt$

$$B(\omega) = \frac{1}{\pi}\int_{-\infty}^{\infty} x(t)\sin(\omega\, t)\, dt$$

Alternative form

$x(t) = \displaystyle\int_{-\infty}^{\infty} X(\omega)\, e^{i\,\omega\, t}\, d\omega$ where $X(\omega) = \dfrac{1}{2\,\pi}\displaystyle\int_{-\infty}^{\infty} x(t)\, e^{-i\,\omega\, t}\, dt$

The Discrete Fourier Transform (DFT)

Let us consider a time signal which is digitised (by an A-D converter)

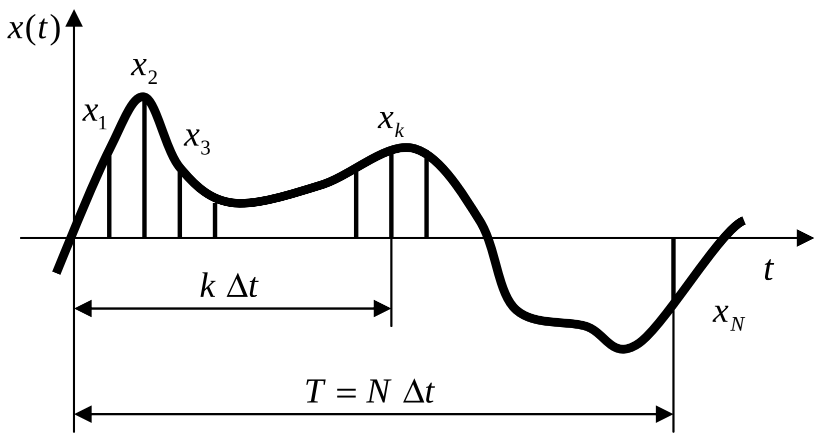

Δt = time resolution

$f_s = \dfrac{1}{\Delta t}$ = sampling rate

$T = N\,\Delta t$ = sample length

$\Delta f = \dfrac{1}{T} = \dfrac{f_s}{N}$ = frequency resolution

The Fourier series of the original signal (**periodicity assumption**) can be written:

$$x(t) = \sum_{n=-\infty}^{\infty} X_n \, e^{i\frac{2\pi n t}{T}} \qquad \text{with} \qquad X_n = \frac{1}{T}\int_0^T x(t)\, e^{-i\frac{2\pi n t}{T}}\, dt$$

If $x(t)$ is discretised at evenly spaced time intervals Δt, we can write at a particular time $t_i = k\,\Delta t$:

$$x(t_k)\, e^{-i\frac{2\,\pi\, n\, t_k}{T}} = x(k\,\Delta t)\, e^{-i\frac{2\,\pi\, n\, k\,\Delta t}{T}} = x_k\, e^{-i\frac{2\,\pi\, n\, k}{N}}$$

In this case, the integral $X_n = \dfrac{1}{T}\displaystyle\int_0^T x(t)\, e^{-i\frac{2\,\pi\, n\, t}{T}}\, dt$

is replaced by $X_n = \dfrac{1}{N\,\Delta t}\displaystyle\sum_{k=1}^{N} x_k\, e^{-i\frac{2\,\pi\, n\, k}{N}}\,\Delta t$

The (complex) DFT is defined by

$$\boxed{X_n = \frac{1}{N}\sum_{k=1}^{N} x_k\, e^{-i\frac{2\,\pi\, n\, k}{N}} \qquad (n = 1,\cdots,N)}$$

The Fast Fourier Transform (FFT)

The calculation of the DFT of a signal using the definition

$$X_n = \frac{1}{N} \sum_{k=0}^{N-1} x_k \, e^{-i\frac{2\pi n k}{N}} \qquad (n = 0, \cdots, N-1)$$

requires N^2 complex multiplications (and additions)

$\Rightarrow$ time-consuming operation.

The basis of the FFT algorithm of radix 2 ($N=2^r$ where r is an integral number) is the partitioning of the full sequence of sample values into a number of shorter sequences:

$$X_n = \frac{1}{N} \left(\sum_{k=0}^{N/2-1} x_{2k} \, e^{-i\frac{2\pi n 2k}{N}} + \sum_{k=0}^{N/2-1} x_{2k+1} \, e^{-i\frac{2\pi n (2k+1)}{N}} \right)$$

$$X_n = \frac{1}{2} \frac{1}{N/2} \left(\sum_{k=0}^{N/2-1} x_{2k} \, e^{-i\frac{2\pi n k}{N/2}} + e^{-i\frac{2\pi n}{N}} \sum_{k=0}^{N/2-1} x_{2k+1} \, e^{-i\frac{2\pi n k}{N/2}} \right)$$

Thus the full FFT computation scheme becomes

$$\left.\begin{aligned} X(n) &= \frac{1}{2}\left(X_y(n) + W^n\ X_z(n)\right) \\ X\left(n + N/2\right) &= \frac{1}{2}\left(X_y(n) - W^n\ X_z(n)\right) \end{aligned}\right\} \quad (n = 0, \cdots, \frac{N}{2} - 1)$$

where $W = e^{-i\frac{2\pi}{N}}$

Example of partitioning : $N=8$ samples

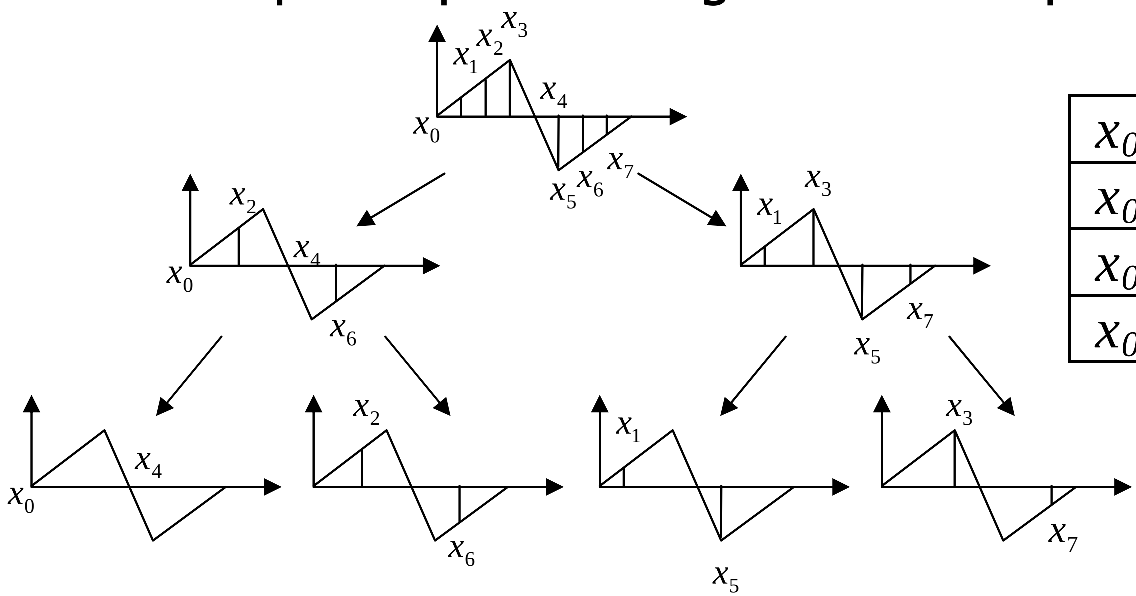

x_0	x_1	x_2	x_3	x_4	x_5	x_6	x_7
x_0	x_2	x_4	x_6	x_1	x_3	x_5	x_7
x_0	x_4	x_2	x_6	x_1	x_5	x_3	x_7
x_0	x_4	x_2	x_6	x_1	x_5	x_3	x_7

Random Vibration

Consider a random process represented by an infinite set of samples

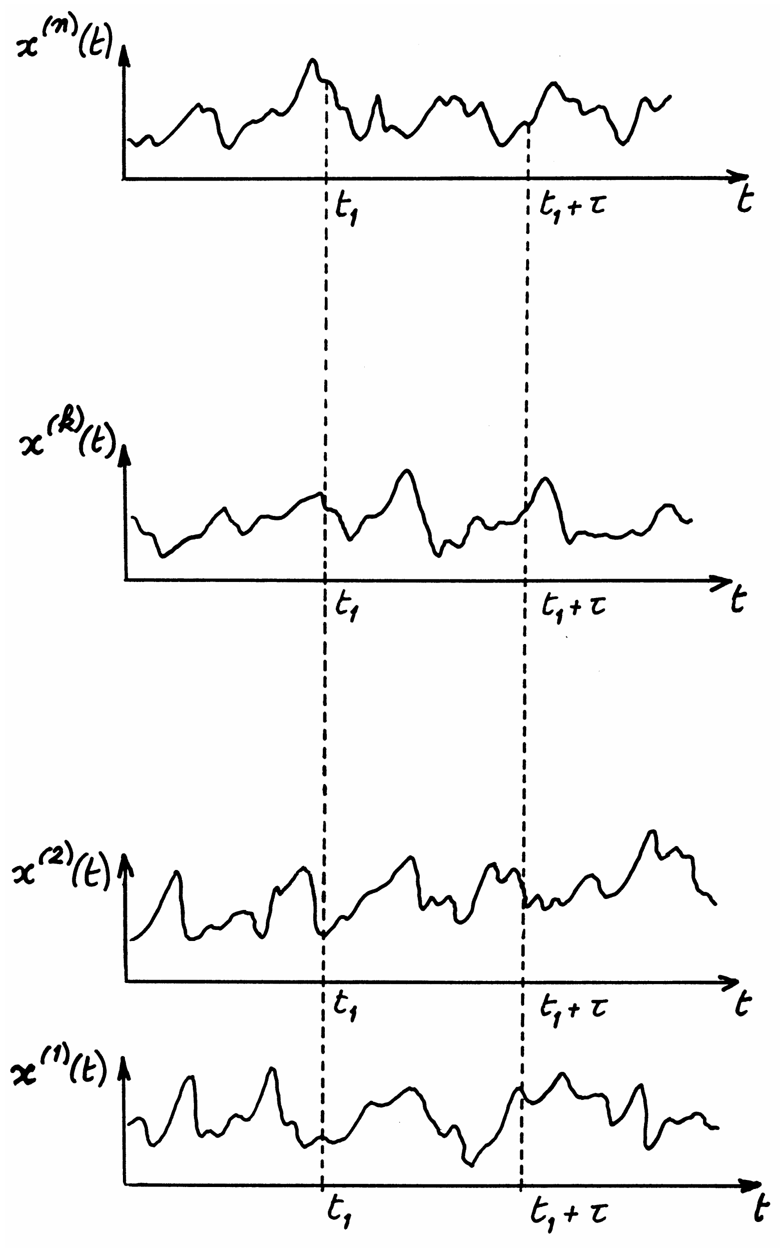

Definitions

Mean Value

$$\mu_x(t_1) = \lim_{n\to\infty} \frac{1}{n} \sum_{k=1}^{n} x^{(k)}(t_1)$$

Root Mean Square Value

$$\overline{X}^2 = \lim_{T\to\infty} \frac{1}{T} \int_{-T/2}^{T/2} x^2(t)\, dt$$

Autocorrelation Function

$$R_{xx}(t_1, t_1+\tau) = \lim_{n\to\infty} \frac{1}{n} \sum_{k=1}^{n} x^{(k)}(t_1)\, x^{(k)}(t_1+\tau)$$

Classes of random process

Random Process

- Non steady-state
- Steady-state

$$\left.\begin{aligned}\mu_x(t_1) &= \mu_x \\ R_{xx}(t_1, t_1+\tau) &= R_{xx}(\tau)\end{aligned}\right\}\ \text{independent of } t_1$$

  - Non ergodic
  - Ergodic

(is a type of random process which requires only a single sample, albeit of considerable length, to portray all the statistical properties required for its definition)

For an ergodic process, it follows that the Autocorrelation function is defined as the ‘expected’ (or average) value of the product $(x(t).x(t+\tau))$

$$R_{xx}(\tau) = E\left[x(t).\,x(t+\tau)\right]$$

It can been seen that:

$$R_{xx}(0) = \overline{X}^{\,2}$$

Power Spectral Density (PSD)

The Auto- or Power Spectral Density (PSD), $S_{xx}(\omega)$, of a signal $x(t)$ is defined as the Fourier Transform of the Autocorrelation Function i.e.

$$S_{xx}(\omega) = \frac{1}{2\pi} \int_{-\infty}^{\infty} R_{xx}(\tau)\, e^{-i\omega\tau}\, d\tau$$

The Auto-Spectral Density is a real and even function of frequency, and does in fact provide a description of the frequency composition of the original signal. For an acceleration signal for example, it has units of $(m/s^2)^2/(rad/s)$.

The inverse transformation gives:

$$R_{xx}(\tau) = \int_{-\infty}^{\infty} S_{xx}(\omega)\, e^{i\omega\tau}\, d\omega$$

Thus, it comes: $$R_{xx}(0) = \int_{-\infty}^{\infty} S_{xx}(\omega)\, d\omega = \overline{X}^2$$

A similar concept can be applied to a pair of functions such as $x(t)$ and $f(t)$ to produce cross correlation and cross spectral density functions.

The cross correlation function, $R_{xf}(t)$, is defined as:

$$R_{xf}(\tau) = E[x(t).\, f(t+\tau)]$$

and the cross spectral density is defined as its Fourier Transform:

$$S_{xf}(\omega) = \frac{1}{2\pi} \int_{-\infty}^{\infty} R_{xf}(\tau)\, e^{-i\,\omega\,\tau}\, d\tau$$

Time Domain | **Autocorrelation function** | **Power Spectral Density**

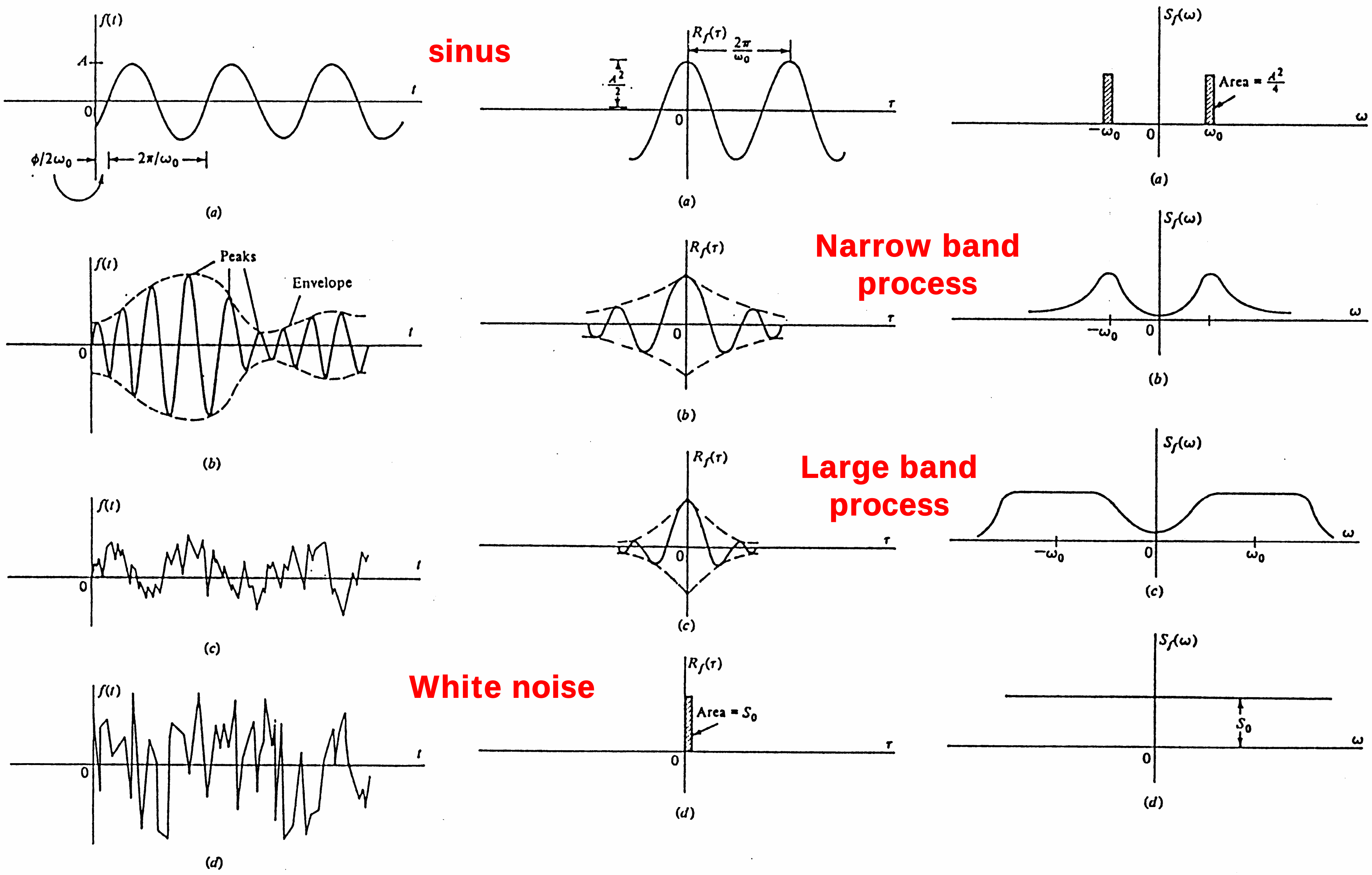

System Response - Time / Frequency Duality

Input: $f(t)$ → Impulse Response $h(t)$ → Output: $x(t) = \int_0^t f(\tau)\, h(t-\tau)\, d\tau$

Input: $F(\omega)$ → Transfert Function (FRF) $H(\omega)$ → Output: $X(\omega) = H(\omega)\, F(\omega)$

In the frequency domain, we can establish the following relations:

$$S_{xx}(\omega) = \left|H(\omega)\right|^2 S_{ff}(\omega)$$

$$S_{fx}(\omega) = H(\omega)\, S_{ff}(\omega)$$

$$S_{xx}(\omega) = H(\omega)\, S_{xf}(\omega)$$

Property of the cross power spectral densities:

$$S_{xf}(\omega) = S^{*}_{fx}(\omega)$$

Some Features of Digital Fourier Analysis

There are a number of features of digital Fourier analysis which, if not properly treated, can give rise to erroneous results. These are generally the result of the discretisation approximation and of the need to limit the length of the time history.

Specific features are:

- *aliasing*,
- *leakage*,
- *windowing*,
- *filtering*,
- *zooming*,
- *averaging*.

Aliasing

Aliasing results from the discretisation of the originally continuous time history.

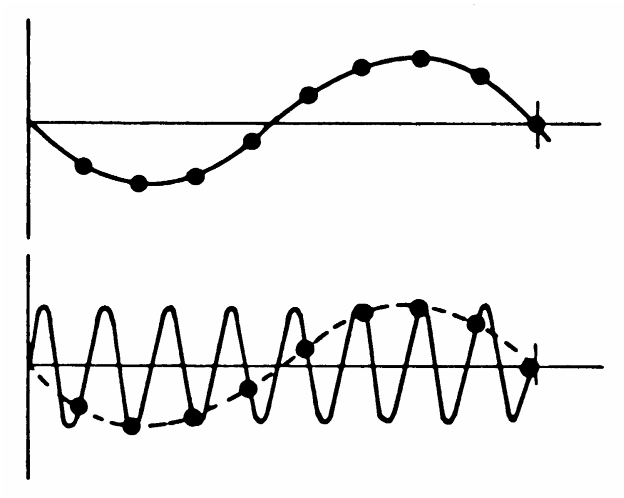

Low-frequency signal

High-frequency signal: the existence of high frequencies is misinterpreted if the sampling rate is too slow.

Thus, a signal of frequency ω and one of $(\omega_s - \omega)$ (where ω_s is the sampling frequency) are indistinguishable when represented as a discretised time history.

Alias distortion of spectrum by DFT

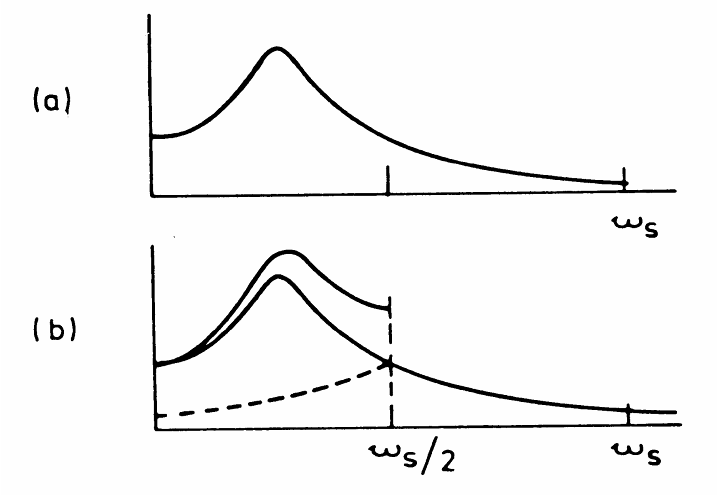

(a) True spectrum of signal

(b) Indicated spectrum from DFT: frequencies higher than $\omega_S / 2$ are "folded back"

Nyquist sampling theorem

$$\boxed{\omega \leq \frac{\omega_s}{2}}$$

$$\omega_{\max} = \frac{\omega_s}{2} = \text{Nyquist (cut-off) frequency}$$

Practically, one often chooses : $\omega_s = 2.56\,\omega$

Solution : use an anti-aliasing filter which subjects the <u>original</u> time signal to a low-pass, sharp cut-off filter.

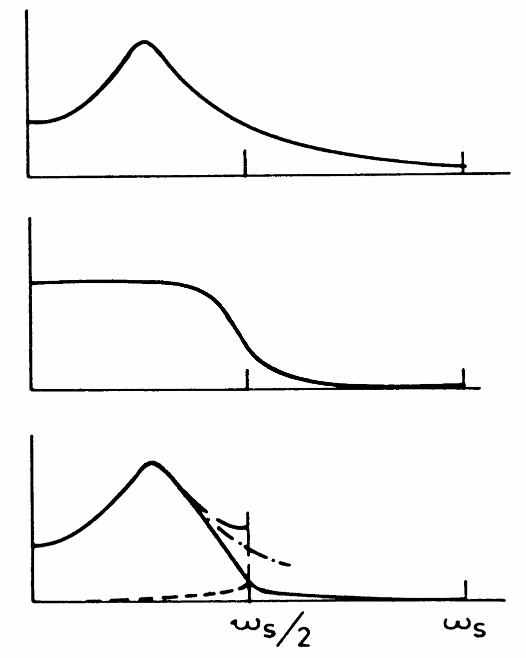

Because the filters are not perfect, it is necessary to reject the spectral measurements in a frequency range approaching the Nyquist frequency. It is for this reason that a 1024-point transform results in a 512-line spectrum and that only the first 400 lines are given on the analyser display.

Leakage

Leakage results from the need to take only a finite length of time history coupled with the assumption of periodicity.

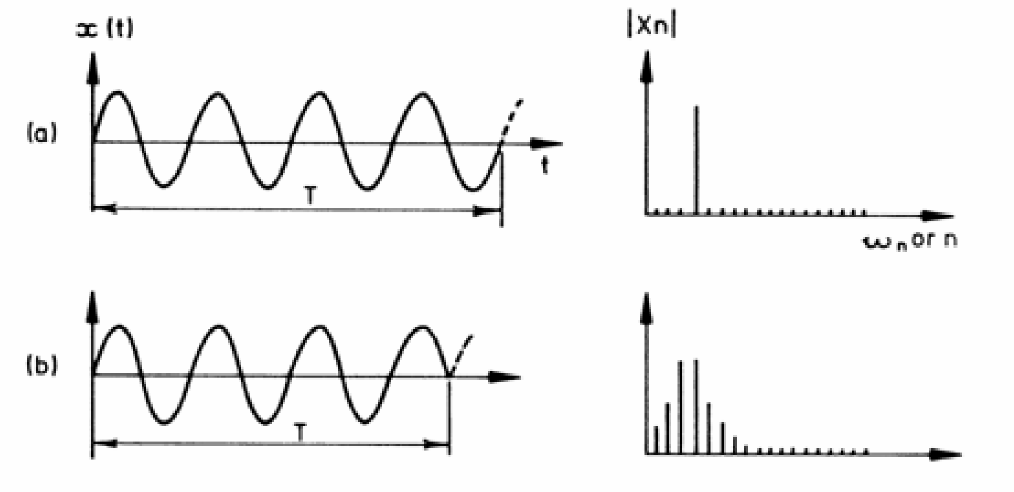

(a) Ideal signal

(b) 'Awkward' signal

(a) The signal is perfectly periodic in the time window T

(b) The periodicity assumption is not strictly valid (discontinuity at the end of the sample)

Time domain

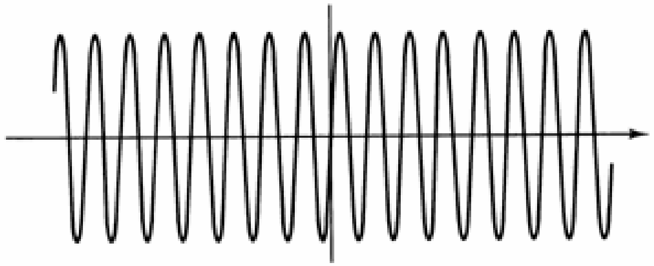

(a)

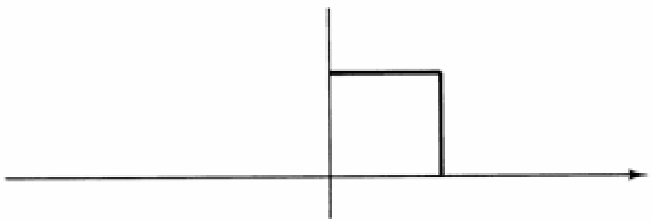

(b)

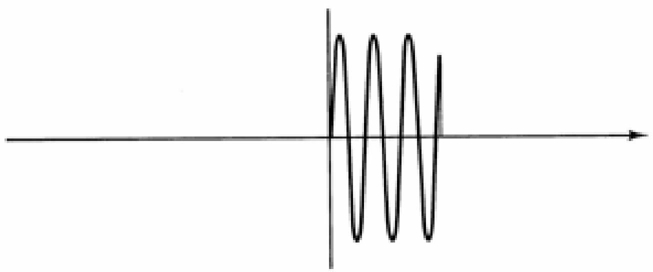

(c)

Frequency domain

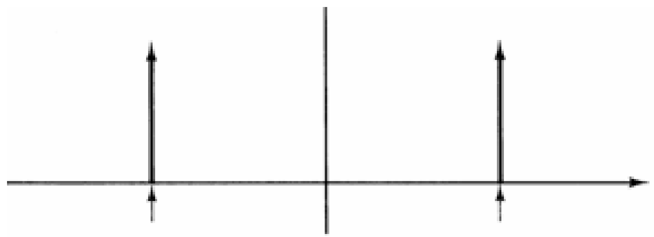

(a)

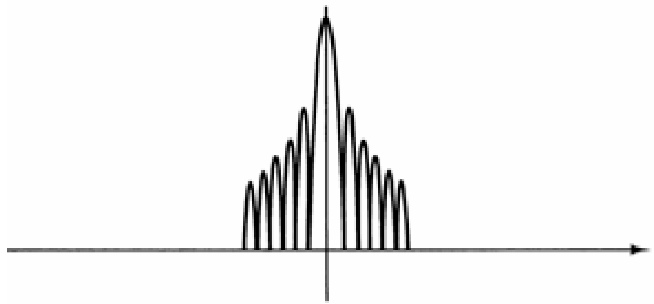

(b)

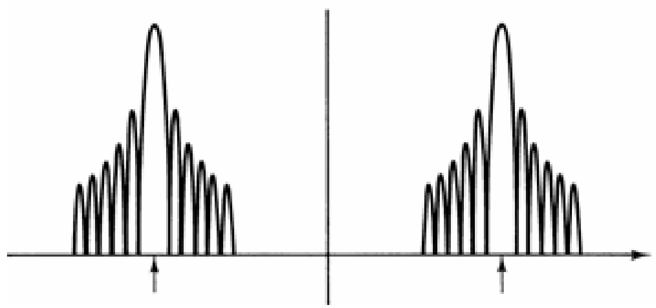

Windowing

$$x'(t) = x(t)\, w(t) \qquad X'(\omega) = X(\omega) \otimes W(\omega)$$

Analysed signal — $x(t)$ **Window** — $w(t)$ **Convolution product**

Different types of window

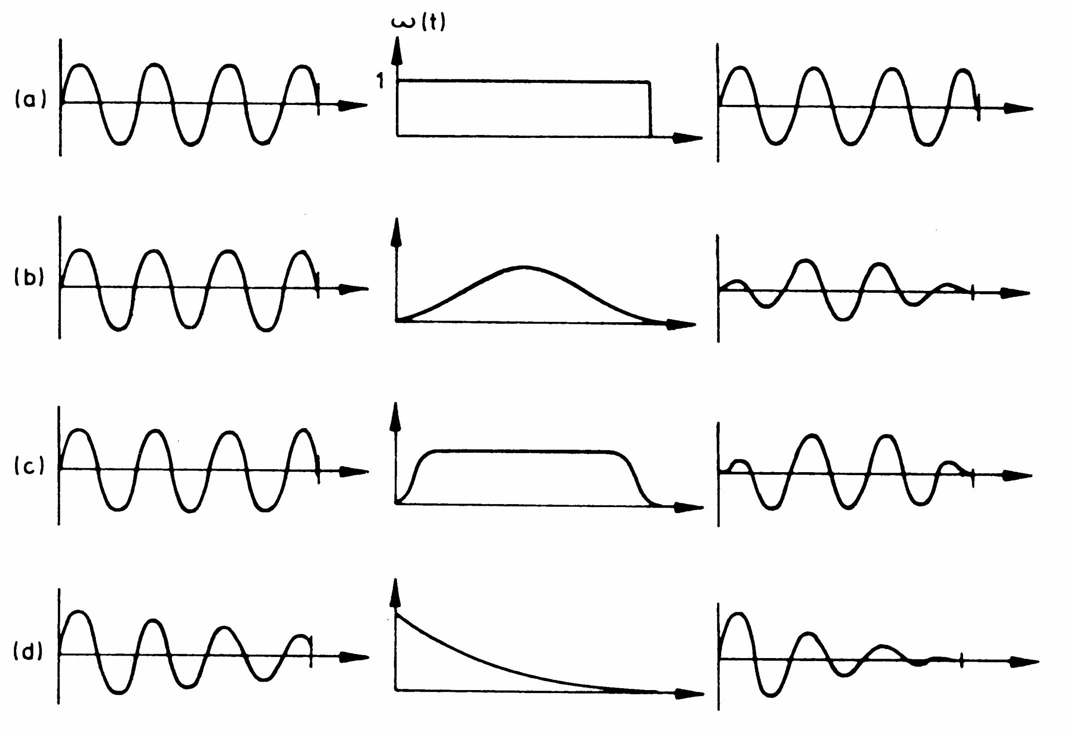

(a) Boxcar

(b) Hanning

(c) Cosine-taper

(d) Exponential

Frequency spectra of different windows

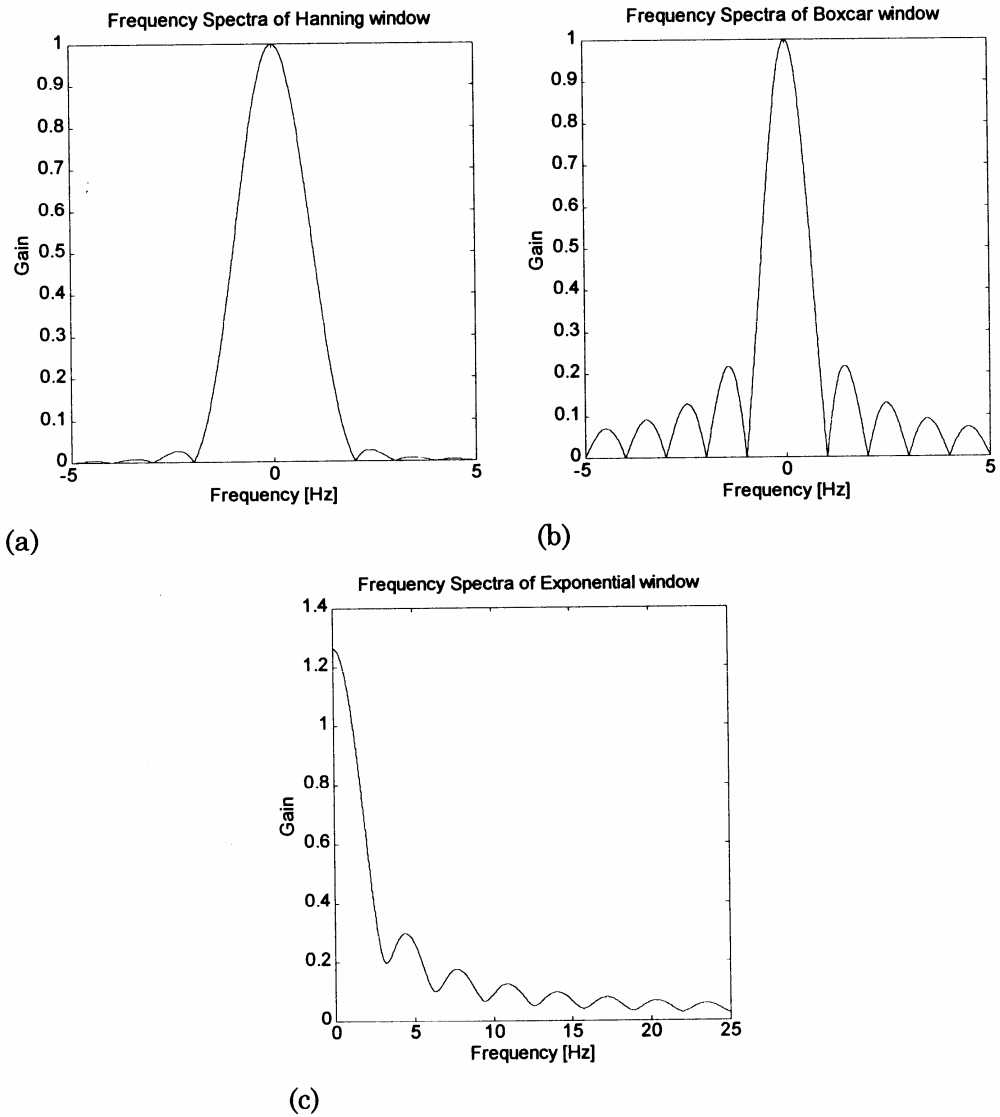

Filtering

Filtering is another signal conditioning process rather like windowing, except that it is applied in the frequency domain rather that the time domain.

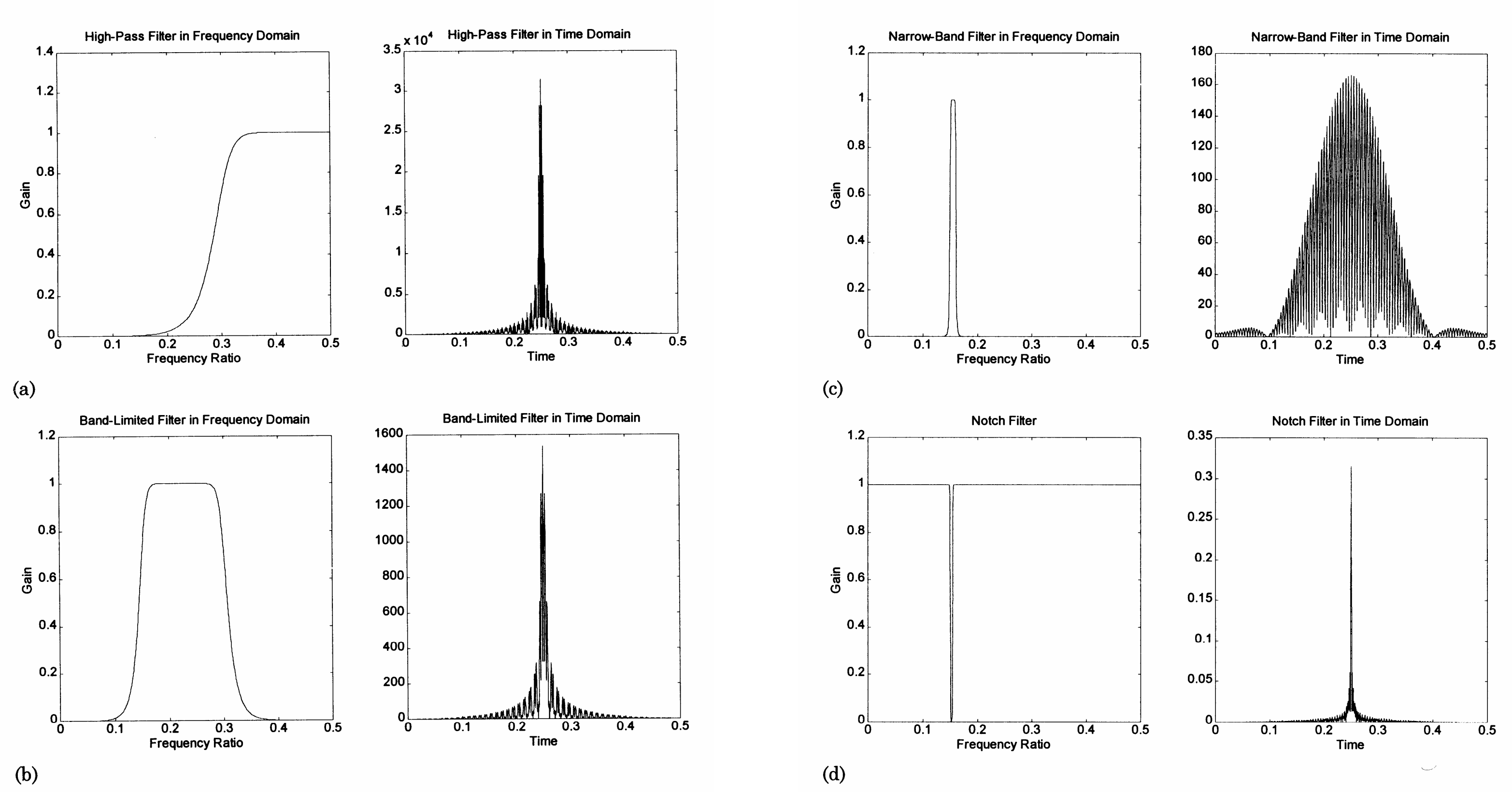

$$X'(\omega) = X(\omega)\,W(\omega) \qquad x'(t) = x(t) \otimes w(t)$$

Improving Resolution

Inadequate frequency resolution (e.g. especially for lightly-damped systems) arises because of the constraints imposed by the DFT process i.e.

- the limited number of discrete points available (N);
- the maximum frequency range to be covered ($\omega_s/2$) and/or the length of time sample available.

Solutions to this problem are:

- Increasing transform size (but it may be counterproductive to increase the fineness of the spectrum overall)
- Zero padding
- Zoom

Zero padding: It consists in adding a series of zeroes to the short sample of actual data, to increase artificially the length of the sample.

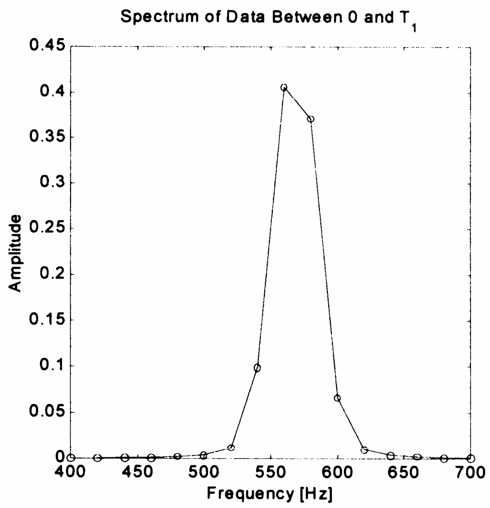

(a)

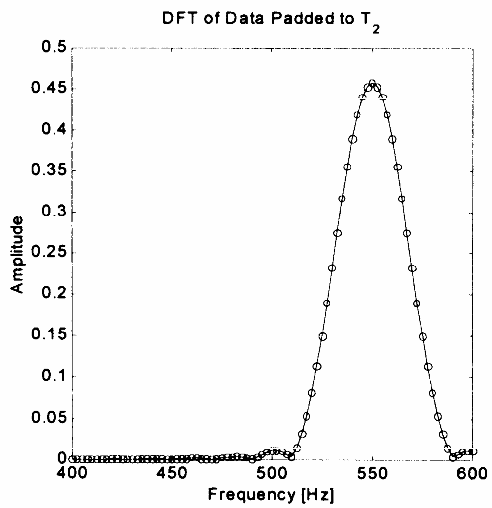

(b)

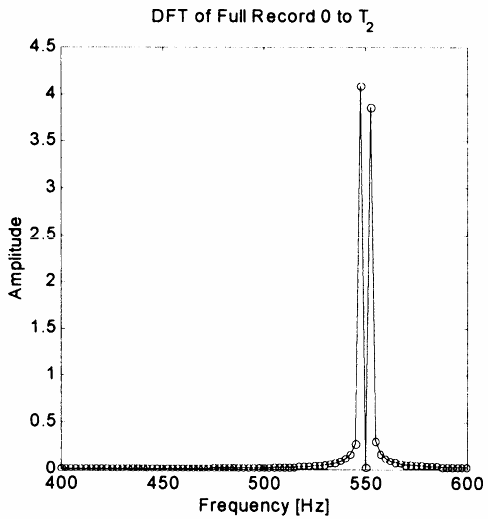

(c)

Results of using zero-padding

(a) DFT of data between 0 and T_1

(b) DFT of data padded to T_2

(c) DFT of full record 0 to T_2.

It reveals the presence of 2 frequency components in the signal !

Zoom

The objective is to obtain a finer frequency resolution by concentrating all the spectral lines (400, 800, …) on the frequency range of interest (between f_1 and f_2 rather than between 0 and f_2).

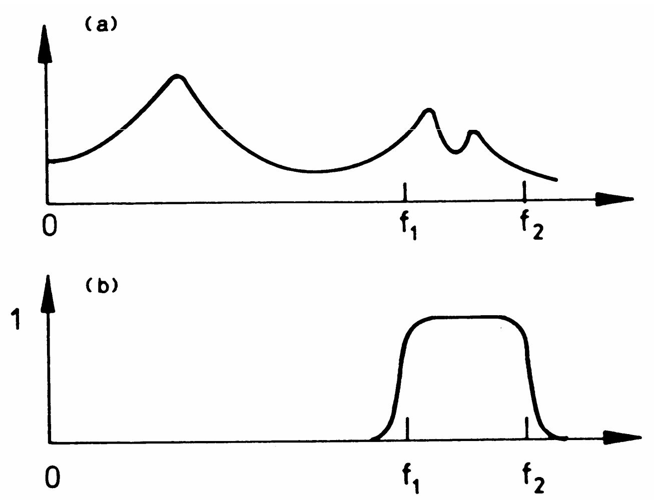

(a) Spectrum of the signal to be analysed

(b) Band-pass filter

A method consists to apply a band-pass filter to the signal and to perform a DFT between 0 and $(\omega_2 - \omega_1)$

Then because of the aliasing phenomenon, the frequency components between f_1 and f_2 will appear aliased in the analysis range 0 to (f_2-f_1) with the advantage of a finer resolution.

Effective frequency translation for zoom

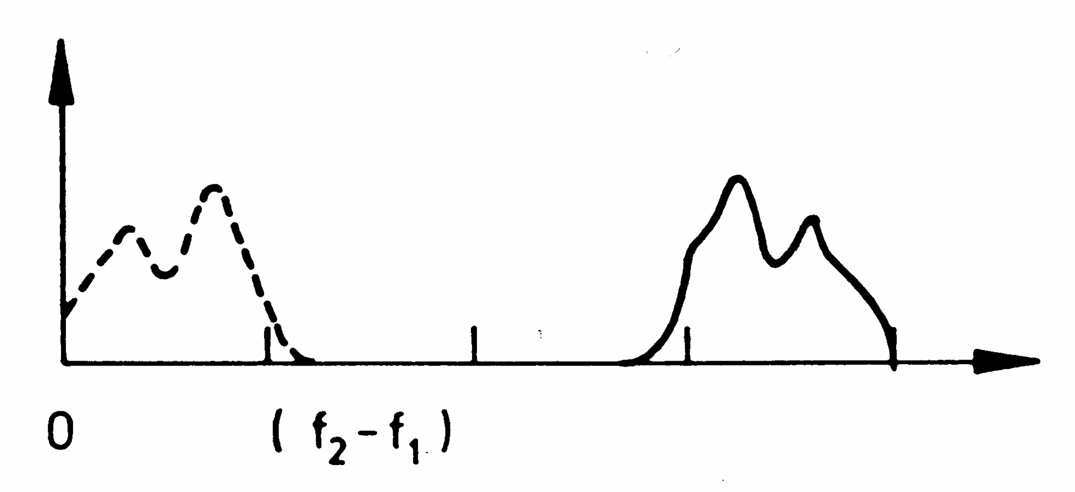

In this example, the resolution is 4 times finer than in the original baseband analysis.

Other methods to achieve a zoom measurement are based on effectively shifting the frequency origin by multiplying the original time history by a $\cos(\omega_1 t)$ function and then filtering the higher of the two components thus produced.

Example : suppose the signal to be analysed is:

$$x(t) = A\sin(\omega t)$$

Multiplying this by $\cos(\omega_1 t)$ yields:

$$x'(t) = A\sin(\omega t)\cos(\omega_1 t) = \frac{A}{2}(\sin(\omega - \omega_1)t + \sin(\omega + \omega_1)t)$$

If we filter out the second component, we are left with the original signal translated down the frequency range by ω_1 . In this method, it is clear that sample times are multiplied by the zoom magnification factor.

Averaging

Need to enhance the quality of the measurements in terms of reliability and accuracy. A high number of samples allows to remove spurious random noise from the signals.

There are several options which can be selected when setting an analyser into average mode (exponential, linear).

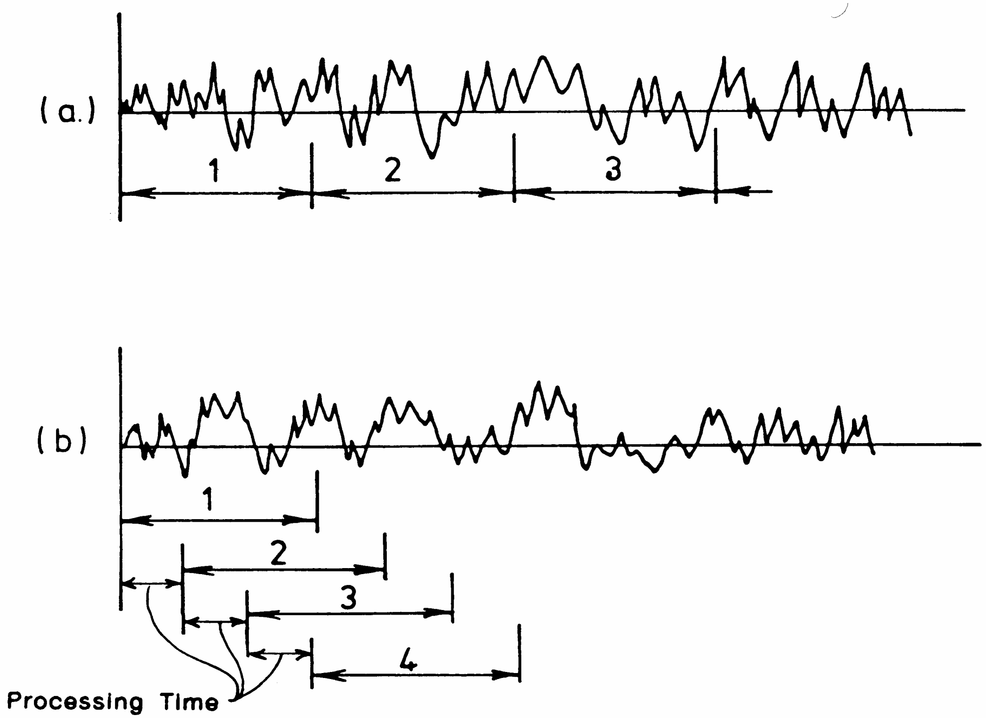

Different interpretations of multi-sample averaging

(a) Sequential

(b) Overlap

Use of Different Excitation Signals

Classes of signal used for modal testing

Periodic excitation

- stepped sine
- slow sine sweep
- periodic
- pseudo-random
- periodic random

Random excitation

- (true) random
- white noise
- narrow-band random

Transient excitation

- burst sine
- burst random
- chirp
- impulse

Periodic Excitation

- **Stepped-sine Testing**

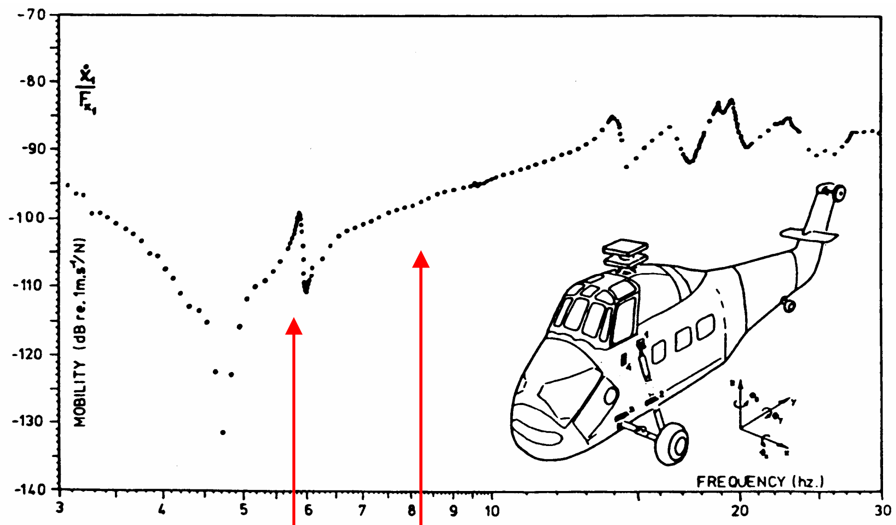

Example of <u>rapid coarse sweep</u> with a large frequency increment, followed by a set of <u>small fine sweeps</u> localised around the resonances of interest.

Features :

- Step-by-step variation of the frequency of the excitation signal;
- Need to ensure steady-state conditions before the measurements are made;
- The extent of the unwanted transient response will depend on:
  - the proximity of a natural frequency,
  - the lightness of the damping,
  - the abruptness of the changeover.

⇨ long measurement time.

• Slow Sine Sweep Testing

(= the traditional method of FRF measurement)

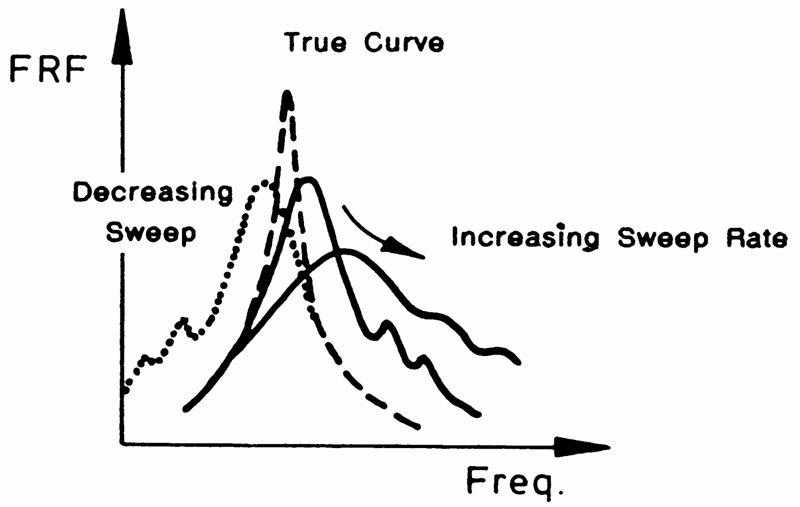

Distorting effect of sweep rate

Features :

- Slow and continuous variation of the excitation frequency;
- Slow sweep rate to achieve steady-state conditions;

Prescriptions of the ISO Standard:

- Linear sweep:

$$S_{\max} < 216\,\omega_r^2\,\zeta_r^2 \qquad \text{Hz/min}$$

- Logarithmic sweep:

$$S_{\max} < 310\,\omega_r^2\,\zeta_r^2 \qquad \text{Hz/min}$$

• Periodic, Pseudo-Random and Periodic Random Excitation

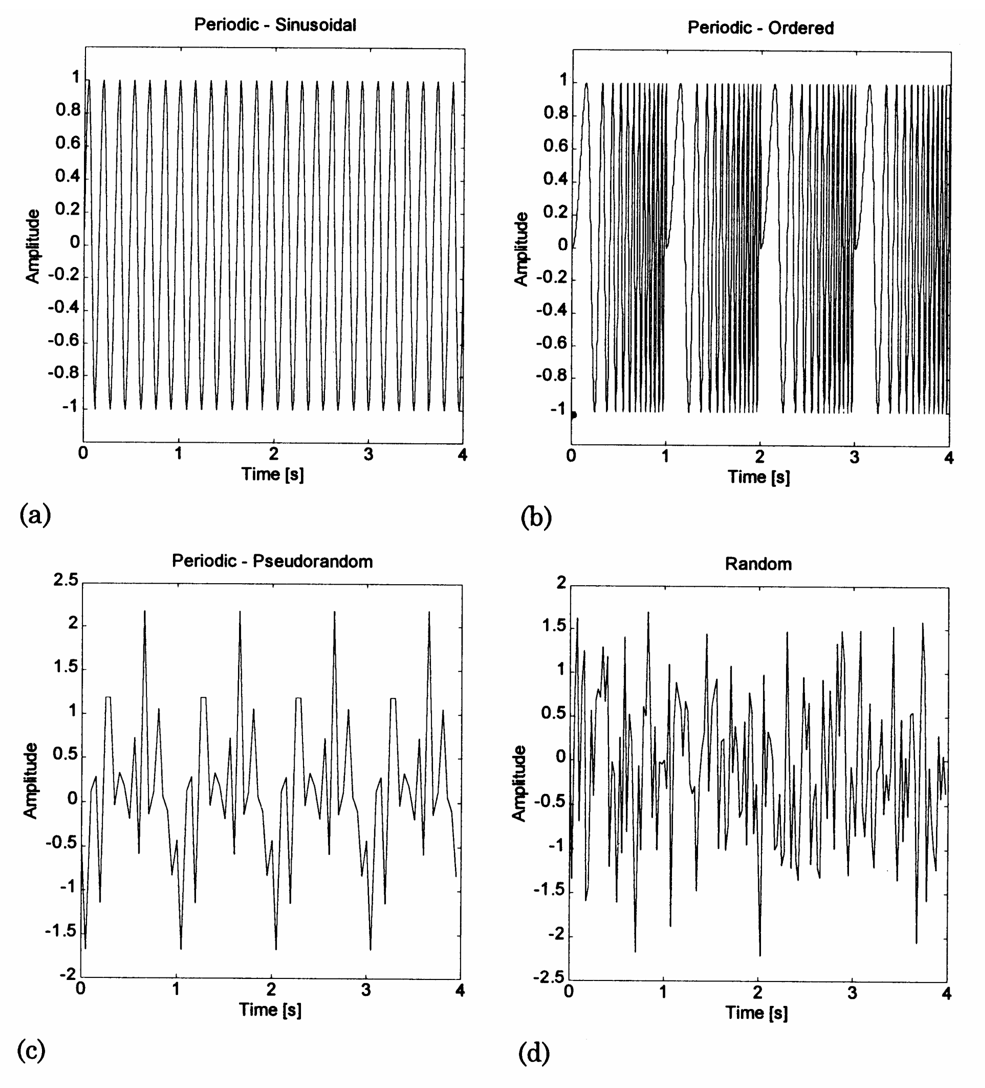

Features :

- Superposition of sinusoids;

or

- Generation of a random mixture of amplitudes and phases for the various frequency components and repetition of this sequence for several successive cycles.

⇨ Optimisation of the energy in the frequency range of interest.

Advantage:

- Exact periodicity of the excitation resulting in zero leakage errors → no need to use a window.

Random Excitation

FRF estimates using random excitation

The principle upon which the FRF is determined using random excitation relies on the following relations:

$$\begin{cases} S_{xx}(\omega) = \left|H(\omega)\right|^2 S_{ff}(\omega) \\ S_{fx}(\omega) = H(\omega)\, S_{ff}(\omega) \\ S_{xx}(\omega) = H(\omega)\, S_{xf}(\omega) \end{cases} \quad \text{rather than} \quad X(\omega) = H(\omega)\, F(\omega)$$

where $S_{xx}(\omega)$, $S_{ff}(\omega)$, $S_{xf}(\omega)$ are the autospectra of the response and excitation signals and the cross spectrum between these two signals, respectively.

The spectrum analyser has the facility to **estimate** these various Power Spectral Densities (PSD). Two estimates for the FRF can be computed using these equations. We shall denote them:

$$H_1(\omega) = \frac{S_{fx}(\omega)}{S_{ff}(\omega)} \quad \text{and} \quad H_2(\omega) = \frac{S_{xx}(\omega)}{S_{xf}(\omega)}$$

Because we have used different quantities for these two estimates, we must be prepared for the eventuality that they are not identical (as, according to theory, they should be) and to this end we shall introduce the coherence function which is defined by:

$\gamma^2 = \dfrac{H_1(\omega)}{H_2(\omega)}$ which can be shown to be always less or equal to 1.

Noisy Data

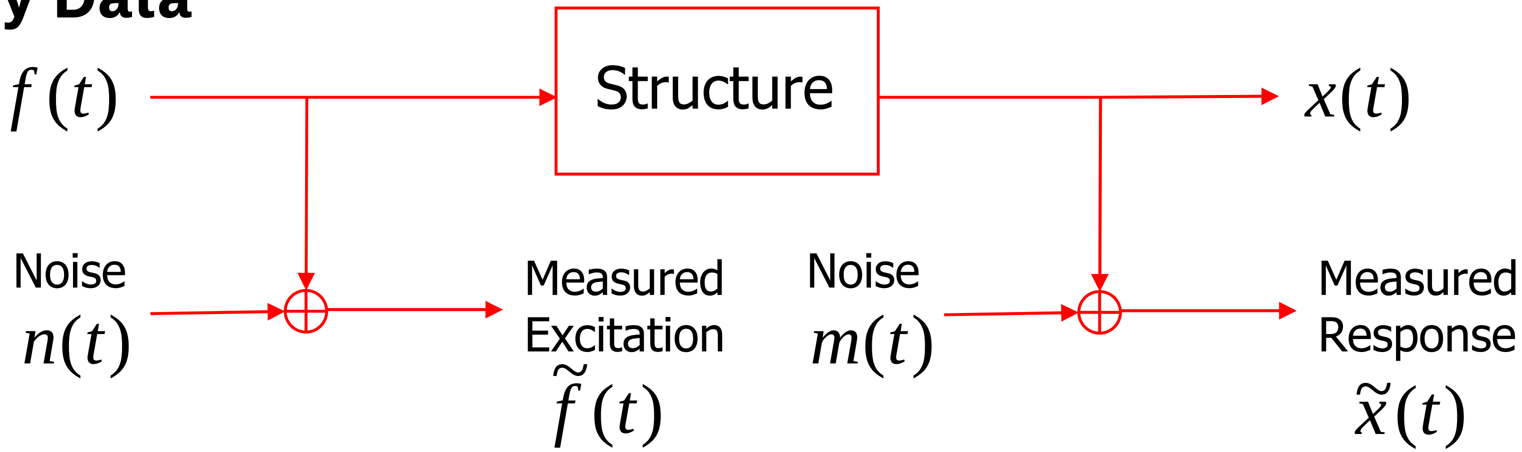

Measured excitation and response signals:

$$\tilde{f}(t) = f(t) + n(t) \qquad\qquad \tilde{x}(t) = x(t) + m(t)$$

Assumption: $m(t)$ and $n(t)$ are not correlated with $x(t)$ and $f(t)$.

$$\Longrightarrow \qquad S_{nm}(\omega) = S_{fn}(\omega) = S_{xm}(\omega) = 0$$

Thus, it follows:

$$S_{\tilde{f}\tilde{f}}(\omega) = S_{ff}(\omega) + S_{nn}(\omega)$$

$$S_{\tilde{x}\tilde{x}}(\omega) = S_{xx}(\omega) + S_{mm}(\omega)$$

and

$$S_{\tilde{f}\tilde{x}}(\omega) = S_{fx}(\omega)$$

FRF estimates:

$$H_1(\omega) = \frac{S_{fx}(\omega)}{S_{ff}(\omega) + S_{nn}(\omega)}$$

is used when noise degrades the response signal (better indicator near antiresonance)

$$H_2(\omega) = \frac{S_{xx}(\omega) + S_{mm}(\omega)}{S_{xf}(\omega)}$$

is used when noise degrades the force signal (better indicator near resonance)

General Case: $H_1(\omega) \leq H(\omega) \leq H_2(\omega)$

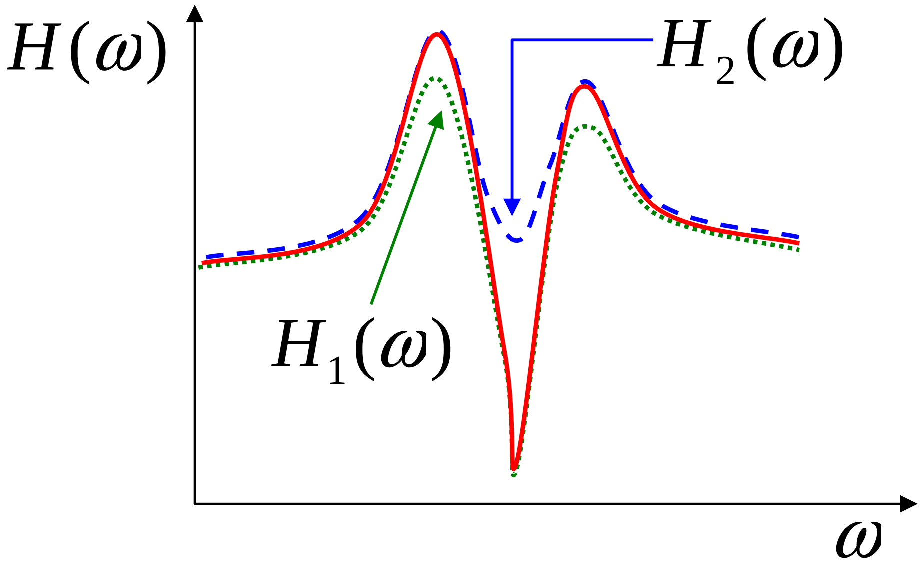

Alternative:

$$H_V(\omega) = \sqrt{H_1(\omega)\, H_2(\omega)}$$

Coherence estimation:

$$\gamma^2 = \frac{H_1(\omega)}{H_2(\omega)} \quad \Rightarrow \quad \gamma^2_{\tilde{f}\tilde{x}} = \frac{S_{fx}(\omega)}{\left(S_{ff}(\omega)+S_{nn}(\omega)\right)} \frac{S_{xf}(\omega)}{\left(S_{xx}(\omega)+S_{mm}(\omega)\right)}$$

$$= \frac{\gamma^2_{fx}(\omega)}{\left(1+\dfrac{S_{nn}(\omega)}{S_{ff}(\omega)}\right)\left(1+\dfrac{S_{mm}(\omega)}{S_{xx}(\omega)}\right)}$$

$$\Rightarrow \quad \gamma^2_{\tilde{f}\tilde{x}} \leq 1$$

Cases when $\gamma^2_{\tilde{f}\tilde{x}} \leq 1$

- There may be noise on one or other of the signals;
- The dynamic behaviour of the structure is nonlinear;
- The structure is excited by a non-recorded source of excitation (e.g. lateral coupling between the structure and the shaker).

Example of FRF measurement using random excitation

Coherence drop due to noise in the response signal

Coherence drop due to noise in the excitation signal

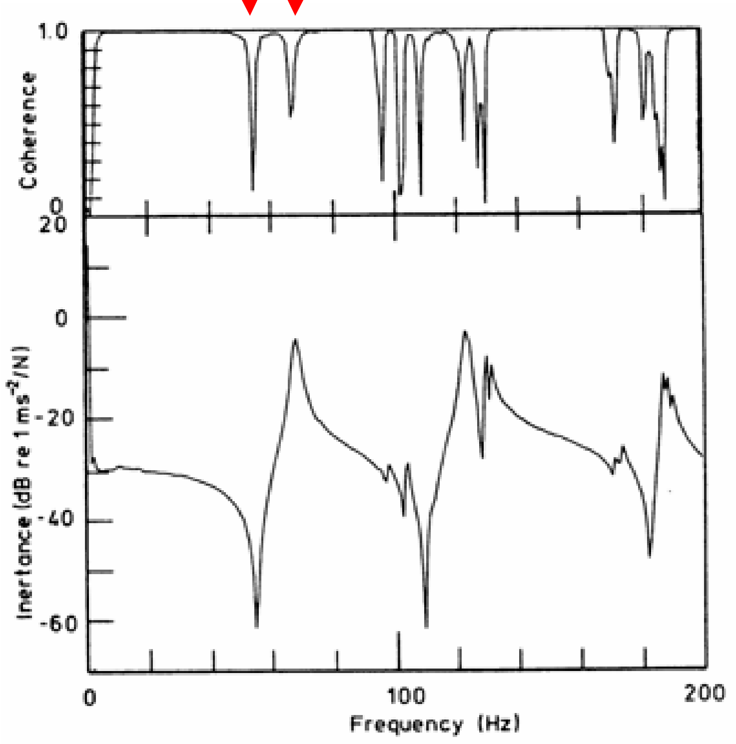

Example of application

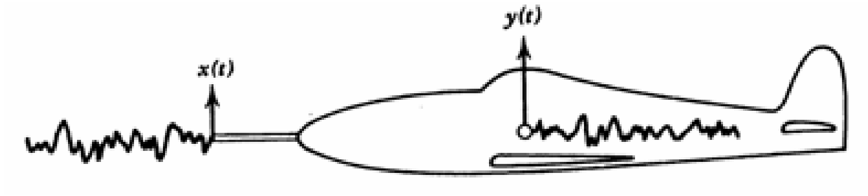

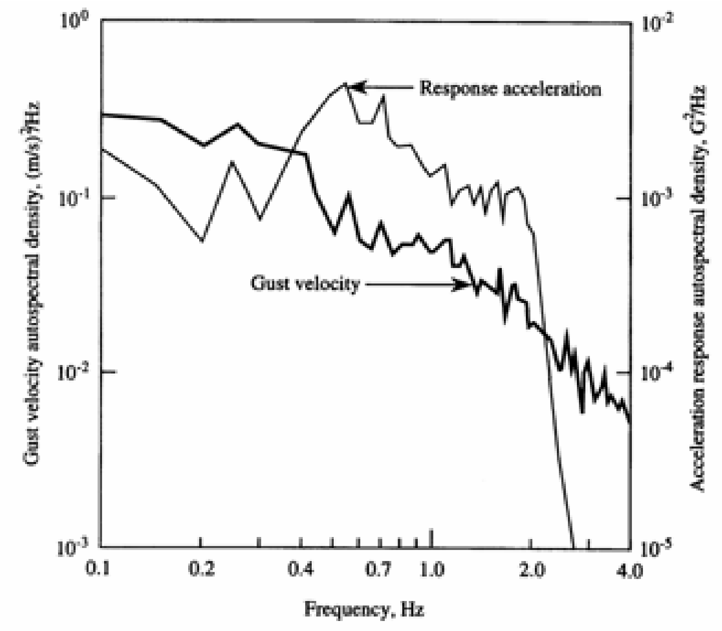

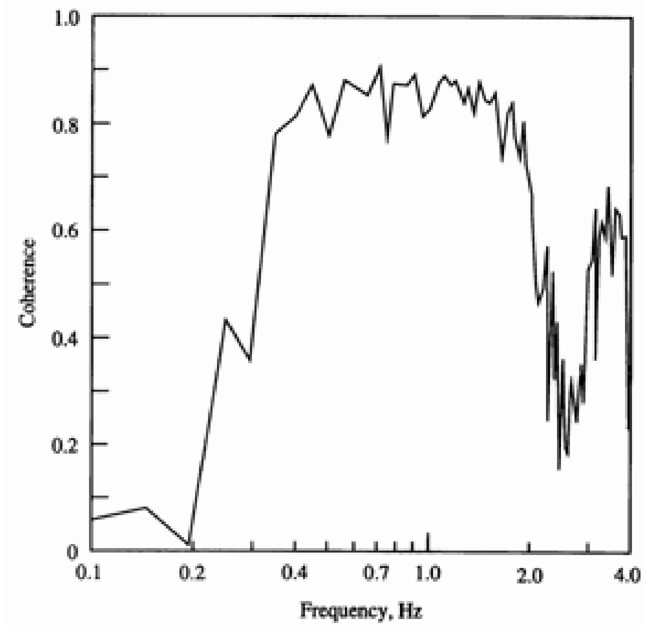

Transient Excitation

There are 3 types of transient excitation signals.

- **Burst excitation signals**

It consists of short sections of an underlying continuous signal (which may be a sine wave, a sine sweep or a random signal) followed by a period of zero input.

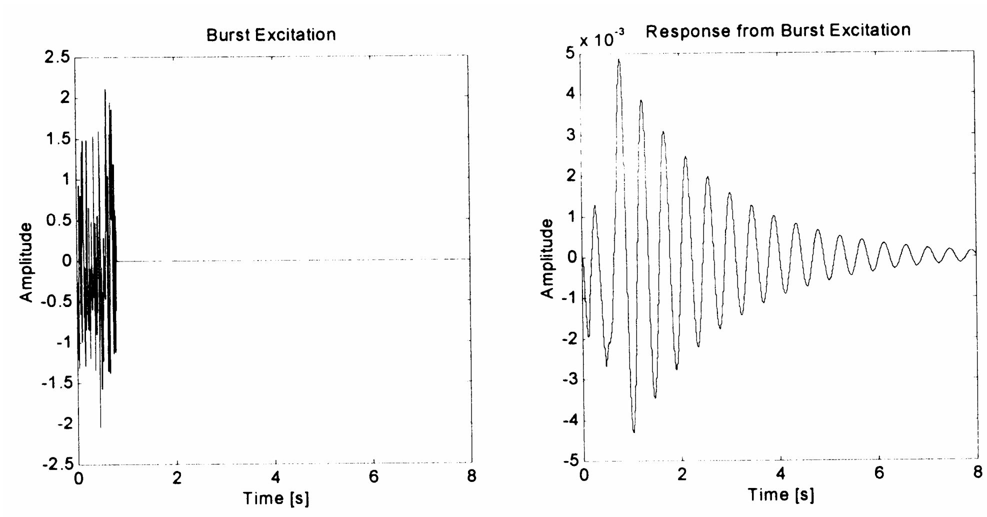

The duration of the burst is selected to allow the damping out of the response by the end of the measurement period (to avoid leakage errors).

- **Rapid sine sweep or 'chirp'**

  (short duration signal)

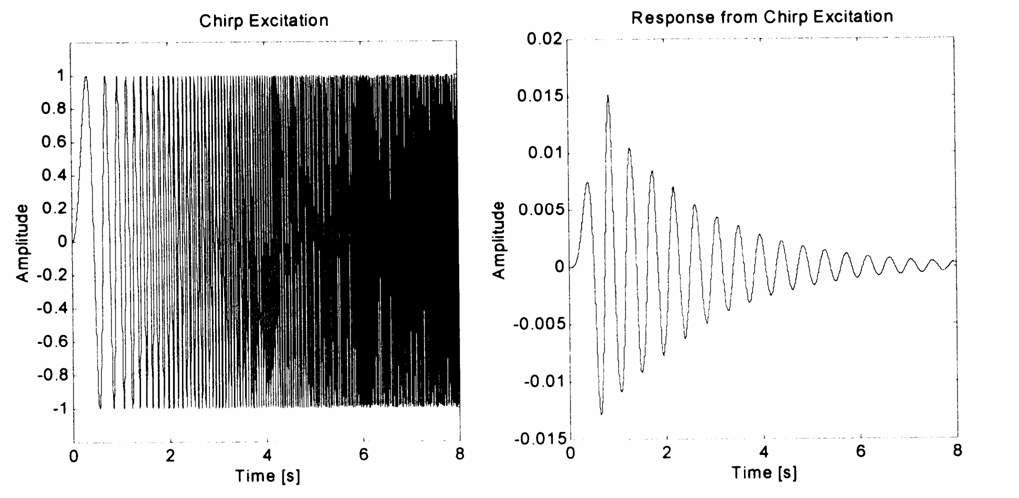

Good control of both the amplitude and the frequency content of the signal.

- **Impulsive excitation**

  - Impact controlled by a shaker attached to the structure

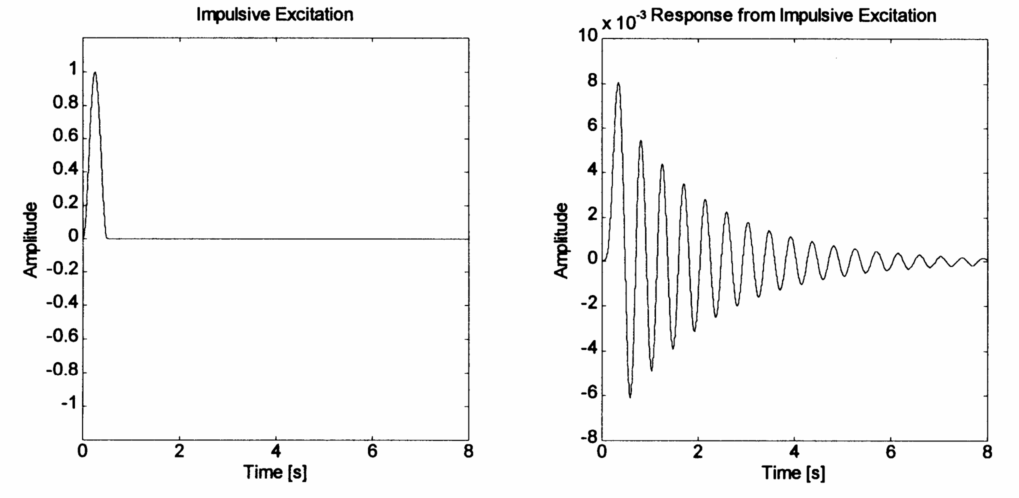

  - Impact from a hammer blow

One practical difficulty encountered when using the hammer excitation is that of the double-hit (rebound).

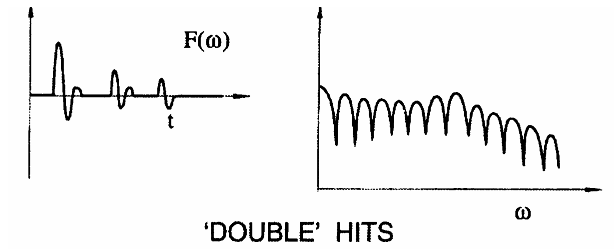

Periodicity assumption

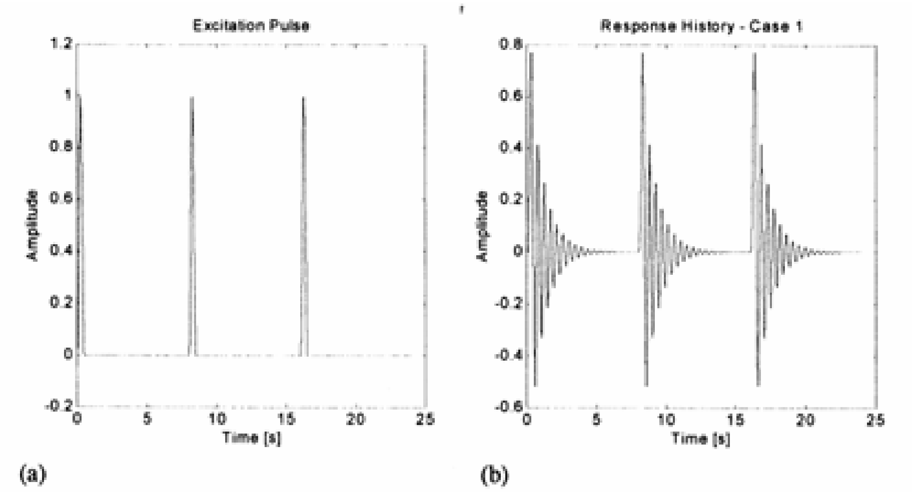

(a) Excitation pulse clearly satisfies the assumption

(b) The response history also satisfies the assumption

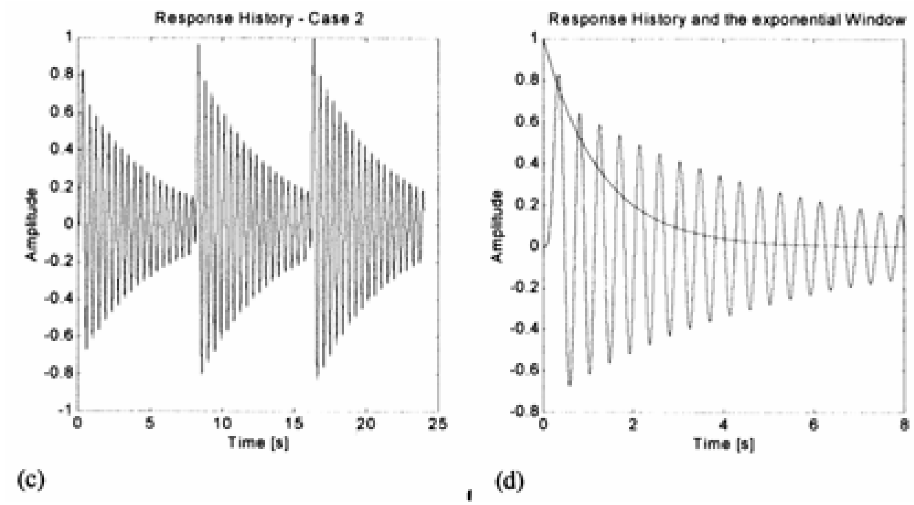

(c) The response history does not satisfy the assumption (for the period T selected)

(d) Exponential window

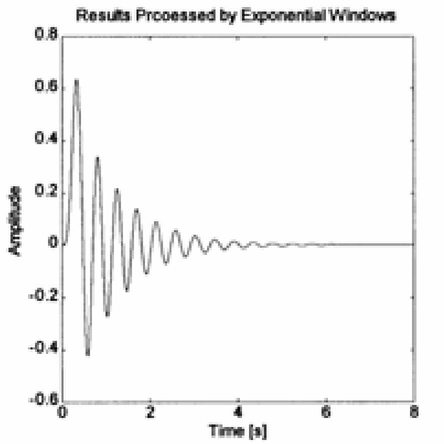

(e)

(e) Results processed by exponential window

Impulsive excitation as pseudo-periodic function

Types of excitation

No single method is the ‘best’ and it is probably worth making use of several types in order to optimise time, effort and accuracy.

SIGNAL	CARACTERISTIQUES DE LA STRUCTURE						EXCITATION LONGUE		MOYENS IMPORTANTS	
	LINEAIRE		PEU AMORTIE		MODES PROCHES					
	OUI	NON	OUI	NON	OUI	NON	OUI	NON	OUI	NON
SINUS	*	*	*	*	*	*	*			*
CHIRP	*	*	*			*		*		*
PSEUDO-RD	*	*	*	*		*		*		*
RANDOM	*	*	*	*	*	*		*		*
TRANSIENT-RD	*	*	*	*	*	*	*		*	
PERIODIC-RD	*	*	*	*	*	*	*		*	
TRANSITOIRE	*		*			*		*		*

Modal Identification Methods

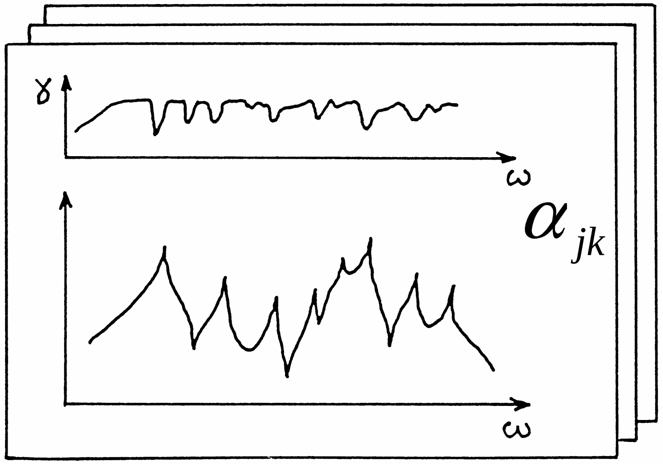

1. FRF measurements

(e.g. 800 lines / spectrum)

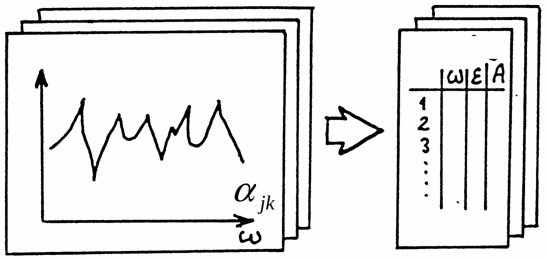

2. Modal parameter extraction

⇨ data reduction

(e.g. 6 modes x 4 values = 24 values/spectrum)

$$H_{rs}(\omega) = \sum_{k=1}^{N} \frac{A_{rs(k)}}{\omega_k^2 - \omega^2 + 2\, i\, \zeta_k\, \omega\, \omega_k}$$

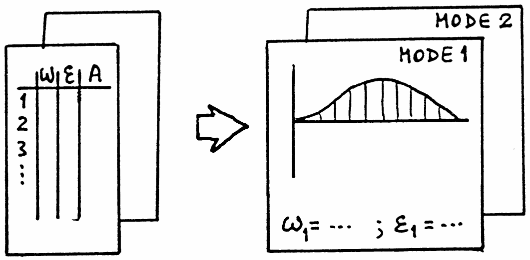

3. Derivation of a mathematical model

(Spatial model, Modal Model)

Classification of modal identification methods

Frequency Domain (FRF's)	↔	Time Domain (IRF's or response histories)
SDOF methods	↔	MDOF methods
Single-FRF methods	↔	Multi-FRF methods

Difficulties :

- modelling of damping effects,
- model order.

SDOF Modal Identification Methods

⚠ SDOF means that just one resonance is considered at a time

Assumption: the modes must appear clearly separated so that they can be analysed sequentially, one after the other.

$$H_{rs}(\omega) = \sum_{k=1}^{N} \frac{A_{rs(k)}}{\omega_k^2 - \omega^2 + 2\,i\,\zeta_k\,\omega\,\omega_k} = \frac{A_{rs(k)}}{\omega_k^2 - \omega^2 + 2\,i\,\zeta_k\,\omega\,\omega_k} + \underbrace{\sum_{\substack{j=1\\ j\neq k}}^{N} \frac{A_{rs(j)}}{\omega_j^2 - \omega^2 + 2\,i\,\zeta_j\,\omega\,\omega_j}}$$

$$\Rightarrow \quad H_{rs}(\omega) \cong \frac{A_{rs(k)}}{\omega_k^2 - \omega^2 + 2\,i\,\zeta_k\,\omega\,\omega_k} + B_{rs(k)}$$

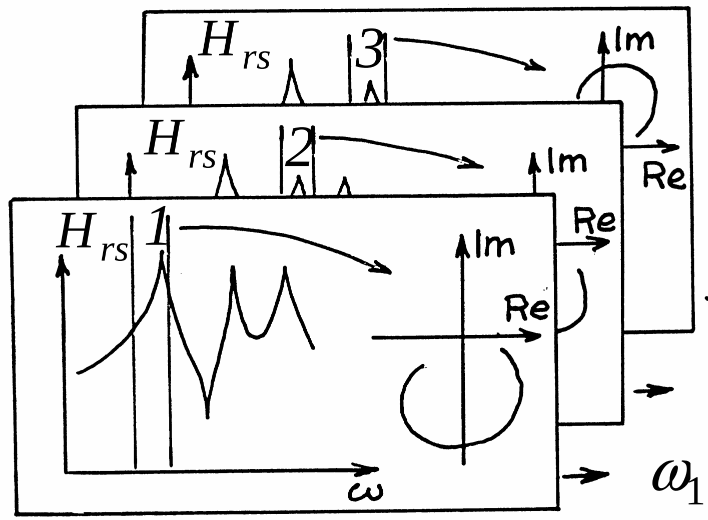

$\rightarrow \omega_3, \zeta_3, A_{rs(3)}$

$\rightarrow \omega_2, \zeta_2, A_{rs(2)}$

$\rightarrow \omega_1, \zeta_1, A_{rs(1)}$

a) Peak-Amplitude Method (Peak-Picking)

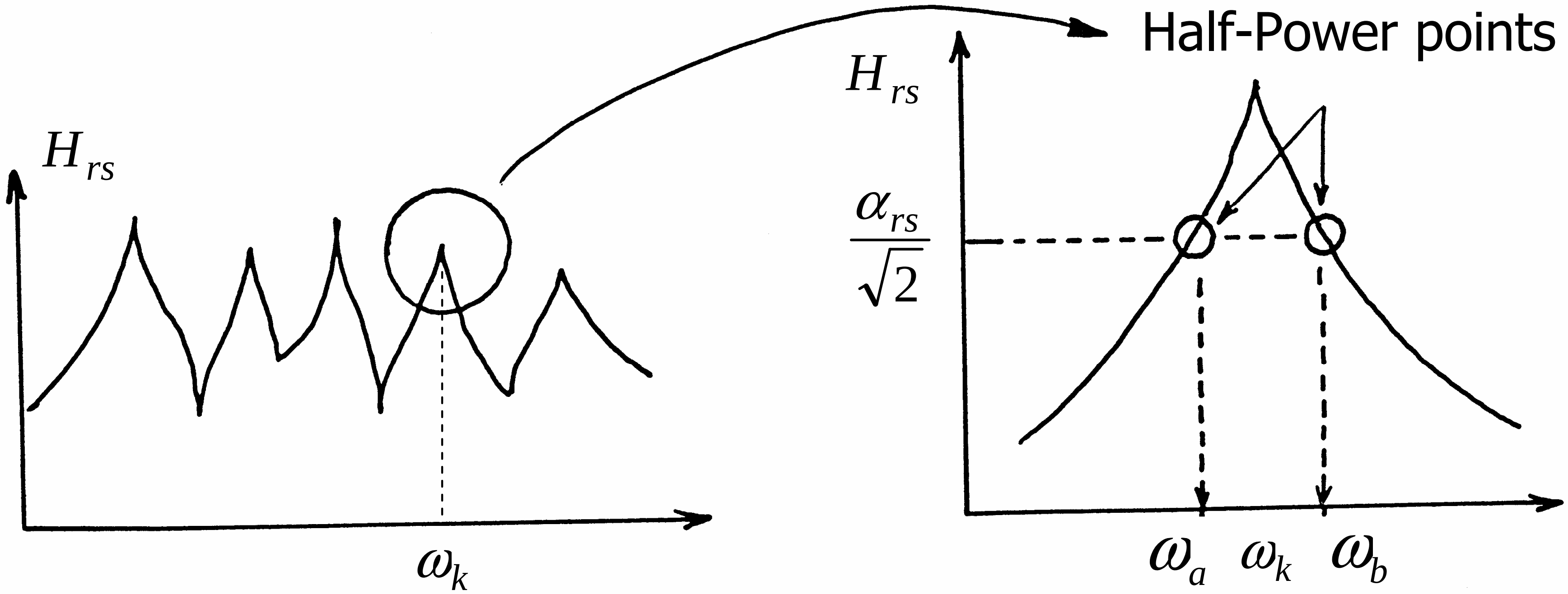

Estimation of the damping ratio using the quality factor:

$$Q = \frac{\omega_k}{\omega_a - \omega_b} = \frac{1}{2\,\zeta_k}$$

b) Circle-Fit Method

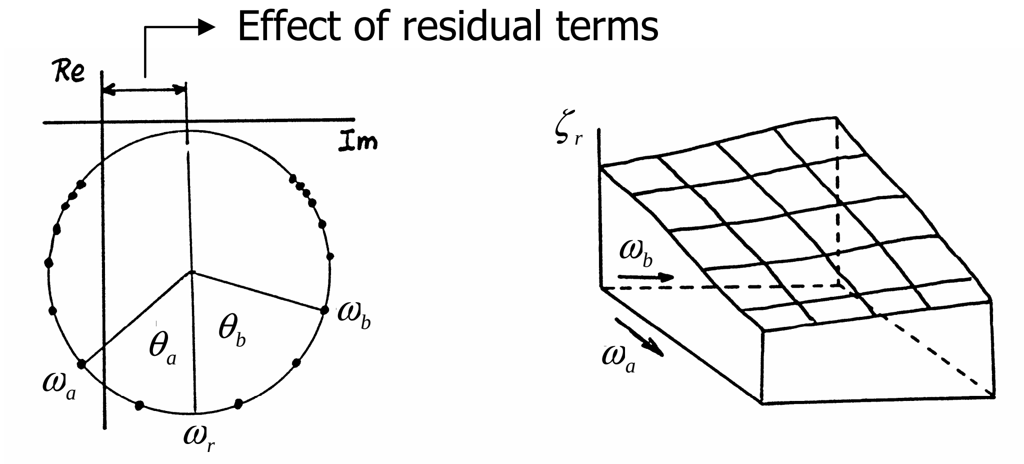

detection of nonlinear behaviour

Circle-fitting FRF plot in the vicinity of resonance

$$\zeta_k = \frac{\omega_a^2 - \omega_b^2}{\omega_k^2 \left(\tan(\theta_a/2) + \tan(\theta_b/2)\right)}$$

Concept of residual terms

To take into account the influence of modes which exist outside the frequency range of measurement and/or analysis, any FRF coefficient may be rewritten as:

$$\alpha_{jk}(\omega) = \sum_{r=1}^{N} \frac{{}_rA_{jk}}{\omega_r^2 - \omega^2 + 2\,i\,\zeta_r\,\omega\,\omega_r}$$

$$= \left(\underbrace{\sum_{r=1}^{m_1-1}}_{\text{Low-frequency modes}} + \underbrace{\sum_{r=m_1}^{m_2}}_{\text{Modes actually identified}} + \underbrace{\sum_{r=m_2+1}^{N}}_{\text{High-frequency modes}} \right) \frac{{}_rA_{jk}}{\omega_r^2 - \omega^2 + 2\,i\,\zeta_r\,\omega\,\omega_r}$$

Contributions of low-, medium- and high frequency modes

$$H_{rs}(\omega) = -\frac{1}{\omega^2 \, M_{rs}^{R}} + \sum_{k=m_1}^{m_2} \frac{A_{rs(k)}}{\omega_k^2 - \omega^2 + 2\, i\, \zeta_k \, \omega\, \omega_k} + \frac{1}{K_{rs}^{R}}$$

Residual mass

Residual stiffness

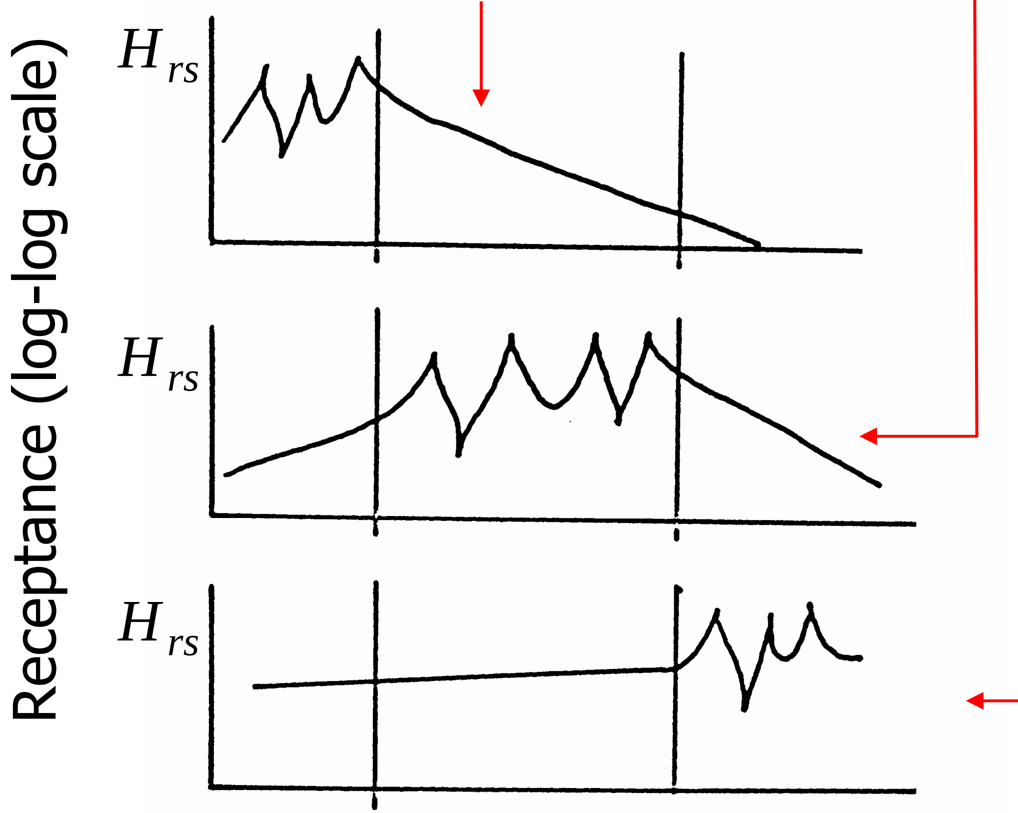

Examples of regenerated FRF's

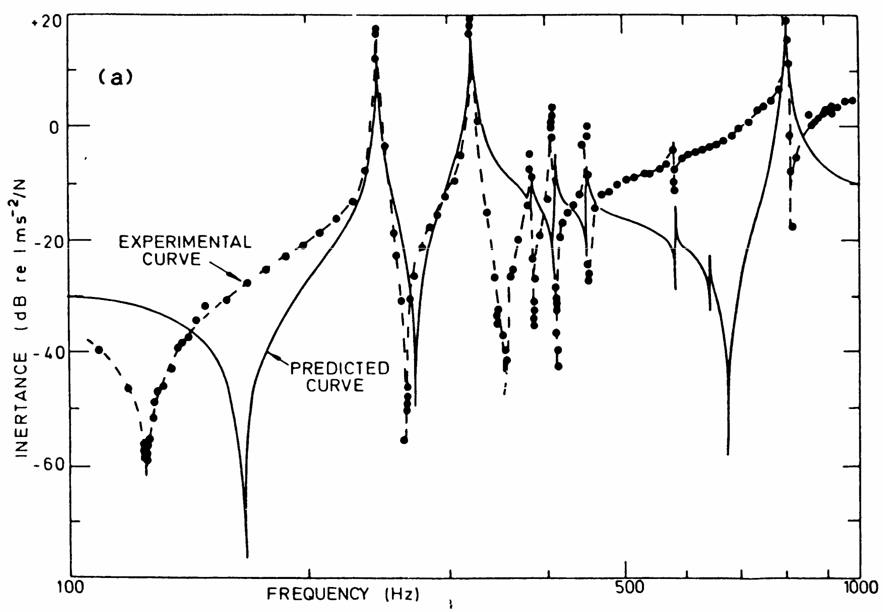

← without residuals

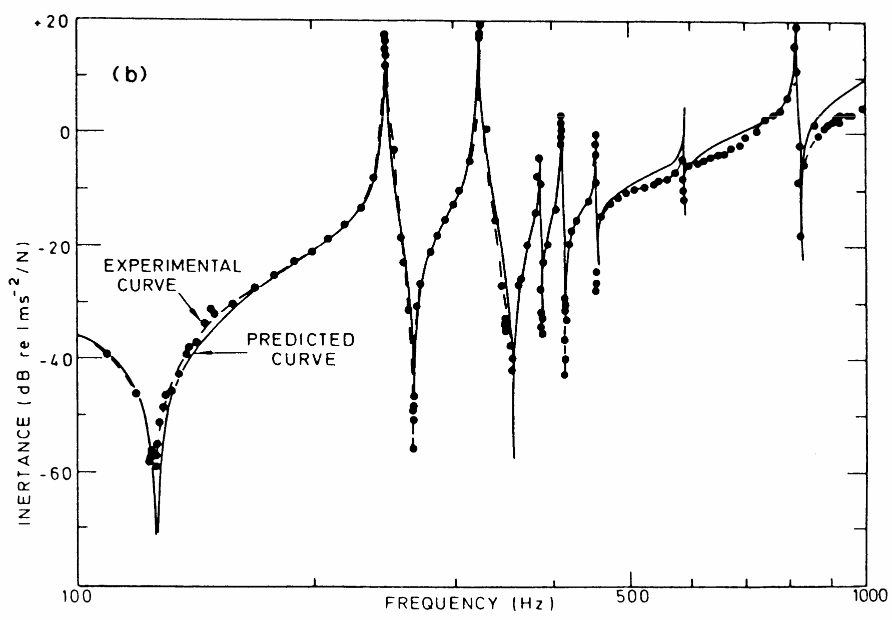

← with residuals

MDOF Modal Identification Methods

a) Least Squares Complex Exponential (LSCE)

Features:

- Time-domain technique
- Global estimation of natural frequency and damping of several modes simultaneously

Theoretical basis:

The general expression used for the FRF of a damped system in terms of modal parameters is:

$$H_{rs}(\omega) = \sum_{k=1}^{N} \frac{z_{r(k)}\, z_{s(k)}}{\rho_k\,(i\,\omega - \lambda_k)} + \frac{z^*_{r(k)}\, z^*_{s(k)}}{\rho^*_k\,(i\,\omega - \lambda^*_k)}$$

$$= \sum_{k=1}^{N} \frac{A_{rs(k)}}{(i\,\omega - \lambda_k)} + \frac{A^*_{rs(k)}}{(i\,\omega - \lambda^*_k)}$$

Taking the inverse Fourier Transform, the expression for an Impulse Response Function (IRF) in terms of modal parameters writes:

$$h_{rs}(t) = \sum_{k=1}^{N} A_{rs(k)}\, e^{\lambda_k t} + A^*_{rs(k)}\, e^{\lambda^*_k t} = 2\,\mathrm{Re}\left(\sum_{k=1}^{N} A_{rs(k)}\, e^{\lambda_k t} \right)$$

Time sampling: $t = j\,\Delta t$

$$h_{rs}(j\,\Delta t) = 2\,\mathrm{Re}\left(\sum_{k=1}^{N} A_{rs(k)}\, Z_k^{\,j} \right)$$

$Z_k = e^{\lambda_k\,\Delta t}$ defines the natural frequency and damping ratio of mode k (= global estimate)

$A_{rs(k)}$ defines the displacement of point r in mode k (= local estimate)

The unknowns Z_k may be considered as the roots of a polynomial of order $2N$:

$$P(Z) = \prod_{\substack{k=-N \\ k\neq 0}}^{N} \left(Z - Z_k\right) = \sum_{p=0}^{2N} \alpha_p \, Z^p$$

where the coefficients α_p have to be estimated using data measured on the system.

For this purpose, let us consider the expression of the IRF

$$h_{rs}(j\,\Delta t) = 2\,\mathrm{Re}\left(\sum_{k=1}^{N} A_{rs(k)}\, Z_k^{\,j} \right)$$

The IRF at a series of $2N$ equally spaced time intervals is:

$$\alpha_0 \times \{ \quad h_{rs}(0) = 2\,\mathrm{Re}\left(\sum_{k=1}^{N} A_{rs(k)}\, Z_k^0 \right) \quad \}$$

$$\vdots$$

$$\alpha_p \times \{ \quad h_{rs}(p\,\Delta t) = 2\,\mathrm{Re}\left(\sum_{k=1}^{N} A_{rs(k)}\, Z_k^p \right) \quad \}$$

$$\vdots$$

$$\alpha_{2N} \times \{ \quad h_{rs}(2N\,\Delta t) = 2\,\mathrm{Re}\left(\sum_{k=1}^{N} A_{rs(k)}\, Z_k^{2N} \right) \quad \}$$

$$\sum_{p=0}^{2N} \alpha_p\, h_{rs}(p\,\Delta t) = 2\,\mathrm{Re}\left(\underbrace{\sum_{k=1}^{N} A_{rs(k)} \sum_{p=0}^{2N} \alpha_p\, Z_k^p}_{} \right)$$

= 0 from the definition

$$\Longrightarrow \quad \sum_{p=0}^{2N} \alpha_p\, h_{rs}(p\,\Delta t) = 0$$

It follows that:

$$\sum_{p=0}^{2N-1} \alpha_p \, h_{rs}(p\,\Delta t) = -h_{rs}(2N\,\Delta t)$$

To estimate the coefficients α_p in a least squares sense, let express this equation:

- for all possible time points: $(2N+\ell)\,\Delta t \quad (\ell = 0, 1, \ldots, n_t)$
- for all possible measured responses: $(r = 1, \ldots, n_o)$
- for all possible excitation points: $(s = 1, \ldots, n_i)$

$$\sum_{p=0}^{2N-1} \alpha_p \, h_{rs}\big((p+\ell)\,\Delta t\big) = -h_{rs}\big((2N+\ell)\,\Delta t\big)$$

Thus the matrix:

$$\underbrace{\begin{bmatrix} h_{11}(0) & h_{11}(\Delta t) & \cdots & h_{11}((2N-1)\Delta t) \\ h_{11}(\Delta t) & h_{11}(2\,\Delta t) & \cdots & h_{11}(2N\,\Delta t) \\ \vdots & \vdots & & \vdots \\ h_{11}(n_t\,\Delta t) & h_{11}((n_t+1)\Delta t) & \cdots & h_{11}((n_t+2N-1)\Delta t) \\ \vdots & \vdots & & \vdots \\ h_{rs}(\ell\,\Delta t) & h_{rs}((1+\ell)\Delta t) & \cdots & h_{rs}((2N-1+\ell)\Delta t) \\ \vdots & \vdots & & \vdots \\ h_{n_o n_i}(n_t\,\Delta t) & h_{n_o n_i}((n_t+1)\Delta t) & \cdots & h_{n_o n_i}((n_t+2N-1)\Delta t) \end{bmatrix}}_{\mathbf{A}} \underbrace{\begin{Bmatrix} \alpha_0 \\ \alpha_1 \\ \vdots \\ \alpha_{2N-1} \end{Bmatrix}}_{\mathbf{x}} = \underbrace{\begin{Bmatrix} -h_{11}(2N\,\Delta t) \\ -h_{11}((2N+1)\Delta t) \\ \vdots \\ -h_{11}((2N+n_t)\Delta t) \\ \vdots \\ -h_{rs}((2N+\ell)\Delta t) \\ \vdots \\ -h_{n_o n_i}((2N+n_t)\Delta t) \end{Bmatrix}}_{\mathbf{b}}$$

Overdetermined system: $\mathbf{A} \quad \mathbf{x} = \mathbf{b}$

which has the solution: $\mathbf{x} = \left(\mathbf{A}^T\,\mathbf{A}\right)^{-1}\mathbf{A}^T\,\mathbf{b}$

The solution: $\mathbf{x}^T = \{\alpha_0 \quad \alpha_1 \quad \cdots \quad \alpha_{2N-1}\}$

allows to reconstruct the polynomial: $P(Z) = \sum_{p=0}^{2N} \alpha_p \, Z^p$

and the roots: $Z_k = e^{\lambda_k \, \Delta t}$

gives the complex eigenvalues: $\lambda_k \quad (k = 1, 2, \ldots, N)$

If the eigenvalues may be further expressed as follows:

$$\lambda_k = \omega_k \left(-\zeta_k + i \sqrt{1 - \zeta_k^2} \right)$$

we obtain the values of the natural frequency ω_k and the damping ratio ζ_k (in the assumption of proportional damping).

Selection of the model order

By using a different number of poles ($2N$) and comparing the error between the regenerated FRF's and the original measured data, it is possible to draw a so-called 'stabilisation diagram':

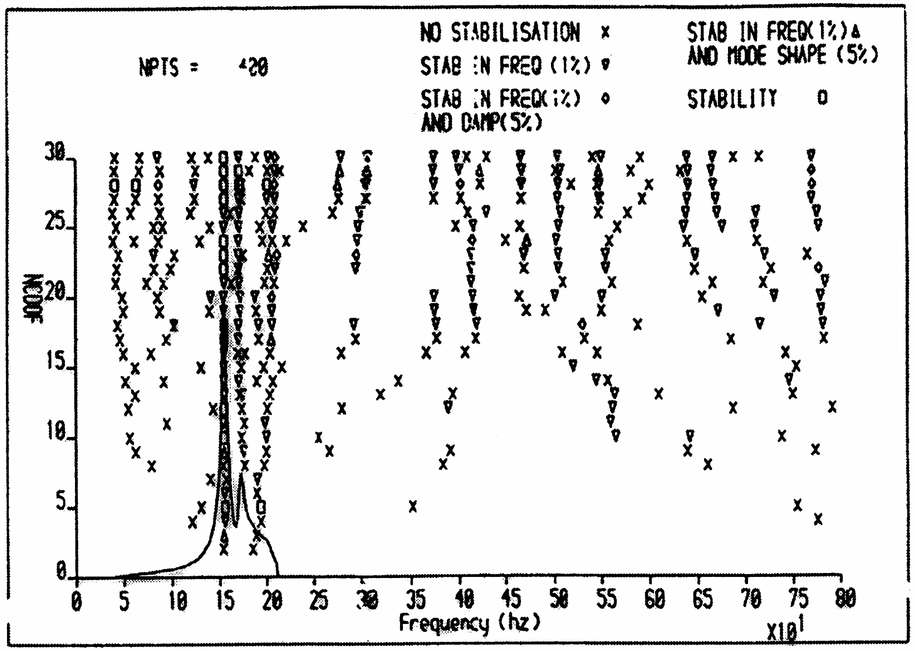

As the number of poles increases, a number of computational modes are created in addition to the genuine physical modes which are of interest.

b) Least Squares Frequency Domain (LSFD)

Features:

- Frequency domain technique
- Global estimation of residues (--> complex modes)

Theoretical basis:

FRF of a damped system in the frequency band $[\omega_{min}, \omega_{max}]$:

$$H_{rs}(\omega) = -\frac{1}{\omega^2 \, M_{rs}^R} + \left(\sum_{k=m_1}^{m_2} \frac{A_{rs(k)}}{(i\,\omega - \lambda_k)} + \frac{A_{rs(k)}^*}{(i\,\omega - \lambda_k^*)} \right) + \frac{1}{K_{rs}^R}$$

$$H_{rs}(\omega) = -\boxed{\frac{1}{\omega^2 M_{rs}^R}} + \left(\sum_{k=m_1}^{m_2} \frac{A_{rs(k)}}{(i\,\omega - \lambda_k)} + \frac{A_{rs(k)}^*}{(i\,\omega - \lambda_k^*)} \right) + \boxed{\frac{1}{K_{rs}^R}}$$

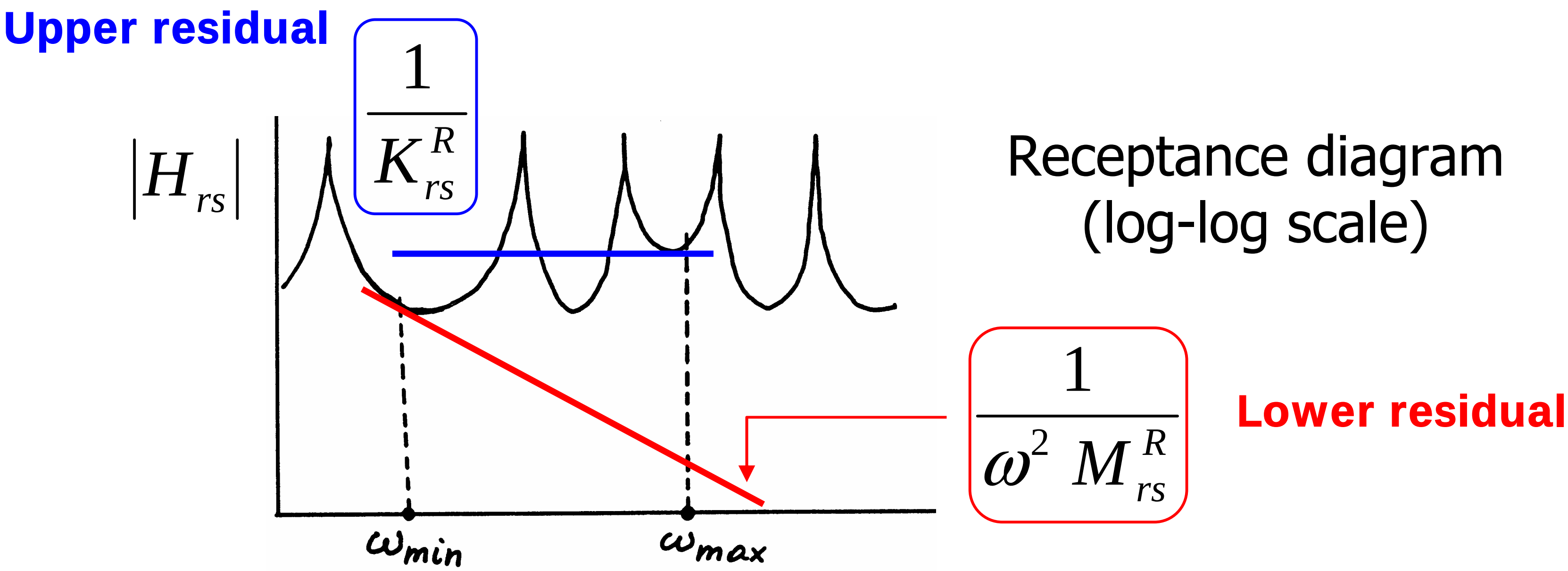

Receptance diagram (log-log scale)

$\left.\begin{array}{l} A_{rs(k)},\ A_{rs(k)}^* \\ K_{rs}^R,\quad M_{rs}^R \end{array}\right\}$ are local estimates (which depend on the locations of the measurement point (r) and of the excitation point (s)

Calculation of the residues $A_{rs(k)}$ and $A^*_{rs(k)}$

Assumption: the poles λ_k have been identified (LSCE method).

Writing:
$$\begin{cases} A_{rs(k)} = U_{rs(k)} + i\, V_{rs(k)} \\ A^*_{rs(k)} = U_{rs(k)} - i\, V_{rs(k)} \end{cases}$$

the FRF takes the form:

$$H_{rs}(\omega) = -\frac{1}{\omega^2\, M^R_{rs}} + \left(\sum_{k=m_1}^{m_2} U_{rs(k)}\, P_k(\omega) + V_{rs(k)}\, Q_k(\omega) \right) + \frac{1}{K^R_{rs}}$$

(2 *m*+2) unknowns with *m* = m_2 - m_1

We define the error as: $$E = \sum_{\omega=\omega_{\min}}^{\omega_{\max}} \left| \underbrace{H_{rs}(\omega)}_{\text{Theoretical value}} - \underbrace{H^{EXP}_{rs}(\omega)}_{\text{Measured data}} \right|^2$$

The error is minimised by differentiating its expression with respect to each unknowns in turn,

$$\frac{\partial E}{\partial U_{rs(k)}} = 0\,; \frac{\partial E}{\partial V_{rs(k)}} = 0\,; \quad (k = m_1, \ldots, m_2)$$

$$\frac{\partial E}{\partial K_{rs}} = 0\,; \frac{\partial E}{\partial M_{rs}} = 0$$

thus generating a set of ($2\ m+2$) equations with ($2\ m+2$) unknowns ($m = m_2 - m_1$).

Extraction of the (complex) eigenmodes.

For each identified pole k $(k = 1,.., m)$, we have:

$$\lambda_k, \quad \begin{aligned} A_{1s(k)} &= z_{1(k)}\ z_{s(k)} \\ A_{2s(k)} &= z_{2(k)}\ z_{s(k)} \\ \vdots &= \vdots \quad \vdots \\ A_{ss(k)} &= z_{s(k)}\ z_{s(k)} = z_{s(k)}^2 \longrightarrow z_{s(k)} = \sqrt{A_{ss(k)}} \\ \vdots &= \vdots \quad \vdots \\ A_{n_o s(k)} &= z_{n_o r}\ z_{s(k)} \end{aligned}$$

and thus:

$$z_{r(k)} = \frac{A_{rs(k)}}{z_{s(k)}} \qquad (r = 1, \ldots, n_o, r \neq s)$$

$\Rightarrow$ A transducer should not be located where $z_{s(k)}$ = 0 (on a vibration node)

In practice:

$$\mathbf{H}(\omega)=\begin{bmatrix} H_{11} & \cdots & H_{1s} & \cdots & H_{1n_i} \\ \vdots & & \vdots & & \vdots \\ H_{r1} & \cdots & H_{rs} & \cdots & H_{rn_i} \\ \vdots & & \vdots & & \vdots \\ H_{n_o1} & \cdots & H_{n_os} & \cdots & H_{n_on_i} \end{bmatrix}$$

« roving hammer »

Remarks

Frequency band

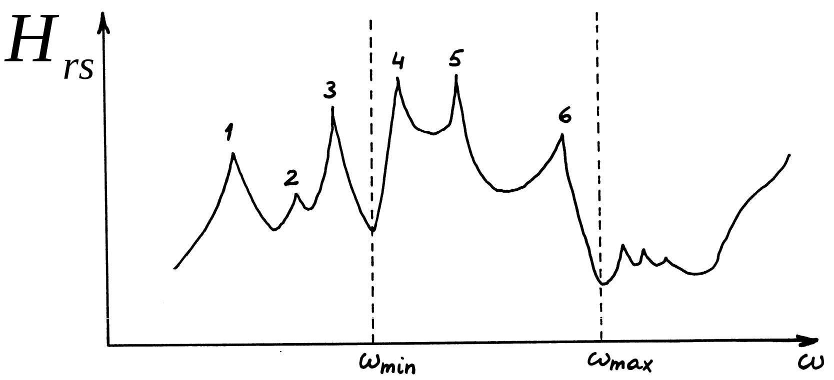

As modes 1, 2, 3 have been identified (poles and residues), their participation in the frequency range $[\omega_{min}, \omega_{max}]$ can be subtracted mathematically before identifying modes 4, 5 et 6.

Partial fitting

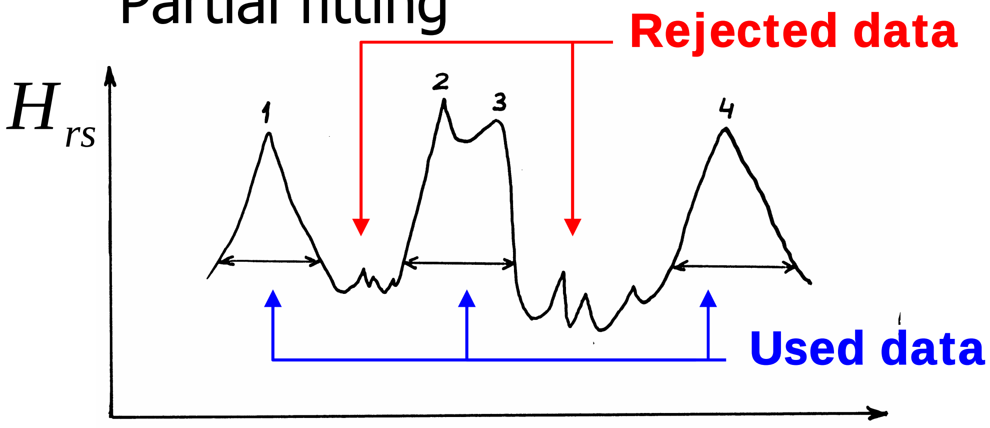

FRF data associated with a bad coherence are not considered for identification

c) Ibrahim Time Domain Method (ITD, 1973-77)

Features :

- Time-domain method
- Global estimation of poles and residues

Theoretical basis:

The free response of a viscously-damped system is given by:

Number of modes in the response

complex eigenvector $\mathbf{z}_{(k)}$ (unscaled mode)

Free response vector

$$\mathbf{q}(t) = \sum_{k=1}^{2n} \mathbf{z}_{(k)} \, e^{\lambda_k t}$$

Considering $2n$ time instants, the free response matrix is given by:

$$\underbrace{\begin{bmatrix}\mathbf{q}(t_1) & \ldots & \mathbf{q}(t_{2n})\end{bmatrix}}_{\substack{\mathbf{Q} \\ n\times 2n}} = \underbrace{\begin{bmatrix}\mathbf{z}_{(1)} & \ldots & \mathbf{z}_{(2n)}\end{bmatrix}}_{\substack{\mathbf{Z} \\ n\times 2n}} \underbrace{\begin{bmatrix} e^{\lambda_1 t_1} & \ldots & e^{\lambda_1 t_{2n}} \\ \vdots & & \vdots \\ e^{\lambda_{2n} t_1} & \ldots & e^{\lambda_{2n} t_{2n}} \end{bmatrix}}_{\substack{\mathbf{\Lambda} \\ 2n\times 2n}}$$

Considering a second set of samples shifted by an interval of time Δt with respect to the first set:

$$\mathbf{q}\left(t_j+\Delta t\right)=\sum_{k=1}^{2n}\mathbf{z}_{(k)}\; e^{\lambda_k\left(t_j+\Delta t\right)}=\sum_{k=1}^{2n}\underbrace{\mathbf{z}_{(k)}\; e^{\lambda_k \Delta t}}\; e^{\lambda_k t_j}$$

$$\underbrace{\left[\mathbf{q}\left(t_1+\Delta t\right)\quad \ldots \quad \mathbf{q}\left(t_{2n}+\Delta t\right)\right]}_{\mathbf{Q}_{\Delta t}}=\underbrace{\overbrace{\left[\hat{\mathbf{z}}_{(1)}\quad \ldots \quad \hat{\mathbf{z}}_{(2n)}\right]}}_{\hat{\mathbf{Z}}}\underbrace{\begin{bmatrix} e^{\lambda_1 t_1} & \ldots & e^{\lambda_1 t_{2n}} \\ \vdots & & \vdots \\ e^{\lambda_{2n} t_1} & \ldots & e^{\lambda_{2n} t_{2n}} \end{bmatrix}}_{\boldsymbol{\Lambda}}$$

$$\Rightarrow\quad \mathbf{Q}_{\Delta t}=\hat{\mathbf{Z}}\,\boldsymbol{\Lambda}$$

In the same way, for a time shift of $2\,\Delta t$

$$\begin{bmatrix}\mathbf{q}(t_1+2\Delta t) & \dots & \mathbf{q}(t_{2n}+2\Delta t)\end{bmatrix}=\begin{bmatrix}\hat{\hat{\mathbf{z}}}_{(1)} & \dots & \hat{\hat{\mathbf{z}}}_{(2n)}\end{bmatrix}\begin{bmatrix} e^{\lambda_1 t_1} & \dots & e^{\lambda_1 t_{2n}} \\ \vdots & & \vdots \\ e^{\lambda_{2n} t_1} & \dots & e^{\lambda_{2n} t_{2n}}\end{bmatrix}$$

with $\hat{\hat{\mathbf{z}}}_{(i)} = \mathbf{z}_{(i)}\, e^{2\,\lambda_i\,\Delta t}$

$$\Rightarrow \quad \mathbf{Q}_{2\,\Delta t} = \hat{\hat{\mathbf{Z}}}\,\mathbf{\Lambda}$$

Thus, we have: $$\begin{bmatrix}\mathbf{Q}\\ \mathbf{Q}_{\Delta t}\end{bmatrix} = \begin{bmatrix}\mathbf{Z}\\ \hat{\mathbf{Z}}\end{bmatrix}\boldsymbol{\Lambda} \quad \text{or} \quad \boldsymbol{\Phi} = \mathbf{A}\ \boldsymbol{\Lambda}$$

and $$\begin{bmatrix}\mathbf{Q}_{\Delta t}\\ \mathbf{Q}_{2\,\Delta t}\end{bmatrix} = \begin{bmatrix}\hat{\mathbf{Z}}\\ \hat{\hat{\mathbf{Z}}}\end{bmatrix}\boldsymbol{\Lambda} \quad \text{or} \quad \hat{\boldsymbol{\Phi}} = \hat{\mathbf{A}}\ \boldsymbol{\Lambda}$$

Eliminating $\boldsymbol{\Lambda}$ gives: $$\hat{\boldsymbol{\Phi}}\,\boldsymbol{\Phi}^{-1}\,\mathbf{A} = \hat{\mathbf{A}}$$

If we define: $\mathbf{A} = [\mathbf{a}_1 \quad \dots \quad \mathbf{a}_n]$ and $\hat{\mathbf{A}} = [\hat{\mathbf{a}}_1 \quad \dots \quad \hat{\mathbf{a}}_n]$

We have: $$\hat{\boldsymbol{\Phi}}\,\boldsymbol{\Phi}^{-1}\,\mathbf{a}_i = \hat{\mathbf{a}}_i \quad \Rightarrow \quad \underbrace{\hat{\boldsymbol{\Phi}}\,\boldsymbol{\Phi}^{-1}\,\mathbf{a}_i = e^{\lambda_i\,\Delta t}\,\mathbf{a}_i}_{\text{Eigenvalue problem}}$$

The eigenvectors $\mathbf{a}_i$ have their first n co-ordinates equal to the eigenmodes of the structure and λ_i are the complex eigenvalues.

If the number of time samples is greater than the number of modes excited, then matrices $\mathbf{\Phi}$ are rectangular and the eigenvalue problem is transformed into:

$$\left(\hat{\mathbf{\Phi}}\;\mathbf{\Phi}^{T}\right)\left[\mathbf{\Phi}\;\mathbf{\Phi}^{T}\right]^{-1}\mathbf{a}_i = e^{\lambda_i\,\Delta t}\;\mathbf{a}_i$$

Modal Confidence Factor

Since the order of matrix $\left(\hat{\mathbf{\Phi}}\ \mathbf{\Phi}^T\right)\left[\mathbf{\Phi}\ \mathbf{\Phi}^T\right]^{-1}$ may exceed the number of modes excited, it remains to separate the structural modes from the numerical modes.

For this purpose, let us write the response of the real stations delayed by a time-interval $\Delta\tau$: $\mathbf{q}(t+\Delta\tau)=\mathbf{q}'(t)$ i.e.

$$\mathbf{q}'(t)=\sum_{k=1}^{2n}\mathbf{z}_{(k)}\ e^{\lambda_k(t+\Delta\tau)}=\sum_{k=1}^{2n}\mathbf{z}_{(k)}\ e^{\lambda_k\Delta\tau}\ e^{\lambda_k t}=\sum_{k=1}^{2n}\mathbf{z}'_{(k)}\ e^{\lambda_k t}$$

If $\mathbf{z}_{i(k)}$ is the i th deflection of the k th mode at the real station, then the value at the assumed station delayed by $\Delta\tau$ is expected to be:

$$\mathbf{z}_{i(k),\text{expected}}=\mathbf{z}_{i(k)}\ e^{\lambda_k\Delta\tau}$$

The Modal Confidence Factor (MCF) is defined as:

$$\mathrm{MCF} = \left| \frac{\mathbf{z}_{i(k),\text{expected}}}{\mathbf{z}'_{i(k)}} \right|$$

and should be near 1.

d) Stochastic Subspace Identification Method

Features:

- Time-domain method
- Global estimation of poles and residues

Theoretical background: Stochastic model in the state-space.

Given a n-dimensional time series $\mathbf{q}[k] = \mathbf{q}(t_k)$, the dynamic behavior of the system may be described by the state space model

State vector

State matrix

$$\mathbf{r}[k+1] = \mathbf{A}\,\mathbf{r}[k] + \mathbf{w}[k]$$

Process noise

$$\mathbf{q}[k] = \mathbf{B}\,\mathbf{x}[k] + \mathbf{v}[k]$$

Measurement noise

Output matrix

Assumption: $\mathbf{w}$ and $\mathbf{v}$ are zero-mean Gaussian white noise.

The covariance matrices of $\mathbf{w}$ and $\mathbf{v}$ are:

Covariance matrices

Expectation

$$E\left[\begin{pmatrix}\mathbf{w}[k]\\ \mathbf{v}[k]\end{pmatrix}\begin{pmatrix}\mathbf{w}[k+t]^T & \mathbf{v}[k+t]^T\end{pmatrix}\right]=\begin{pmatrix}\mathbf{Q} & \mathbf{S}\\ \mathbf{S} & \mathbf{R}\end{pmatrix}\delta(t)$$

The output covariance matrices are defined as

$$\mathbf{\Lambda}_0 = E\left[\mathbf{q}[k] \quad \mathbf{q}[k]^T\right]$$

$$\mathbf{\Lambda}_i = E\left[\mathbf{q}[k+i] \quad \mathbf{q}[k]^T\right]$$

As $\mathbf{w}[k]$ and $\mathbf{v}[k]$ are independent of the state vector $\mathbf{r}[k]$, the following properties can be established:

$$E\left[\mathbf{r}[k]\,\mathbf{r}[k]^T\right] = \mathbf{A}\,\mathbf{\Sigma}_0\,\mathbf{A}^T + \mathbf{Q}$$

$$E\left[\mathbf{r}[k+1]\,\mathbf{r}[k]^T\right] = \mathbf{G} = \mathbf{A}\,\mathbf{\Sigma}_0\,\mathbf{B}^T + \mathbf{S}$$

$$\mathbf{\Lambda}_0 = \mathbf{B}\,\mathbf{\Sigma}_0\,\mathbf{B}^T + \mathbf{R}$$

$$\mathbf{\Lambda}_i = \mathbf{B}\,\mathbf{A}^{i-1}\,\mathbf{G}$$

where $\mathbf{\Sigma}_0$ is the state covariance matrix and $\mathbf{G}$ is referred as the next state-output covariance matrix.

Covariance-Driven Stochastic Subspace Method

Let us construct the Hankel matrix with p block rows and q block columns of the output covariance matrix $\mathbf{\Lambda}_i$

$$\mathbf{H}_{p,q} = \begin{bmatrix} \mathbf{\Lambda}_1 & \mathbf{\Lambda}_2 & \cdots & \cdots & \mathbf{\Lambda}_q \\ \mathbf{\Lambda}_2 & \mathbf{\Lambda}_3 & \cdots & \cdots & \mathbf{\Lambda}_{q+1} \\ \cdots & \cdots & \cdots & \cdots & \cdots \\ \mathbf{\Lambda}_p & \mathbf{\Lambda}_{p+1} & \cdots & \cdots & \mathbf{\Lambda}_{p+q+1} \end{bmatrix} \qquad (q \geq p)$$

The pth-order observability and controllability matrices are respectively:

$$\mathbf{O}_p = \begin{bmatrix} \mathbf{B} & \mathbf{B\,A} & \cdots & \mathbf{B\,A}^{p-1} \end{bmatrix}^T$$

$$\mathbf{C}_q = \begin{bmatrix} \mathbf{G} & \mathbf{A\,G} & \cdots & \mathbf{A}^{q-1}\,\mathbf{G} \end{bmatrix}$$

The previous relationship $\mathbf{\Lambda}_i = \mathbf{B}\,\mathbf{A}^{i-1}\,\mathbf{G}$

leads to the following factorisation property

$$\mathbf{H}_{p,q} = \mathbf{O}_p\,\mathbf{C}_q$$

Let $\mathbf{W}_1$ and $\mathbf{W}_2$ be two user-defined invertible weighting matrices of dimension p x m and q x m respectively. Performing the following singular value decomposition gives:

$$\mathbf{W}_1\,\mathbf{H}_{p,q}\,\mathbf{W}_2 = [\mathbf{U}_1 \quad \mathbf{U}_2]\begin{bmatrix} \mathbf{S}_1 & 0 \\ 0 & 0 \end{bmatrix}[\mathbf{V}_1 \quad \mathbf{V}_2]^T = \mathbf{U}_1\,\mathbf{S}_1\,\mathbf{V}_1^T$$

S1 contains $2\,N_m$ non-zero singular values where N_m is the number of system modes.

It follows that the observability and controllability matrices can be recovered as

$$\mathbf{O}_p = \mathbf{U}_1\, \mathbf{S}_1^{1/2}$$

$$\mathbf{C}_q = \mathbf{S}_1^{1/2}\, \mathbf{V}_1^T$$

Let us write

$$\mathbf{O}_p^{\uparrow} = \begin{bmatrix} \mathbf{B}\,\mathbf{A} & \mathbf{B}\,\mathbf{A}^2 & \cdots & \mathbf{B}\,\mathbf{A}^{p-1} \end{bmatrix}^T = \mathbf{O}_{p-1}\, \mathbf{A}$$

may be determined by making use of $\mathbf{O}_p$ matrix

Matrices $\mathbf{A}$ and $\mathbf{B}$ then the eigenvalues and eigenvectors of the system may be easily computed.

Comparison and Correlation Techniques

- Visual inspection experimental / calculated mode-shapes.
- Visual inspection of regenerated / predicted FRFs.
- Use of mathematical tools.

Let us note:

x_X an experimental (complex) eigenvector;

x_A an analytical eigenvector (predicted by a model);

Modal Scale Factor (MSF)

$$MSF = \frac{\mathbf{x}_X^T \ \mathbf{x}_A}{\mathbf{x}_A^T \ \mathbf{x}_A} \qquad \text{or} \qquad MSF = \frac{\mathbf{x}_X^T \ \mathbf{x}_A}{\mathbf{x}_X^T \ \mathbf{x}_X}$$

depending upon which mode-shape is taken as the reference one.

$$MAC = \frac{\left| \mathbf{x}_X^T \ \mathbf{x}_A \right|^2}{(\mathbf{x}_X^T \ \mathbf{x}_X)\,(\mathbf{x}_A^T \ \mathbf{x}_A)} \qquad (0 \leq MAC \leq 1)$$

Graphical representations

Analytical mode number \ Experimental mode number	1	2	3	4	5	6	7	8	9	10
1	100	0	1	0	0	0	0	0	0	0
2	0	100	1	1	0	0	0	0	0	0
3	0	1	94	3	2	0	0	0	0	0
4	0	0	2	92	5	3	0	0	0	0
5	0	0	0	4	86	7	4	0	0	0
6	0	0	0	0	7	81	9	5	0	0
7	0	0	0	0	0	10	75	10	5	0
8	0	0	0	0	0	0	12	71	11	5
9	0	0	0	0	0	0	0	14	68	11
10	0	0	0	0	0	0	0	0	16	65

MODAL ASSURANCE CRITERION (MAC) %

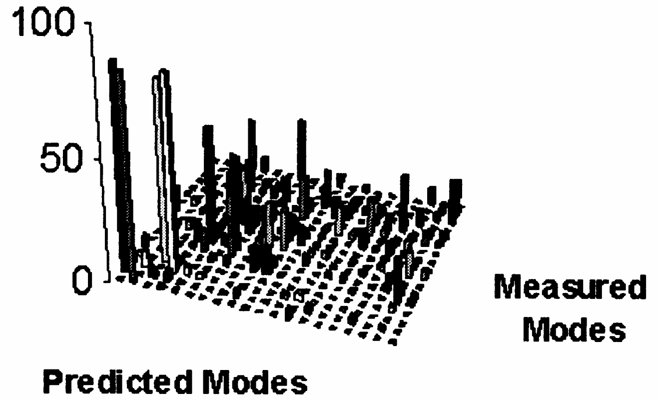

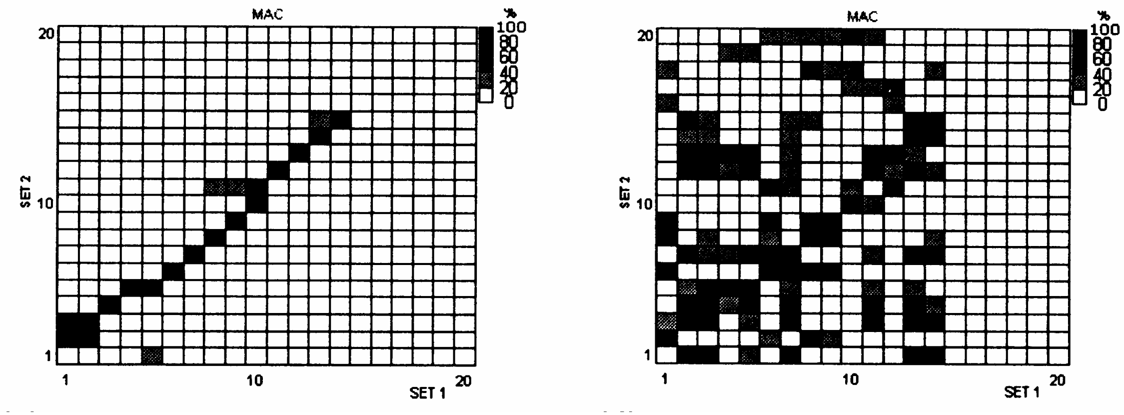

Causes of bad correlation:

- presence of non-linearities, noisy data
- bad modal identification
- inappropriate choice of measurement coordinates
- modelling uncertainties (physical parameters, geometry)
- modelling errors (FEM)